University of Alberta

Functional and Structural Studies of the Mammalian Na^+/H^+ Exchanger Isoform 1

by

Emily R. Slepkov ©

A thesis submitted to the Faculty of Graduate Studies and Research
in partial fulfillment of the requirements for the degree of Doctor of Philosophy

Department of Biochemistry

Edmonton, Alberta

Fall 2006

Library and Archives Canada

Published Heritage Branch

395 Wellington Street
Ottawa ON K1A 0N4
Canada

Bibliothèque et Archives Canada

Direction du Patrimoine de l'édition

395, rue Wellington
Ottawa ON K1A 0N4
Canada

Your file Votre référence
ISBN: 978-0-494-23110-4
Our file Notre référence
ISBN: 978-0-494-23110-4

NOTICE:
The author has granted a non-exclusive license allowing Library and Archives Canada to reproduce, publish, archive, preserve, conserve, communicate to the public by telecommunication or on the Internet, loan, distribute and sell theses worldwide, for commercial or non-commercial purposes, in microform, paper, electronic and/or any other formats.

The author retains copyright ownership and moral rights in this thesis. Neither the thesis nor substantial extracts from it may be printed or otherwise reproduced without the author's permission.

AVIS:
L'auteur a accordé une licence non exclusive permettant à la Bibliothèque et Archives Canada de reproduire, publier, archiver, sauvegarder, conserver, transmettre au public par télécommunication ou par l'Internet, prêter, distribuer et vendre des thèses partout dans le monde, à des fins commerciales ou autres, sur support microforme, papier, électronique et/ou autres formats.

L'auteur conserve la propriété du droit d'auteur et des droits moraux qui protège cette thèse. Ni la thèse ni des extraits substantiels de celle-ci ne doivent être imprimés ou autrement reproduits sans son autorisation.

In compliance with the Canadian Privacy Act some supporting forms may have been removed from this thesis.

While these forms may be included in the document page count, their removal does not represent any loss of content from the thesis.

Conformément à la loi canadienne sur la protection de la vie privée, quelques formulaires secondaires ont été enlevés de cette thèse.

Bien que ces formulaires aient inclus dans la pagination, il n'y aura aucun contenu manquant.

Canada

Abstract

The mammalian Na^+/H^+ exchanger isoform 1 (NHE1) is an integral membrane protein that exchanges one intracellular H^+ for one extracellular Na^+. NHE1 is involved in the damage that occurs to the myocardium during ischemia and reperfusion, and inhibition of NHE1 reduces Na^+/Ca^{2+} exchanger-mitigated Ca^{2+} overload. We studied the function and structure of NHE1, specifically focusing on residues in transmembrane (TM) segment IV. To accomplish this, we characterized the expression, surface targeting, and activity of NHE1 mutants in stably transfected cells that lack an endogenous Na^+/H^+ exchanger. We used site-directed mutagenesis to study the importance of three highly conserved proline residues, mutating Pro167 and Pro168 to alanine, glycine, and cysteine, and Pro178 to alanine. All mutations of Pro167 and Pro168 caused significantly reduced activity, while mutation of Pro178 had no effect on activity. We next used cysteine-scanning mutagenesis in combination with reaction with sulfhydryl reactive reagents to identify residues in TM IV that line the ion transport pore. In this case we individually mutated each residue in TM IV to cysteine in a cysteineless NHE1 protein, and we found that residues in TM IV are exceptionally sensitive to mutation, with all of the single cysteine mutants displaying partially impaired activity. We treated the most active single-cysteine mutants with sulfhydryl reactive reagents and found that Phe161Cys was the only mutant that had significantly reduced activity following treatment, indicating that

Phe161 likely lines the ion transport pore of NHE1. Based on this result and the NMR structure of a TM IV peptide, we mutated Phe161 to alanine, leucine, and lysine, and Asp159 and Asp172 to glutamic acid, asparagine, and glutamine. After correction for expression and plasma membrane targeting the only mutant that had decreased activity was Asp159Glu. We suggest that in the Asp159Glu mutant the increased length of the side chain causes the acidic functional group to protrude into the pore, thereby reducing transport. Overall, our results support the importance of TM IV in NHE1 structure and function, with Pro167 and Pro168 being essential for function, and with Phe161 and possibly Asp159 lining the ion transport pore of NHE1.

Acknowledgements

First and foremost, a heartfelt thank you goes to Dr. Larry Fliegel for his patient and enduring supervision during my graduate studies. He took me into his laboratory on short notice and helped me to regain confidence in my own research capabilities. His encouragement, enthusiasm, and constant support have been invaluable to me.

Next, I would like to recognize my committee members, Dr. Joe Casey and Dr. Charles Holmes, for their support and advice throughout my degree. I would also like to recognize my external examiners, Dr. Xing-Zhen Chen and Dr. Balwant Tuana, for their input with this thesis.

I would also like to thank the past and present members of the Fliegel lab, who have always been so helpful, have taught me so much, and have patiently answered all of my questions: Brenda Brix, Bonnie Bullis, Heng Chen, Ersilia Coccaro, Xiuju Li, Yongsheng Liu, Fatima Mraiche, Carmen Rieder, Heather Vandertol-Vanier, and Christine Wiebe.

A special thank you goes to two fellow graduate students who became excellent friends throughout my time in the lab: Angelika Duffy, who was with me from the start; and Mackenzie Malo, who was with me through the end. You made my time in the lab (and out for coffee breaks) especially fun and entertaining.

My husband, Aaron deserves more thanks than I can express in words. He has been my strength, my very best friend, and a pillar of support. I could not have done this without him, and I appreciate that he did not hurry to finish his Ph.D. first!

Finally, I am grateful to the Natural Sciences and Engineering Research Council of Canada, the Alberta Heritage Foundation for Medical Research, and the Heart and Stroke Foundation of Canada for financial support throughout my graduate studies.

To my husband, Aaron, whose support never wavered, even as the years grew long
To my daughter, Beth, who has brightened every day since she came into my life
To Mom, Dad, and Jeff, who believed in me from the very start

Table of Contents

Chapter 1: Introduction 1

1.1 **pH and Volume Regulation in Mammalian Cells** 2

1.2 **The Mammalian Na^+/H^+ Exchanger Family** 2
- 1.2.1 The Mammalian Na^+/H^+ Exchanger Isoform 1 5
- 1.2.2 Physiological functions of NHE1 7
  - 1.2.2.1 Role of NHE1 in disease 9
- 1.2.3 NHE1 as a structural anchor 12

1.3 **Regulation of NHE1** 13
- 1.3.1 Regulation by phosphorylation 14
- 1.3.2 Interaction with signaling molecules 16
- 1.3.3 Transcriptional regulation 19
- 1.3.4 NHE1 Inhibitors 20

1.4 **NHE1 Structure** 23
- 1.4.1 Post-translational modifications 23
- 1.4.2 Dimerization of NHE1 24
- 1.4.3 Putative structure of the membrane domain 25
- 1.4.4 Structure of the cytoplasmic domain 28
- 1.4.5 Structure of the Prokaryotic Na^+/H^+ Antiporter 29

1.5 **Residues involved in NHE1 function** 34
- 1.5.1 TM IV 38
- 1.5.2 TM VII 40
- 1.5.3 TM IX 41
- 1.5.4 TM XI 42
- 1.5.5 Other regions involved in NHE1 function 43

1.6 **Thesis objectives** 46

Chapter 2: Materials and Methods 48

2.1 Materials 49

2.2 Methods 51
2.2.1 Plasmids and site-directed mutagenesis 51
2.2.2 Cell culture and stable transfection 57
2.2.3 SDS-PAGE and immunoblotting 59
2.2.4 Cell surface expression 60
2.2.5 Immunocytochemistry 61
2.2.6 Na^+/H^+ exchange activity 63
2.2.7 Reaction with sulfhydryl-reactive reagents 66
2.2.8 Random mutagenesis using XL1-Red *E. coli* cells 67
2.2.9 Restriction endonuclease digestion, gel purification, and ligation of randomly mutagenized DNA 68
2.2.10 Acid-load selection of cells 70
2.2.11 Isolation and amplification of genomic DNA from acid-load tolerant colonies 72

Chapter 3: The Role of Proline Residues in TM IV of NHE1 76

3.1 Introduction 77

3.2 Results 83
3.2.1 Expression of mutant NHE1 proteins 83
3.2.2 Subcellular localization of mutants and wild-type NHE1 85
3.2.3 Effect of mutations on NHE1 activity 91
3.2.4 Secondary-structure prediction of TM IV 94

3.3 Discussion 96

Chapter 4: Structural and Functional Characterization of TM IV of NHE1 101

4.1 Introduction 102

4.2 Results 108
4.2.1 Expression of NHE1 Mutants 108
4.2.2 Subcellular localization of single cysteine mutants 110
4.2.3 Activity of NHE1 single-cysteine mutants 114
4.2.4 Cysteine-accessibility analysis of NHE1 mutants 116
4.2.5 Solution structure of TM IV 119
4.2.6 Further characterization of Phe161, Asp159, and Asp172 121

4.3 Discussion 127

Chapter 5: Identification of Second-site Revertant Mutations of Pro167Gly using Random Mutagenesis 136

5.1 Introduction 137

5.2 Results 140
5.2.1 Random mutagenesis 140
5.2.2 Isolation of acid-load tolerant cells 142
5.2.3 Na^+/H^+ exchange activity of acid-load tolerant colonies 143
5.2.4 NHE1 expression in acid-load tolerant colonies having high Na^+/H^+ exchange activity 145
5.2.5 Identification of second-site mutations 147

5.3 Discussion 149

Chapter 6: Conclusions and Future Directions 152

6.1 Conclusions 153

6.2 Future Directions 158

Chapter 7: References 162

List of Tables

Table 1.1 Summary of important amino acids in the membrane domain of NHE1 36

Table 2.1 Oligonucleotide primers for site-directed mutagenesis 53

Table 2.2 Site-directed mutagenesis cycling parameters 56

Table 2.3 Solutions for Na^+/H^+ Exchanger Activity Assays 64

Table 2.4 Solutions for Acid Load Selection of PS120 Cells 71

Table 2.5 Oligonucleotide primers for PCR amplification 73

Table 2.6 Cycling parameters for PCR amplification 74

Table 3.1 α-Helical characteristics of amino acids 82

Table 3.2 Quantification of plasma membrane localization for Pro167, Pro168, and Pro178 mutants 88

Table 3.3 Secondary structure analysis of transmembrane segment IV of NHE1 95

Table 4.1 Summary of plasma membrane localization for single-cysteine mutants 113

Table 4.2 Summary of plasma membrane localization for Asp159, Phe161, and Asp172 NHE1 mutants 122

List of Figures

Figure 1.1 Model of NHE1 showing the membrane and cytoplasmic domains 6

Figure 1.2 Molecular structures Na^+/H^+ exchange inhibitors 22

Figure 1.3 Detailed model of the topology of the membrane domain of NHE1 27

Figure 1.4 Structure of the *E. coli* Na^+/H^+ antiporter NhaA 30

Figure 1.5 Proposed mechanism of pH regulation and translocation by NhaA 32

Figure 3.1 Model of TM IV 78

Figure 3.2 Sequence alignment of Na^+/H^+ exchanger isoforms 79

Figure 3.3 Western blot analysis of cells stably expressing Pro167, Pro168, and Pro178 mutants 84

Figure 3.4 Surface expression of Pro167, Pro168, and Pro178 Mutants 87

Figure 3.5 Subcellular localization of Pro167, Pro168, and Pro178 Mutants 90

Figure 3.6 Representative rates of recovery from an acid load 92

Figure 3.7 Rate of recovery from an acid load by Pro167, Pro168, and Pro178 mutants 93

Figure 4.1 Molecular structures of sulfhydryl-reactive reagents 104

Figure 4.2 Western blot analysis of cells stably expressing single-cysteine mutants 109

Figure 4.3 Example Western blots for determination of plasma membrane targeting of single-cysteine mutants 112

Figure 4.4 Activity of single-cysteine NHE1 mutants 115

Figure 4.5 Effect of pCMBS on cysteineless NHE1 activity 117

Figure 4.6 Effect of MTSET and MTSES on activity of cNHE1 and single-cysteine NHE1 mutants 118

Figure 4.7 Structure of the TM IV peptide in CD_3OH:$CDCl_3$:H_2O at 30°C 120

Figure 4.8 Western blot analysis of cells stably expressing Asp159, Phe161, and Asp172 mutants of NHE1 123

Figure 4.9 Activity of Asp159, Phe161, and Asp172 mutants of NHE1 .. 126

Figure 5.1 Strategy for identification of Pro167Gly second-site revertants 141

Figure 5.2 Uncorrected activity of RandomPro167Gly clones 144

Figure 5.3 Expression of RandomPro167Gly mutants 146

Figure 5.4 Corrected activity of RandomPro167Gly mutants 148

Abbreviations

aa	Amino acid
α-MEM	Modified Eagle's medium, α-modification
AE1	Anion exchanger isoform 1
Amiloride	3,5 diamino-6-chloro-N-(diaminomethylene)pyrazine-carboxamide
AP-2	Activator protein-2
ATP	Adenosine triphosphate
BCECF-AM	2'-7'-bis(2-carboxyethyl)-5(6)-carboxyfluorescein acetoxy methyl ester
bp	Base pair
CAII	Carbonic anhydrase II
CaM	Calmodulin
cDNA	Complementary deoxyribonucleic acid
CHP	Calcineurin B homologous protein
cNHE1	Cysteineless NHE1
COUP-TFs	Chicken ovalbumin upstream promoter transcription factors
DAPI	4',6-diamidino-2-phenyl indole
D-MEM	Dulbecco's modified Eagle's medium
DNA	Deoxyribonucleic acid
DNDS	4,4'-dinitrostilbene-2,2'disulfonic acid
dNTP	Deoxyribonucleoside triphosphate
ECL	Enhanced Chemiluminescence
EIPA	5-(N-ethyl-N-isopropyl) amiloride
EL	Extracellular loop
ERK	Extracellular signal-regulated kinase
ERM	Ezrin, radixin, and moesin
G418	Geneticin
GLUT1	Human glucose transporter
HA	Hemagglutinin
HEPES	N-2-hydroxyethypiperazine-N'-2-ethanesulfonic acid
HMA	5-(N,N-hexamethylene) amiloride
HSP70	Mammalian 70 kDa heat shock protein

IC_{50}	Half maximal inhibitory concentration
IgG	Immunoglobulin G
IL	Intracellular loop
kb	Kilobase
kDa	KiloDaltons
K_i	Inhibition constant
K_m	Michaelis-Menten constant
LF2000	LIPOFECTAMINE™ 2000 Reagent
MAPK	Mitogen-activated protein kinase
MjNhaP1	*Methanococcus jannaschii* Na^+/H^+ antiporter
MPA	N^5-methyl-N^5-propylamiloride
mRNA	Messenger ribonucleic acid
MTSEA	2-aminoethylmethane thiosulfonate
MTSES	2-sulfonatoethylmethane thiosulfonate
MTSET	2-trimethylammoniumethylmethane thiosulfonate
NhaA	Bacterial Na^+/H^+ antiporter
NHE(#)	Na^+/H^+ exchanger isoform (#)
NIK	Nck-interacting kinase
NMR	Nuclear magnetic resonance
$P90^{rsk}$	p90 ribosomal S6 kinase
PBS	Phosphate buffered saline
pCMBS	*p*-chloromercuribenzosulfonate
PCR	Polymerase chain reaction
pH_i	Intracellular pH
PIP_2	Phosphatidylinositol 4,5-bisphosphate
pK	Negative log dissociation constant
PP1	Protein phosphatase 1
PP2A	Protein phosphatase 2A
PP2B	Protein phosphatase 2B (calcineurin)
SAM	Sequence Alignment and Modeling
SDS-PAGE	Sodium Dodecyl Sulfate Polyacrylamide Gel Electrophoresis
SE	Standard error
TM	Transmembrane

CHAPTER ONE:

Introduction

1.1 pH and Volume Regulation in Mammalian Cells

It is essential that mammalian cells maintain pH values that are close to neutrality. In mammalian cells the intracellular pH (pH_i) is tightly regulated such that it remains at approximately 7.2 with very narrow fluctuations. Changes in intracellular pH drive a number of physiological processes such as cell growth, differentiation, and migration. Thus, various mechanisms exist to regulate proton fluxes at the plasma membrane, and the Na^+/H^+ exchanger (NHE) is a major pH-regulating system in mammalian cells [1,2]. In addition, because the Na^+/H^+ exchanger removes one intracellular proton (H^+) in exchange for one extracellular sodium ion (Na^+), it is also involved in volume regulation in mammalian cells. When cell shrinking occurs, extracellular Na^+ and Cl^- are brought into the cell, and in many cell types this uptake of Na^+ is accomplished by Na^+/H^+ exchange [2]. Thus, the Na^+/H^+ exchanger plays a central role in important housekeeping functions in mammalian cells.

1.2 The Mammalian Na^+/H^+ Exchanger Family

The mammalian Na^+/H^+ exchangers are a family of integral membrane proteins that mediate the electroneutral exchange of Na^+ for H^+. To date, nine isoforms (NHE1-NHE9) have been identified [3,4]. Each isoform represents a distinct gene product exhibiting specific patterns of tissue expression, membrane

localization, kinetic properties, physiological roles, and sensitivities to pharmacological inhibitors. The isoforms share ~25-70% amino acid identity with calculated molecular masses ranging from ~74,000 to 93,000 [3,5]. Hydropathy analysis of the exchangers predicts that they have similar membrane topologies, with an N-terminal membrane domain consisting of twelve predicted transmembrane (TM) segments (~450-500 amino acids) and a more divergent C-terminal cytoplasmic domain (~130-450 amino acids depending on the isoform) [3]. The NHE1 isoform of the exchanger is the most extensively studied isoform of the Na^+/H^+ exchanger family. This "housekeeping" isoform of the exchanger is ubiquitously expressed in the plasma membrane of virtually all tissues and is the primary NHE isoform found in the mammalian cardiac cell [6]. The NHE2-NHE5 isoforms are also localized to the plasma membrane, but have more restricted tissue distributions. NHE2 and NHE3 are predominantly located in the apical membrane of epithelia and are highly expressed in kidney and intestine [7,8]. While NHE2 is thought to mainly function in secretory processes of certain glands, it is known that NHE3 is essential for absorptive processes that influence systemic electrolyte, acid-base, and blood pressure homeostasis [3]. NHE4, which may have a similar role to NHE1, is most abundant in stomach, but is also expressed in intestine, kidney, brain, uterus, and skeletal muscle [7]. NHE5 is expressed predominantly in brain, but may also be present at low levels in other non-epithelial tissues including spleen, testis, and skeletal muscle [9,10].

Although the physiological role of NHE5 in neuronal function is currently unknown, it has been speculated that it may modulate the acidity of synaptic vesicles [3,11]. Isoforms NHE6-NHE9 are ubiquitously expressed and are distributed to intracellular compartments [4]. These organellar membrane NHEs are presumed to regulate luminal pH and the cation concentration of the intracellular compartments [4]. NHE6 expression is highest in metabolically active tissues including heart, brain, and skeletal muscle, and is localized to early recycling endosomes [4,12]. The NHE7 isoform is localized predominantly to the *trans*-Golgi network, and differs from the other NHE isoforms in that it mediates the influx of either Na^+ or K^+ in exchange for H^+ [13]. The highest levels of NHE8 expression are found in skeletal muscle and kidney, and this isoform is mainly localized to the mid- to trans-Golgi compartments [4]. The recently identified NHE9 isoform is localized to late recycling endosomes [4].

1.2.1 The Mammalian Na^+/H^+ Exchanger Isoform 1

The NHE1 isoform of the Na^+/H^+ exchanger is the best characterized isoform of the family. This isoform was first cloned in 1989 by Jacques Pouysségur's laboratory [14]. NHE1 is 815 amino acids in length, with amino acids 1-500 comprising the membrane domain and residues 501-815 comprising the cytoplasmic tail. Figure 1.1 shows a basic model of NHE1 illustrating both the membrane domain and the cytoplasmic tail. Although NHE1 has a predicted molecular weight of 91 kDa, when resolved by SDS-PAGE it has an apparent molecular weight of 110 kDa because it is glycosylated [15,16]. The membrane domain of NHE1 is both necessary and sufficient for ion transport, while the cytosolic domain is involved in regulation of the activity of the exchanger [17]. Ion flux via the exchanger is driven by the transmembrane Na^+ gradient and requires no direct metabolic energy input. NHE1 exhibits simple Michaelis-Menten dependence on extracellular Na^+ with a reported apparent K_m of 5-50 mM [18,19]. Extracellular Li^+ and H^+ compete with Na^+ for binding at the Na^+-binding site, and high extracellular concentrations of K^+ inhibit NHE1 [20]. In contrast to the simple Michaelis-Menten dependence on extracellular Na^+, intracellular acidification allosterically increases the activity of the Na^+/H^+ exchanger, resulting in a rapid increase in pH_i.

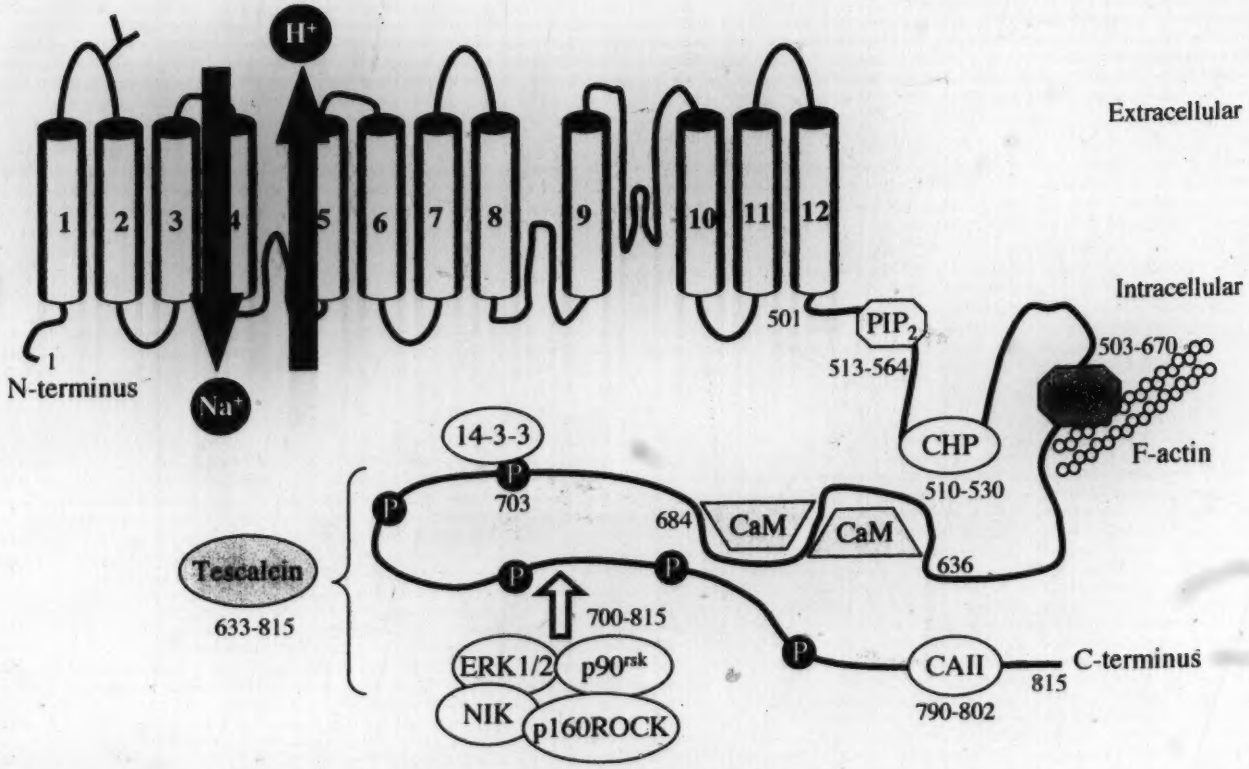

Figure 1.1 Model of NHE1 showing the membrane and cytoplasmic domains

Model of NHE1 illustrating both the membrane and cytoplasmic domains. The membrane domain functions to transport cations, while the cytoplasmic domain regulates the function of the membrane domain through interactions with signaling molecules. PIP_2, phosphatidylinositol 4,5-bisphosphate; CHP, calcineurin homologous protein; ERM, ezrin, radixin, moesin; CaM, calmodulin; CAII, carbonic anhydrase II; ERK 1/2, extracellular signal regulated kinase 1/2; $p90^{rsk}$, p90 ribosomal S6 kinase; NIK, Nck-interacting kinase.

1.2.2 Physiological Functions of NHE1

Na^+/H^+ exchange is critical for a variety of physiological functions. The most important role of the mammalian Na^+/H^+ exchanger is to regulate cytosolic pH. The exchanger protects cells from intracellular acidification, as evidenced by the fact that mutant cell lines devoid of Na^+/H^+ exchange activity are extremely sensitive to acidosis [2,21]. Because the Na^+/H^+ exchanger is activated by decreased intracellular pH, when acidosis occurs, it increases the activity NHE1, resulting in a return of the intracellular pH to resting values. The Na^+/H^+ exchanger also serves as a major Na^+ entry pathway in many cell types, and as such it regulates both sodium fluxes and cell volume after osmotic shrinkage [17,22,23]. Osmotic shrinking causes an alkaline shift of the pH_i dependence of NHE1, resulting in its activation at resting pH [24]. Thus, NHE1 functions to increase the Na^+ concentration within the cytoplasm, as well as causing cytoplasmic alkalinization. The resulting elevated pH_i subsequently activates Cl^-/HCO_3^- exchange, which concurrently increases the Cl^- concentration within the cytoplasm. The net gain of Na^+ and Cl^- causes osmotically obliged water to enter the cell, resulting in cell swelling [23]. While the mechanism by which NHE1 regulates cell volume remains elusive, it is known that the volume or osmolarity-sensitive site within NHE1 is located in the N-terminal 566 amino acids of this protein [25].

In addition to its role in regulating cellular pH and volume, the Na^+/H^+ exchanger also initiates shifts in intracellular pH that stimulate changes in the growth or functional state of cells [1,2]. NHE1 is required for normal cell growth and proliferation [26,27]. Cell proliferation is significantly reduced in cells expressing an inactive NHE1 mutant because NHE1 activity is required to induce a transient increase in pH_i that is essential for the timing of the G2/M transition of the cell cycle [26]. NHE1 activity is also important for cell differentiation. Transcription of NHE1 increases during differentiation in both human leukemic cells and P19 embryonal carcinoma cells [28,29]. In addition, P19 cells that do not express an active NHE1 protein or that have NHE1 inhibited are markedly deficient in their ability to differentiate [27].

There is also data that supports a role for NHE1 in apoptosis, although results have varied with cell type. Apoptosis results in cell shrinkage and intracellular acidification, both of which are processes that are opposed by NHE1. Not surprisingly, in both renal proximal tubule cell lines and human leukemic cell lines Na^+/H^+ exchange activity serves to protect cells from apoptosis [30-32]. However, in two cytokine-dependent cell lines the Na^+/H^+ exchanger mediates an elevation in intracellular pH that triggers an apoptotic pathway [33]. Thus, it is evident that the role that the Na^+/H^+ exchanger plays in apoptosis differs in various cell lines and tissues, and that more research must be done in this area to fully understand the role of NHE1 in apoptosis.

1.2.2.1 Role of NHE1 in Disease

NHE1 has been implicated in the physiology of several diseases. The majority of research about the role of NHE1 in disease has focused on heart disease and cancer. Heart disease accounts for the death of more Canadians than any other disease, and is financially the most costly disease in Canada (www.healthcanada.ca). NHE1 is the only isoform of the exchanger that is present on the plasma membrane of myocardial cells [34]. Moreover, pH regulation by the Na^+/H^+ exchanger plays an important role in the damage that occurs to the human myocardium during and following a myocardial infarction. During a myocardial infarction blood flow to the heart is severely reduced, resulting in a condition that is termed ischemia. During ischemia, protons accumulate within the cell and the intracellular pH drops. Thus, during ischemia and the subsequent restoration of blood flow to the heart (reperfusion), the Na^+/H^+ exchanger is activated to remove intracellular protons, resulting in an accumulation of intracellular Na^+. Under normal conditions, the Na^+-K^+ ATPase would function to remove excess Na^+ from within the cell. However, ischemia leads to a rapid inhibition of the Na^+-K^+ ATPase [35]. Thus, the intracellular Na^+ remains high, causing a reversal of the bidirectional Na^+/Ca^{2+} exchanger to bring Ca^{2+} into the cell [6,36,37]. Consequently, excess Ca^{2+} accumulates inside the cell and causes cell necrosis, contracture, and cardiac arrhythmias. It is known that inhibiting NHE1 can have beneficial effects on the myocardium during ischemia

and reperfusion, and the use of NHE1 inhibitors to protect the heart against ischemic damage is well established in animal studies [38-41]. The importance of NHE1 in ischemia-reperfusion injury is further supported by the fact that genetic ablation of NHE1 in mice protects the heart from ischemia-reperfusion injury [42].

Despite the promising results generated in animal models, results from clinical studies of NHE1 inhibition have not been stellar. Two large studies have failed to find any significant benefit of an NHE1 inhibitor, although a small study of 100 patients did reveal that the NHE1 inhibitor cariporide reduced infarct size and improved left ventricular function in post-infarction patients undergoing angioplasty [43-45]. A more recent study showed that cariporide administration caused a modest but significant reduction in myocardial infarction after coronary artery bypass graft surgery, but in this study a concurrent increase in cerebrovascular events occurred in high-risk patients, and this risk outweighed the positive results [46].

Recently, the Na^+/H^+ exchanger has also been shown to play an important role in myocardial hypertrophy. Hypertrophy of the myocardium is an early, maladaptive response to congestive heart failure and its attenuation is a primary objective for therapeutic treatments. Studies in animal models have shown that inhibition of Na^+/H^+ exchanger activity can prevent myocardial hypertrophy [47-50]. The mechanism by which this occurs has not yet been determined, but the

prevention of hypertrophy supports the potential usefulness of NHE1 inhibition in cardiac surgery.

Cancer is the leading cause of premature death in Canada. The Canadian Cancer Society (www.cancer.ca) estimates that 149,000 new cases of cancer and 69,500 deaths due to cancer occurred in Canada in 2005. It has long been known that the Na^+/H^+ exchanger is important for tumor growth because tumor cells deficient in Na^+/H^+ exchange activity either fail to grow tumors or show severely retarded growth when implanted into immune-deprived mice [51]. It is now thought that NHE1 activity is crucial for causing a reversal of the pH gradient in many types of transformed and/or malignant cells such that the intracellular environment is alkaline and the extracellular environment is acidic [52]. This "malignant acidosis" is considered to represent one of the most specific characteristics of the cancerous state [32,53]. The activation of NHE1 is has been demonstrated to result in the cellular alkalinization that is a key step in oncogenic transformation and is necessary for the development and maintenance of a transformed phenotype [54]. In addition, serum deprivation, a common tumor microenvironmental condition, results in an activation of NHE1 that confers increased motility and invasion in breast cancer cells, characteristics that are required for metastasis to occur [52,55]. Thus, NHE1 inhibitors have a potential use in treating various types of cancers. To date, NHE1 inhibitors have been shown to induce apoptosis in leukemic and breast cancer cell lines

[32,56,57]. The efficacy of NHE1 inhibitors for treating cancer currently awaits preclinical and clinical trials.

1.2.3 NHE1 as a Structural Anchor

In addition to regulating cytosolic pH, NHE1 also acts as a structural anchor that is involved in regulating cytoskeletal organization. It was first suggested that NHE1 may interact with the cytoskeleton in 1992, when Grinstein *et al.* determined that NHE1 was activated during cell volume regulation via a phosphorylation-independent mechanism [58]. Several years later Diane Barber's group confirmed that NHE1 does indeed interact with the cytoskeleton via a direct interaction with the actin binding proteins ezrin, radixin, and moesin (ERM) at residues 553-564 in the C-terminal tail of NHE1 [59,60]. This interaction between NHE1 and ERM proteins serves to regulate focal adhesion assembly, cell shape determination, and cortical cytoskeleton organization independently of the ion translocation function of NHE1 [59]. Additionally, a direct association between NHE1 and ezrin is required to restrict the distribution of these proteins to the lamellipodia of fibroblast cells [59]. A second study by this group found that both cytoskeletal anchoring and ion transport by NHE1 are necessary for establishing polarity and for directed cell migration [61]. Thus, the structural role of NHE1 is thought to regulate membrane integrity and cell shape, to restrict

transmembrane proteins to localized microdomains, and to control cell migration [62]. Furthermore, it may mediate an actin-dependent regulation of NHE1 activity, and it could result in a restricted distribution of NHE1 to maintain a localized H^+ efflux [62]. Moreover, it has recently been suggested that NHE1 likely acts as a plasma membrane scaffold that promotes protein interactions and activities, assembles signaling complexes in specialized plasma membrane domains, and coordinates divergent signaling pathways [63]. This role of NHE1 as a scaffold is supported by a recent study that found that NHE1 promotes cell survival by assembling a signaling complex that includes ERM, phosphoinositide 3-kinase, and the pro-survival kinase Akt [30].

1.3 Regulation of NHE1

The NHE1 isoform of the Na^+/H^+ exchanger is highly regulated. Intracellular acidosis is the major stimulus that regulates NHE1 activity, which is negligible under normal physiological conditions but is rapidly activated as the intracellular pH decreases [37]. This activation exhibits a Hill coefficient of around three, indicating that more than one H^+ binds to NHE1 during the transport cycle [64]. Thus, it has been suggested that NHE1 contains a non-transporting H^+-binding site, sometimes referred to as a proton modifier site. It is thought that as pH_i falls and this proton modifier site becomes increasingly occupied, an

allosteric regulatory mechanism leads to a greater increase in NHE activity than would be expected from the increase in intracellular H^+ alone [64]. In addition to responding to intracellular protons, NHE1 is also regulated by phosphorylation by various kinases in response to hormones and growth factors, and by interactions with other cellular proteins, as depicted in Figure 1.1. NHE1 is also regulated at the transcriptional level, allowing both mRNA levels and the amount of NHE1 protein produced to be controlled. Finally, the exchanger is inhibited by the diuretic compound amiloride and its analogues, and by benzoylguanidinium compounds.

1.3.1 Regulation by Phosphorylation

The distal region of the C-terminal tail of NHE1 that encompasses amino acids ~700-815 contains a number of serine and threonine residues that are phosphorylated by protein kinases in response to sustained acidosis or to hormone and growth factor stimulation [15,65,66]. Phosphorylation of residues in this region shifts the set point of the exchanger, changing the maximal exchange activity from an acidic pH of ~6.5 to a more alkaline pH. For example, sustained intracellular acidosis for ≥3 minutes significantly increases NHE1 activity, and this stimulatory effect is thought to occur through activation of the extracellular signal-regulated kinase (ERK) pathway [66]. In addition, growth factors and

hormones such as thrombin, endothelin, and angiotensin can cause an alkaline shift in the set point of NHE1 via phosphorylation [15,65]. The pathways leading to the phosphorylation of NHE1 are complex and involve a number of signaling molecules, second messengers, binding proteins, and protein kinases. Numerous studies have investigated the phosphorylation of the exchanger, resulting in the identification of several kinases that are involved in regulating NHE1 activity. Kinases that phosphorylate NHE1 and stimulate its activity include: ERK 1/2, via the mitogen-activated protein kinase (MAPK) cascade [67-69]; p90 ribosomal S6 kinase ($p90^{rsk}$), a downstream substrate of ERK 1/2 [67,70,71]; the Rho-associated kinase, p160ROCK [72]; the Nck-interacting kinase, NIK [73]; and the Ca^{2+}/calmodulin-dependent kinase II (CaMKII) [74]. NHE1 is also directly phosphorylated by p38 MAPK [33]. This kinase inhibits NHE1 activity in response to angiotensin II, via inhibition of ERK 1/2 [75], but it may also stimulate NHE1 and induce alkalinization in an apoptotic pathway [33]. Other kinases, such as protein kinase C and protein kinase D, are also able to regulate the exchanger but do not appear to phosphorylate it directly [69,74,76,77].

The regulation of NHE1 by dephosphorylation has also been studied. The phosphatase inhibitor okadaic acid stimulates Na^+/H^+ exchange, suggesting that protein phosphatases 1 (PP1) and 2A (PP2A) may be involved in NHE1 regulation [65,78]. Indeed, further studies proved that NHE1 was completely dephosphorylated by PP1 and poorly dephosphorylated by PP2A, while a third

phosphatase, PP2B did not dephosphorylate the exchanger [78]. In addition, PP1 binds to NHE1 both *in vitro* and *in vivo*. These results suggest that PP1 is an important regulatory phosphatase of NHE1.

1.3.2 Interaction with Signaling Molecules

Na^+/H^+ exchanger activity is also regulated by interaction with a variety of signaling molecules, and these interactions are illustrated in Figure 1.1. To date, three calcium-binding proteins have been shown to interact with the exchanger. Both calmodulin and calcineurin homologous protein act to stimulate NHE1, while tescalcin has an inhibitory effect. Calmodulin (CaM) binds to the cytoplasmic C-terminal tail of NHE1 at two sites: a high affinity site that is located at amino acids 636-656 (CaM-A; $K_d \sim 20$ nM) and a low affinity site that is located at amino acids 657-700 (CaM-B; $K_d \sim 350$ nM) [79]. The high affinity site regulates NHE1 activity by functioning as an autoinhibitory domain, and either deletion of this site or binding of Ca^{2+}/CaM to this site abolishes the inhibitory effect [80]. It is likely that CaM binding requires a very specific conformation to be present at the high-affinity binding site, because mutation of an acidic sequence that is over 100 amino acids downstream from this site disrupts CaM binding [81]. A second Ca^{2+}-binding protein that interacts with NHE1 is calcineurin B homologous protein (CHP) [82]. Endogenous CHP

always contains two tightly bound Ca^{2+} ions when it is associated with NHE1, and it binds to amino acids 515-530 in the C-terminal cytoplasmic domain of NHE1 [83,84]. CHP serves as an essential cofactor for NHE1 and is crucial for maintenance of the pH_i sensitivity of NHE1 [83,84]. A second isoform of CHP, designated CHP2, also interacts strongly with NHE1 and increases its activity. CHP2 is expressed at high levels in tumor cells and appears to protect cells from serum deprivation-induced death by increasing pH_i [85]. The final Ca^{2+}-binding protein that is known to interact with NHE1 is tescalcin [86]. The binding site for tescalcin is located within the last 180 amino acids of the C-terminal tail of NHE1 [87]. Binding of tescalcin to NHE1 inhibits the activity of the exchanger [87].

Three other proteins that are known to bind to NHE1 are: carbonic anhydrase II, the adaptor protein 14-3-3, and mammalian 70 kDa heat shock protein (HSP70). Carbonic anhydrase II (CAII) binds to amino acids 790-802 at the distal end of the C-terminal tail of NHE1 [88]. This interaction has been shown to occur with both *in vitro* and *in vivo* experiments, and CAII expression increases the activity of NHE1 [89]. The double mutation, Ser796Ala/Asp797Asn, within the binding site eliminates CAII binding and the ability of CAII to stimulate NHE1 activity [88]. Phosphorylation at a site within amino acids 634-789 causes an increased interaction between NHE1 and CAII, suggesting that this region of the tail may act as an inhibitor of CAII binding when it is not phosphorylated [88,89]. The binding of 14-3-3 protein to NHE1 is

also dependent on phosphorylation of the exchanger, with binding occurring only when Ser703 is phosphorylated [90]. In this case, 14-3-3 binding is thought to participate in serum-stimulated exchanger activation by preventing dephosphorylation of Ser703 and by stabilizing an active conformation [90]. Finally, HSP70 can also bind directly to the C-terminal regulatory domain of NHE1 [91]. This interaction is likely involved in folding and processing of the antiporter.

A final signaling molecule that is known to bind to and regulate NHE1 is phosphatidylinositol 4,5-bisphosphate (PIP_2). Although the Na^+/H^+ exchanger does not directly use ATP, acute depletion of cellular ATP markedly decreases NHE1 activity [92]. For this reason, it was hypothesized that polyphosphoinositides such as PIP_2 may be involved in the metabolic regulation of NHE1, because depletion of ATP results in a decrease in PIP_2. Indeed, two putative PIP_2 binding motifs were identified within the C-terminal domain at residues 513-520 and 556-564 [92]. *In vitro* experiments proved that these motifs were indeed capable of binding PIP_2, and deletion of these binding motifs resulted in greatly reduced transport activity *in vivo* [92]. Thus, PIP_2 associates with NHE1, and this association is required for optimal activity of the exchanger and at least partially accounts for the ATP-dependence of NHE1 because ATP-depletion results in a net dephosphorylation of PIP_2.

1.3.3 Transcriptional Regulation

The Na^+/H^+ exchanger is also regulated at the transcriptional level. This occurs by regulation of the NHE1 promoter, affecting both mRNA levels and the production of NHE1 protein. Consequently, regulation of the NHE1 promoter affects the maximal velocity of ion exchange, and a number of environmental stimuli have been shown to affect the level of mRNA for NHE1, the amount of the protein itself, and Na^+/H^+ exchange activity [93]. Several groups have examined the effects of ischemia on the expression of NHE1. In isolated perfused hearts, ischemia caused levels of mRNA for the Na^+/H^+ exchanger to increase, and isolated cardiac cells that are subjected to external acidosis have increased exchanger activity [94,95]. Furthermore, NHE1 message and protein levels are both increased at one day and seven days following a myocardial infarction [96].

A proximal region of the NHE1 gene that contains an activator protein-2 (AP-2) site contributes to transcriptional regulation [97]. Deletions upstream of this AP-2 site reduce basal activity of the promoter [98]. The transcription factor AP-2α is likely not the critical transcription factor for regulating the NHE1 promoter at this site because in intact animals with a knockout of the AP-2α transcription factor, NHE1 expression is not reduced [99]. A poly(dA:dT)-rich region of the promoter is also involved in regulation of NHE1 expression [100]. In addition, both serum and growth factors stimulate promoter activity at a more distal region of the promoter. In this case, the chicken ovalbumin upstream

promoter transcription factors (COUP-TFs) act to regulate Na^+/H^+ exchanger expression [101]. Finally, a number of studies have demonstrated that thyroid hormone stimulates an increase in transcription, protein levels, and activity of NHE1 [102]. This increase in expression is due to an interaction between the NHE1 promoter and the thyroid hormone receptor $TR\alpha_1$, at a site that is distinct from but near to the COUP-TF binding site [103].

1.3.4 NHE1 Inhibitors

The Na^+/H^+ exchangers are known targets for inhibition by the diuretic compound, amiloride, and its analogues, and by novel benzoylguanidine derivatives [104]. Comparisons of the different isoforms of the Na^+/H^+ exchanger show that they have varying affinities for these inhibitors, with the following order of sensitivity under similar experimental conditions: NHE1 ≥ NHE2 > NHE5 > NHE3 > NHE4 [3,20]. Because NHE1 is the isoform that is most sensitive to inhibition and is the only isoform that is present in mammalian cardiac cells, the selective properties of these inhibitors can be exploited therapeutically.

Figure 1.2 shows the structure of some NHE inhibitors. The first known inhibitor of NHE was 3,5 diamino-6-chloro-N-(diaminomethylene)pyrazine-carboxamide (amiloride). It contains a guanidine group that is thought to have a structure that is similar in size to a hydrated sodium ion [104]. While amiloride does not have a high specificity for the Na^+/H^+ exchanger, amiloride analogues such as 5-(N-ethyl-N-isopropyl) amiloride (EIPA) and 5-(N,N-hexamethylene) amiloride (HMA) are more selective for the Na^+/H^+ exchanger [105]. Unfortunately, amiloride analogues are not suitable for use in humans due to a number of side effects [106]. Consequently, a new class of inhibitors, the benzoylguanidines, was developed. Members of this family of inhibitors include Hoe-694, cariporide, and eniporide. These compounds have high potency and selectivity for NHE1 and are currently being used in clinical trials [60]. Although these benzoylguanidine derivatives do show potential for treating diseases such as cancer and heart disease, in a recent clinical study cariporide treatment caused an increased cerebrovascular risk [46]. Thus, it is imperative that we continue to increase our knowledge about the Na^+/H^+ exchanger so that even more potent and specific inhibitors of NHE1 can be developed.

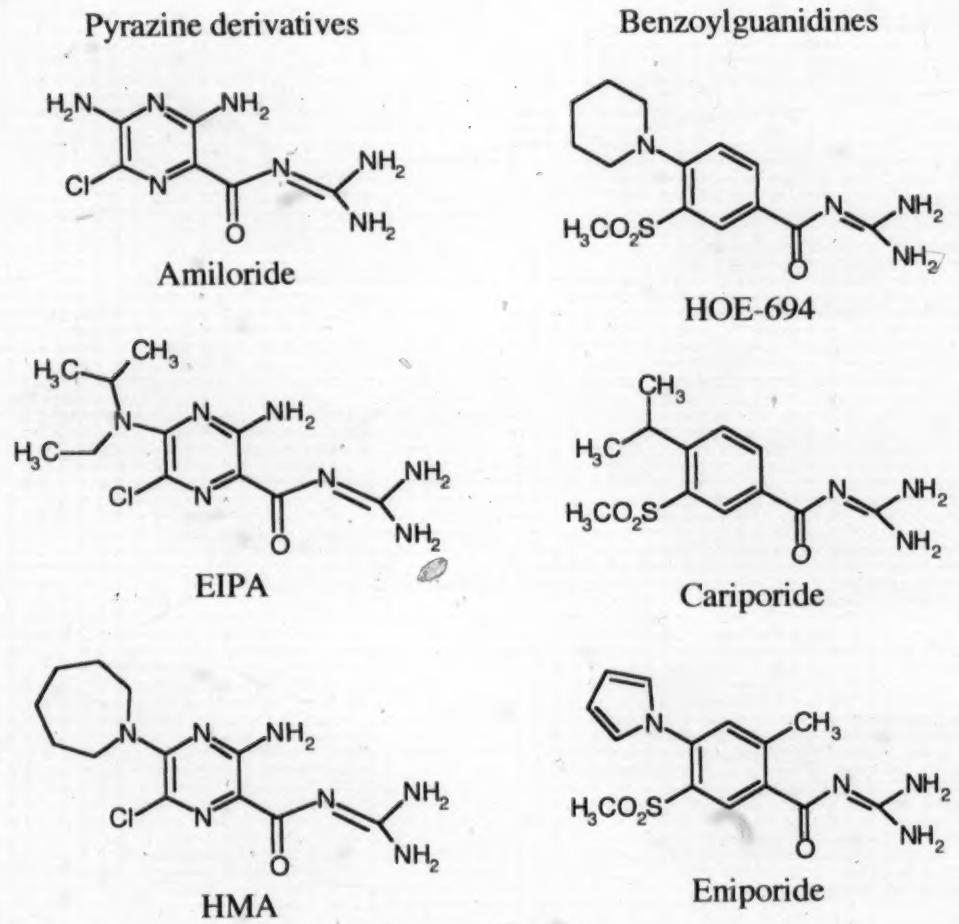

Figure 1.2 Molecular structures Na^+/H^+ exchange inhibitors

Structures of inhibitors of the Na^+/H^+ exchanger. The pyrazine derivatives 3,5 diamino-6-chloro-N-(diaminomethylene)pyrazine-carboxamide (amiloride), and its derivatives 5-(N-ethyl-N-isopropyl) amiloride (EIPA) and 5-(N,N-hexamethylene) amiloride (HMA) are shown on the left panel. The benzoylguanidines compounds HOE-694, HOE-642 (cariporide) and EMD-85131 (eniporide) are shown on the right panel.

1.4 NHE1 Structure

Relatively little is known about the tertiary structure of NHE1 because of the inherent difficulties associated with crystallizing membrane proteins. However, some understanding of the general structure of NHE1 has been gained using molecular biology techniques. In addition, the recently solved high-resolution structure of the bacterial Na^+/H^+ antiporter, NhaA, may also provide some insight to the structure of NHE1 [107].

1.4.1 Post-translational Modifications

The mature form of the Na^+/H^+ exchanger isoform 1 that has a molecular mass of 110 kDa and that is localized to the plasma membrane is glycosylated at both N- and O-linked sites. Each of these glycosylation sites is located within the first extracellular loop, with Asn75 being the target for the N-linked site [16,108]. A second form of the exchanger with a molecular mass of 90 kDa remains present in the endoplasmic reticulum and contains only N-linked high-mannose oligosaccharide [108]. Although NHE1 is glycosylated, it has been clearly shown that N-linked glycosylation is not necessary for normal Na^+/H^+ exchange function. This is evidenced by the fact that neither enzymatic deglycosylation nor removal of Asn75 by site-directed mutagenesis results in decreased Na^+/H^+ exchanger activity [16,108].

1.4.2 Dimerization of NHE1

The first information about the oligomeric state of NHE1 came from our laboratory in 1993 when it was demonstrated that under non-reducing conditions a 205 kDa protein became apparent. This protein was assumed to be an NHE1 dimer [109]. Further studies confirmed that NHE1 forms homodimers in intact cells, and that the deletion of the C-terminal cytoplasmic domain did not disrupt dimerization, suggesting that the membrane domain alone is sufficient to allow dimerization [110]. However, a recent study found that intermolecular cross-linking occurred predominantly at Cys794 in the C-terminal cytoplasmic domain, suggesting that the two C-termini of the NHE1 dimer may also be located in close proximity [111]. Furthermore, coimmunoprecipitation experiments showed that the proximal C-termini (aa 503-580) have a strong propensity to interact directly with each other, and that deletion of aa 562-579 resulted in a disruption of cross-linking between C-termini [111].

With regard to Na^+/H^+ exchange activity, co-expression of active NHE1 and an inactive NHE1 mutant did not result in a dominant negative effect, suggesting that individual subunits of NHE1 function independently within the oligomeric state [110]. However, in mutants with the aa 562-579 deletion that results in disrupted cross-linking between C-termini, the intracellular pH sensitivity of the Na^+/H^+ exchanger is markedly reduced, suggesting that the

dimeric interaction may be involved in the control of the pH-dependent regulation of NHE1 [111].

1.4.3 Putative Structure of the Membrane Domain

Despite over forty years of experimentation on the Na^+/H^+ exchanger, much remains unknown about the structure of this critically important protein. Initial topology models of the membrane domain were based on hydropathy analysis of the primary sequence and predicted a structure consisting of twelve transmembrane (TM) segments. In 2000, Wakabayashi *et al.* experimentally determined the membrane topology of NHE1 by means of substituted-cysteine-accessibility analysis [112]. In this study they individually introduced eighty-three cysteine residues within the membrane domain of a functional cysteineless NHE1. They subsequently determined the topological disposition of each introduced cysteine by labeling with biotin maleimide in the presence or absence of a membrane-impermeant sulfhydryl reagent, in either streptolysin O-permeabilized or nonpermeabilized cells. Their model confirmed that NHE1 has twelve TM segments with both the N- and C-termini located in the cytosol. This model is illustrated in the representation of the membrane domain of NHE1 in Figure 1.3. In addition, they identified three membrane-associated loop regions. Two intracellular loops, IL2 and IL4, were accessible to sulfhydryl reagents from

the extracellular surface. One extracellular loop, EL5, had a long stretch of hydrophobic amino acids that were not accessible to sulfhydryl reagents from either side of the membrane, but this stretch of amino acids is not long enough to span the lipid bilayer twice if it forms an α-helix. Thus, this hydrophobic segment was deemed to be membrane-associated without spanning the bilayer, and is reminiscent of the selectivity filter of the K^+ channel.

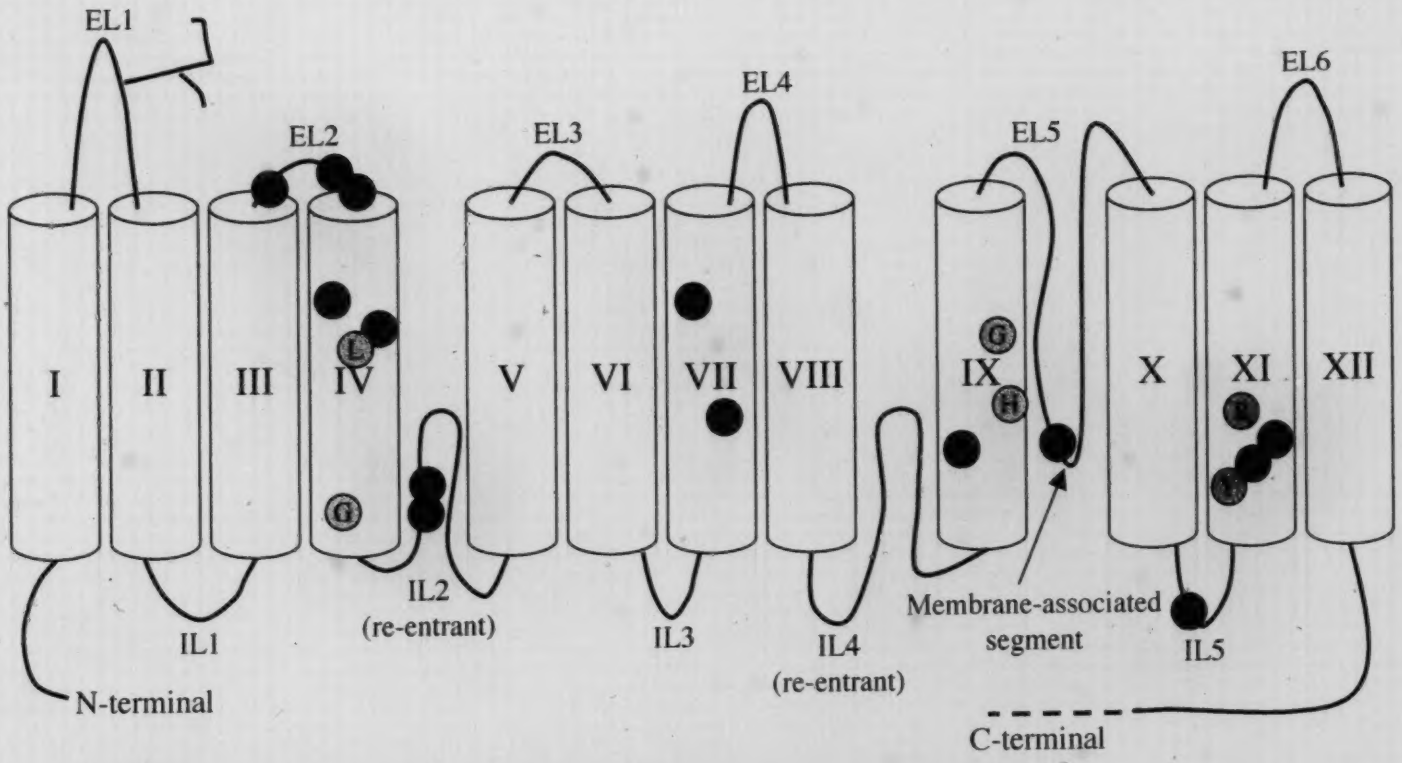

Figure 1.3 Detailed model of the topology of the membrane domain of NHE1

Model of NHE1 illustrating the topology of the membrane domain based on the findings of Wakabayashi *el al.* [112]. *Purple circles*, residues implicated in both ion transport and inhibitor binding; *Red circles*, residues implicated in ion binding and transport; *Blue circles*, residues implicated in inhibitor binding, *Green circles*, residues implicated in NHE1 folding and targeting to the plasma membrane. IL, intracellular loop; EL, extracellular loop.

1.4.4 Structure of the Cytoplasmic Domain

For several membrane proteins it has been possible to obtain a high-resolution crystal of the cytoplasmic domain [113-116]. Unfortunately, attempts to crystallize the C-terminal cytoplasmic domain of NHE1 have been unsuccessful thus far. Consequently, the only structural information known about this hydrophilic region of NHE1 has been determined using circular dichroism spectroscopy. This method revealed that the NHE1 cytoplasmic tail is 35% α-helix, 17% β-turn, and 48% random coil. The structure of the cytoplasmic tail is more compact at regions proximal to the membrane domain while regions distal to the membrane domain are more flexible in nature [117]. More recently, circular dichroism analysis using only the C-terminal 182 amino acids of NHE1 showed that the structure observed in the tail displayed calcium dependent conformational changes [87].

1.4.5 Structure of the Prokaryotic Na^+/H^+ Antiporter

While no high-resolution structure is available for NHE1, some insight into the tertiary structure of this protein may be gained from the recently solved crystal structure of the Na^+/H^+ antiporter, NhaA, from *Escherichia coli*. Although NhaA shares little sequence homology with NHE1, these proteins share a similar basic topology with 12 membrane spanning segments and both the C- and N-termini in the cytoplasm. Figure 1.4 shows the recently published 3.45 Å resolution structure of NhaA in an acid-locked conformation. This structure revealed a negatively charged funnel that opens to the cytoplasm and ends in the middle of the membrane at the putative ion-binding site [107]. Of the 12 TM segments, ten span the bilayer as α-helices, while two (TMs IV and XI) are composed of a short helix, and extended polypeptide chain, and a short helix (Figure 1.4A). TM segments IV and XI form a unique assembly at the binding site, with the two pairs of short helices connected by the crossed, extended chains, creating a balanced electrostatic environment.

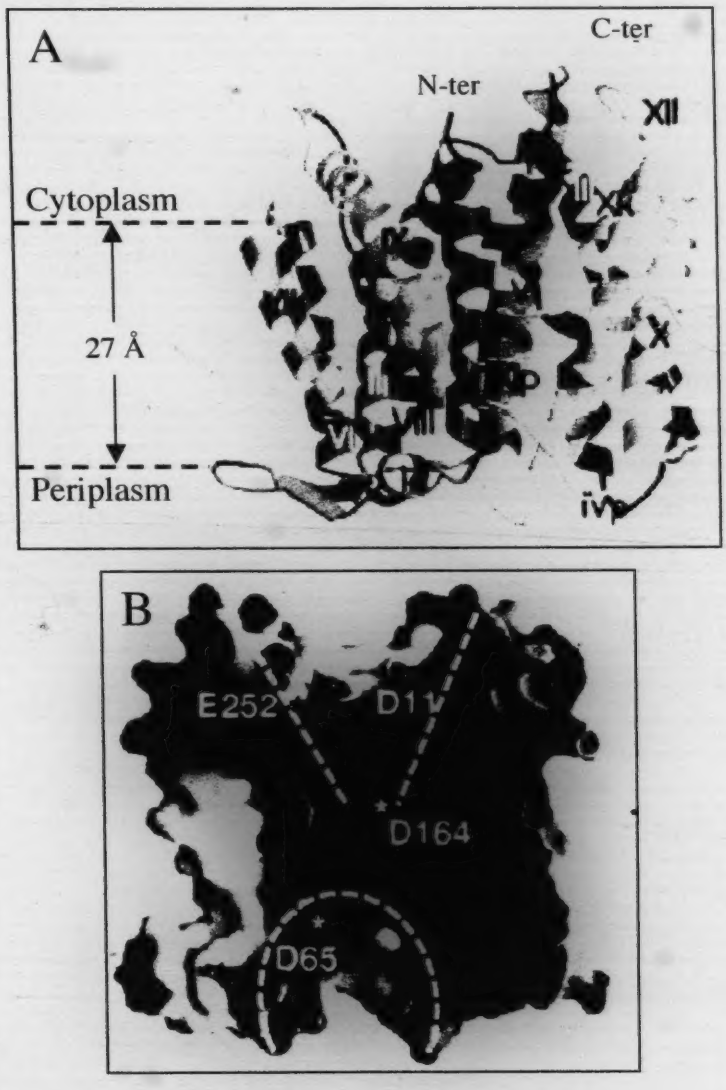

Figure 1.4 Structure of the *E. coli* Na^+/H^+ antiporter NhaA

A, Ribbon representation of NhaA viewed parallel to the membrane. The 12 TM segments are labeled with roman numerals. TM segments IV and XI have a helix-extended chain-helix conformation. B, Cross-section of the electrostatic potential surface of NhaA coloured according to charge (positive in blue, negative in red). The cytoplasmic (top) and periplasmic (bottom) funnels are marked by broken lines. Adapted by permission from Macmillan Publishers Ltd: Nature, copyright 2005 [107].

The mechanism of NhaA is thought to be dependent on TM IX, which is known to contribute to the "pH sensor" and undergo a pH-induced conformation change. In the structure, TM IX is a distorted helix that is in direct contact with the TM IV/XI assembly at the center of the membrane. Thus, it is thought that at alkaline pH the conformation of TM IX changes, resulting in a reorientation of the TM IV/XI assembly that would fully expose the Na^+ binding site to the cytoplasm. Subsequent binding of Na^+ would then trigger another small movement of the TM IV/XI assembly, thereby exposing the cation-loaded binding site to the periplasm. Figure 1.5 shows a schematic representation of this proposed mechanism of pH regulation and ion translocation. This mechanism, which requires only a small conformational change, is consistent with the extremely high catalytic activity of NhaA.

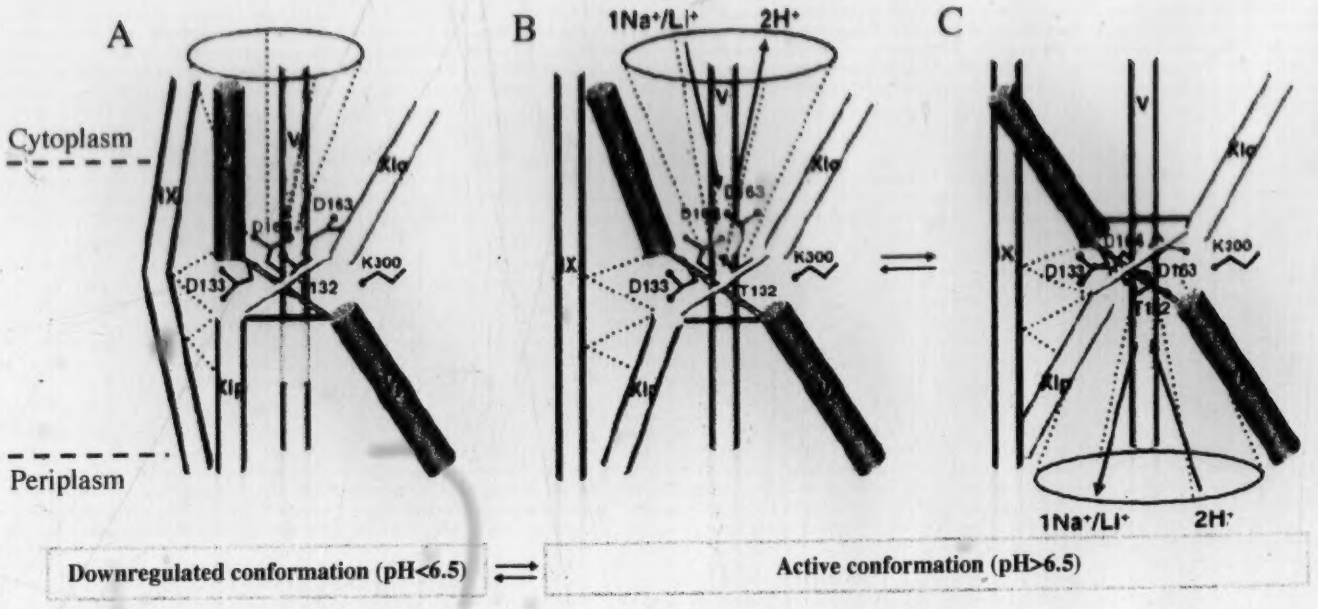

Figure 1.5 Proposed mechanism of pH regulation and translocation by NhaA

Schematic showing the TM IV/XI assembly and its interaction with TM IX. A, Acidic pH-locked conformation. TM IX is bent, and the conformation of the TM IV/XI assembly only partly exposes the Na^+-binding site. B, Activation by alkaline pH causes a conformational change in helix IX that results in a reorientation of the TM IV/XI assembly. This exposes the Na^+-binding site (yellow circle) to the cytoplasmic funnel (red dotted lines and red circle) and blocks it from the periplasm (orange bar). C, Na^+ binding causes the exposure of the cation-loaded binding site to the periplasm. Upon release of the cation, key aspartic acid residues are protonated, shifting NhaA back to the cytoplasm exposed conformation in B. Adapted by permission from Macmillan Publishers Ltd: Nature, copyright 2005 [107].

It has been proposed that the three-dimensional architecture of bacterial NhaA and the mammalian Na^+/H^+ exchangers may be similar, despite the fact that these proteins share little sequence homology [118-120]. This is supported by the fact that many membrane proteins of known structure have symmetry within their three-dimensional architecture although there is little sequence homology between the symmetrical regions [107,121,122]. Thus, it is possible for polypeptide chains with very little homology in their primary sequences to adopt a similar structure within a folded protein. In addition, the distantly related proteins NHE1 and NhaA do share similar characteristics. In each of these proteins the pH regulatory site is different from the active site, a loop participates in the pH response, and each protein exists as an oligomer within the membrane [6,118,123-125]. In contrast to the speculation of a similar overall architecture for all Na^+/H^+ exchangers, a recently published 8 Å electron cryomicroscopy projection map of the MjNhaP1 Na^+/H^+ antiporter from the hyperthermophilic archaeon *Methanococcus jannaschii* showed that the structure of this protein differed significantly from that of the *E. coli* NhaA [126]. Although this finding would argue against NHE1 having a similar tertiary structure to *E. coli* NhaA, little is known about the physiological role of MjNhaP1, making it difficult to draw conclusions about the relevance of this structure with relation to the other Na^+/H^+ exchangers. Ultimately, the final verdict as to the possibility of a conserved

three-dimensional architecture awaits the atomic resolution of more members of this group of transporters.

1.5 Residues Involved in NHE1 Function

Despite the fact that NHE1 has been extensively studied, it remains unknown how this antiporter actually binds and transports Na^+ and H^+ or how it interacts with inhibitors. For some time it was thought that Na^+ and inhibitors bind at a common site on NHE1 because amiloride and HOE694 competitively inhibit Na^+ binding [105]. However, there is also evidence to the contrary, as several studies have demonstrated that the Na^+ and inhibitor binding sites can be altered independently of each other [127-129]. In addition, under chloride-free buffer conditions, amiloride and its derivatives also inhibit transport noncompetitively [5]. Thus, it appears that Na^+ and inhibitors compete for physically distinct binding sites that function cooperatively with respect to Na^+/H^+ exchanger function, such that competitive behavior is observed [105].

Although the exact mechanisms of transport and inhibitor binding are not known, specific residues within the membrane domain of NHE1 have been implicated as being important for ion binding and transport. Figure 1.3 shows the location of these residues within NHE1, and Table 1.1 highlights the mutations that have been studied and summarizes the effects of these mutations. The

majority of residues that are implicated in ion transport and inhibitor binding reside in TM IV. In contrast to TM IV, little is known about other regions of NHE1 that are involved in function.

Amino acid	Location	Mutational studies	Effect of mutation	Reference
Glu346 (Rat: Glu350)	TM IX	Glu→Asp	250-fold increase in K_i for EIPA 2000-fold increase in K_i for HOE-694 Decrease in transport Increase in K_m for Na^+	[5,134]
		Glu→Asn, Gln	Increase in K_i for EIPA Decrease in transport	[5]
Gly352 (Rat: Gly356)	TM IX	Gly→Ala, Ser, Asp	Increase in K_i for EIPA Decrease in transport	[5]
Glu391	EL5	Glu→Gln	Decreased Na^+/H^+ transport	[133]
		Glu→Asp	Restores Na^+/H^+ transport	
Arg440	IL5	Arg→Cys, Lys, His, Asp, Glu, Leu	Shifts pH_i dependence to acidic side	[124]
Tyr454	TM XI	Tyr→Cys	Retained in endoplasmic reticulum	[135]
Gly455	TM XI	Gly→Cys, Gln, Thr, Val	Shift pH_i dependence to alkaline side	[124]
		Gly→Ala, Asp, Asn, Ser	No effect on pH_i dependence	
Gly456	TM XI	Gly→Cys	Shifts pH_i dependence to alkaline side	[124]
Arg458	TM XI	Tyr→Cys	Retained in endoplasmic reticulum	[135]

Table 1.1 Summary of important amino acids in the membrane domain of NHE1

Overview of residues in the membrane domain of NHE1 that are required for ion transport, inhibitor binding, and/or expression and targeting of the exchanger. For simplicity, the amino acid numbering corresponding to the human NHE1 sequence is used. For mutants that were studied in other mammalian models, the species used and the corresponding amino acid number are shown in brackets under the human residue number. The location of the residue within the topology of the exchanger, the specific mutations studied, and the effects of the mutations are summarized.

Amino acid	Location	Mutational studies	Effect of mutation	Reference
Gly148 (Rat: Gly152)	EL2	Gly→Ala	Increase in K_i for EIPA	[5]
Pro153/Pro154 (Rat: Pro157/Pro158)	EL2	Pro→Ser/Pro→Phe	Increase in K_i for EIPA Decrease in transport	[5]
Phe161 (Hamster: Phe165)	TM IV	Phe→Tyr	Increase in K_i for amiloride and MPA Decrease in transport	[130]
Phe162	TM IV	Phe→Ser	1500-fold increase in K_i for cariporide Increase in K_m for Na^+	[132]
Leu163 (Hamster: Leu167)	TM IV	Leu→Phe, Ala, Arg, Trp Leu→Tyr	Increase in K_i for amiloride, MPA, and HOE-694 Eliminates Na^+/H^+ transport	[130]
Gly174	TMIV	Gly→Ser,Asp	Increase in K_i for amiloride and HOE-694	[131]
Leu163/Gly174	TM IV	Leu→Phe/Gly→Ser	>100-fold increase in K_i for HOE-694 Increase in K_m for Na^+	[131]
Arg180	IL2	Arg→Cys	MTSET treatment decreases activity	[112]
Gln181	IL2	Gln→Cys	MTSET treatment decreases activity	[112]
Glu262	TM VII	Glu→Gln Glu→Asp	Eliminates Na^+/H^+ transport Restores partial Na^+/H^+ transport Increases K_m for Li^+	[133]
Asp267	TM VII	Asp→Asn Asp→Glu	Eliminates Na^+/H^+ transport Restores Na^+/H^+ transport	[133]
His349	TM IX	His→Gly, Leu His→Tyr, Phe	Increase in K_i for amiloride Decrease in K_i for amiloride	[129]

1.5.1 TM IV

Numerous residues in TM IV have been implicated in NHE1 function. The sequence of transmembrane IV in the human Na^+/H^+ exchanger isoform 1 is ^{155}FLQSDVFFLFLLPPIILDAGYFL^{177}. In 1993, Counillon *et al.* found that a Phe165Tyr mutation in TM IV of the hamster NHE1 sequence (corresponding to Phe161 in the human sequence) causes both a 40-fold increase in resistance to the amiloride derivative N^5-methyl-N^5-propylamiloride (MPA) and a 3- to 4-fold decrease in Na^+ transport rate, indicating that phenylalanine 165 affects both amiloride binding and the V_{max} for Na^+ [130]. In the same study they used an H^+-killing selection technique and found that a Leu167Phe mutation (corresponding to Leu163 in the human sequence) causes a 30-fold increase in MPA resistance with no effect on Na^+ transport. In 1997, the same group used random mutagenesis and found that a Gly174Ser mutation in TM IV causes a modest 3.3-fold increase in resistance to amiloride with no effect on Na^+ transport [131]. They also made an NHE1 mutant with a Leu163Phe/Gly174Ser double mutation, and found that this mutant possesses a strongly reduced affinity for HOE-694 and a 2-fold decrease in sodium affinity, further implicating TM IV as being important for ion binding and transport. Recently, a Phe162Ser mutation in TM IV was found to cause a dramatic decrease in affinity for cariporide and a 10-fold decrease in Na^+ affinity [132].

The loop regions at either end of TM IV also contain residues that are important for NHE1 function. Mutation of three residues in the second exomembrane loop at the N-terminal end of TM IV (EL2) affects both the drug sensitivity and the activity of the exchanger. Specifically, a single Gly152Ala (corresponding to Gly148 in the human sequence) or a double Pro157Ser/Pro158Phe (corresponding to Pro153/Pro154 in the human sequence) substitution mutation in this loop both modestly influence the drug sensitivity of NHE1, and the Pro157Ser/Pro158Phe double mutation also decreases the catalytic turnover of the exchanger [5]. The intracellular loop at the C-terminal end of TM IV (IL2) also contains residues that may interact with transported cations, as evidenced by the recent substituted-cysteine-accessibility study of the exchanger. In this study, Wakabayashi *et al.* found that parts of IL2 are accessible from both sides of the membrane [112]. In addition, treating Arg180Cys or Gln181Cys in IL2 with the membrane-impermeant sulfhydryl reagent 2-trimethylammoniumethyl-methanethiosulfonate (MTSET) severely inhibits transport. Based on these results, they hypothesized that IL2 is located in a pore-lining region of NHE1 that is involved in ion transport [112]. Further evidence for the importance of this loop comes from the prediction that IL2 is part of the putative H^+-sensor region of NHE1 [6,123]. Overall, these studies provide a strong case for the involvement of TM IV in the ion binding and transport properties of NHE1.

1.5.2 TM VII

Our lab demonstrated that residues Glu262 and Asp267 are essential for NHE1 activity. Thus, TM VII is clearly involved in the ion binding and transport capabilities of NHE1 [133]. Each of the mutations Glu262Gln and Asp267Asn abolished Na^+/H^+ exchange activity, while the conservative mutations Glu262Asp and Asp267Glu that retain the acidic side chain restored Na^+/H^+ exchanger activity. It is unlikely that these effects are due to an altered structure of NHE1 because similar mutations to other regions of the exchanger had little effect, the proteins were properly targeted to the plasma membrane, and limited proteolytic digestion did not indicate that the conformation was altered with respect to the wild-type protein. In addition, the mutant Glu262Asp had a lower affinity for Li^+ than did the wild-type exchanger. Because Li^+ has a smaller ionic radius than Na^+, this decreased affinity may be due to the shorter side-chain length of Asp reducing the ability of the exchanger to coordinate the smaller lithium ion. Thus, these results support the involvement of TM VII in the cation exchange mechanism of NHE1, and specifically implicate Glu262 as a likely target for directly interacting with transported cations.

1.5.3 TM IX

Transmembrane segment IX is also involved in NHE1 function. The importance of TM IX in amiloride binding was first illustrated in 1995, when it was determined that mutating His349 to either glycine or leucine increases resistance to amiloride, whereas mutating this residue to either tyrosine or phenylalanine decreases resistance to amiloride [129]. Moreover, in 1996 Orlowski and Kandasamy made chimeric NHE proteins by interchanging a 66-amino acid segment containing TM IX and its adjacent loops from NHE1 and NHE3. The chimeric NHE proteins displayed reciprocal alterations in their sensitivities to amiloride, EIPA, HOE694, and cimetidine [127]. Again, the chimeric NHE1 mutants retained their normal Na^+ transport properties. Recently, two residues within TM IX of rat NHE1, Glu350 and Gly356 (corresponding to Glu346 and Gly352 in human NHE1), were identified as major determinants of drug sensitivity [5]. Gly356 was mutated to alanine, which is the residue that is located at the corresponding position in the sequence of the NHE3 isoform. This mutation markedly reduced the half-maximal inhibition of the exchanger by the drugs amiloride, EIPA, and HOE694, suggesting that Gly356 may be a key residue in the inhibition of NHE1 [5]. Surprisingly, mutation of the highly conserved residue Glu350 (corresponding to Glu346 in the human sequence) to glutamine also resulted in a decreased sensitivity to amiloride and EIPA, suggesting that this residue may be required for drug recognition in all

mammalian NHEs, regardless of their drug sensitivities. The importance of this residue within human NHE1 was further investigated by Noël *et. al.*, who identified a Glu346Asp mutation in an NHE1 variant with up to 2000-fold higher resistance to HOE694 than wild-type NHE1 [134]. Their studies found that mutation of nearby amino acids had no effect on the IC_{50} values for various drugs, indicating that the Glu346Asp mutation was unlikely to be causing a gross conformational change in the protein structure. In addition, they found that the Glu346Asp mutation caused a 4-fold increase in the K_m for Na^+ as compared to wild-type NHE1. Thus, TM IX not only interacts with NHE1 inhibitors, but also interacts with transported cations. This finding further supports the previously suggested hypothesis that Na^+ and inhibitors have overlapping but distinct binding sites in the NHE1 protein.

1.5.4 TM XI

Several papers published by Munekazu Shigekawa's group have suggested that TM XI plays a role in NHE1 function. First, in their substituted-cysteine-accessibility analysis of NHE1, a number of cysteine mutants in TM XI displayed altered function, indicating that these residues may be involved in either ion transport or proper targeting to the plasma membrane [112]. In a second paper, localization studies determined that two of the mutants in TM XI, Tyr454Cys and Arg458Cys, are retained in the endoplasmic reticulum [135]. These results

suggested that TM XI was important, but it remained unclear whether TM XI was directly involved in NHE1 function or rather if it was required for proper folding and targeting of the transporter. More recent data from this group have shown that TM XI does indeed play a role in NHE1 function. The mutation Gly455Cys or Gly456Cys in TM XI shifts the pH_i dependence of the exchanger to the alkaline side (pK ~ 7), whereas the mutation Arg440Cys in IL5 at the N-terminal end of TM XI shifts the pH_i dependence to the acidic side (pK < 6.2) [124]. The shift in pK observed with mutation of Gly455 was dependent on the size of the substituted side chain residue, implying that these mutations may perturb the structure of TM XI, thereby indirectly affecting the H^+-modifier site. In the case of Arg440, mutation to lysine had a more modest effect on the pK than did other mutations, indicating that a positive charge at this site may be important for normal pH_i sensitivity. Further experiments measuring $^{22}Na^+$ efflux from cells in which the Na^+/H^+ exchanger was functioning in the reverse mode also support the conclusion that both IL5 and TM XI play a crucial role in the proper functioning of the H^+ modifier site [136].

1.5.5 Other regions involved in NHE1 function

The first extracellular loop (EL1), the membrane-associated segment (EL5), and the proximal region of the cytoplasmic domain also contain residues that are involved in NHE1 function. The first extracellular loop is involved in the

differences in volume sensitivity between isoforms of the Na^+/H^+ exchanger. Specifically, amino acids 41-53 are responsible for inhibiting hyperosmolarity-induced activation of NHE2, resulting in the lack of regulatory volume increase (RVI) that is evident in this isoform [137]. Either point mutations within this region of NHE2 or replacement of the N-terminus of NHE2 with the corresponding region of NHE1 resulted in the ability of NHE2 to respond to cell shrinkage [137]. However, deletion and point mutations within amino acids 1-95 of NHE1 had no effect on RVI, suggesting that the N-terminal region is not involved in the volume-sensing mechanism of this isoform [137].

The possible functional involvement of the membrane-associated segment, EL5, within NHE1 is of interest because this segment contains several polar amino acids, and is reminiscent of the selectivity filter of potassium channels [133]. Our group demonstrated that Glu391 in the membrane-associated segment is important for activity [133]. Mutation of Glu391 to glutamine resulted in a partial reduction in activity. Again, mutation to Asp, an alternative acidic residue, restored Na^+/H^+ exchanger activity indicating that the effects of mutating Glu391 are almost certainly not due to an altered structure of NHE1. Thus, the membrane-associated segment also plays a role in the ion binding and transport properties of NHE1.

A highly conserved histidine-rich sequence of amino acids in the proximal region of the cytoplasmic domain, ^{540}HYGHHH^{545}, is also involved in NHE1

function. Mutation of this sequence to ^{540}HHHHHH^{545} has no effect on the activation of NHE1 by protons, but did cause a decrease in the maximal velocity of the exchanger [138]. Thus, this conserved sequence is involved in NHE1 function, but is not involved in proton sensing.

1.6 Thesis objectives

The objective of my thesis was to identify specific amino acids that are important for the function of NHE1, and to begin to elucidate the structure of NHE1 by identifying pore-lining residues within transmembrane segment IV of the exchanger and by identifying long-range interactions between TM IV and other transmembrane segments in NHE1. Initially, we were intrigued by suggestions that three highly conserved proline residues in TM IV were important for the function of NHE1, for the structure of TM IV, and to allow for conformational changes within this transmembrane segment [112,131]. Thus, we used site-specific mutagenesis to investigate the role of these conserved proline residues for the function and membrane targeting of NHE1. Based on findings of other groups that identified numerous amino acids in TM IV that are important for NHE1 function, we hypothesized that TM IV lines the ion transport pore of NHE1. To test this hypothesis, we used cysteine-scanning mutagenesis in combination with reaction with sulfhydryl reactive reagents to identify pore-lining residues in TM IV. In addition to identifying pore-lining residues by reaction with the sulfhydryl reactive reagents, this method will also identify residues in TM IV that are sensitive to mutation. Thus, residues that are sensitive to mutation that may potentially be involved in cation binding and transport can be further studied by using site-specific mutagenesis to mutate the residues to amino acids

other than cysteine. Finally, we attempted to identify long-range interactions between TM IV and other transmembrane segments in NHE1 by isolating and identifying second-site revertant mutations of an inactive Na^+/H^+ exchanger that has a mutation in TM IV.

CHAPTER TWO:

Materials and Methods

2.1 Materials

The pOPRSVICAT plasmid used to create the NHE1 expression vector was purchased from Stratagene. Site-directed mutagenesis was performed using the Stratagene QuikChange™ site-directed mutagenesis kit in combination with PWO DNA polymerase from Roche Molecular Biochemicals. All other DNA modifying enzymes were from either Gibco BRL or New England Biolabs. Random mutations were introduced in the NHE1 gene by propagating DNA in the XL1-Red *E. coli* mutator strain from Stratagene. Commercial kits used to isolate and purify DNA included the GenElute ™ Mammalian Genomic DNA Miniprep Kit from Sigma and the QiaQuick PCR Purification Kit, the Qiagen Maxiprep Kit, and the Qiaex II Gel Purification Kit from Qiagen. Oligonucleotides used as PCR primers and for sequencing were synthesized by either Qiagen or MWG Biotech, Inc. DNA samples were sent to the University of Alberta, Department of Biochemistry, DNA Core Services lab for DNA sequencing.

AP-1 cells were a generous gift from Dr. Sergio Grinstein (University of Toronto, Toronto, ON, Canada) and PS120 cells were kindly provided by Dr. Mark Donowitz (Johns Hopkins School of Medicine, Baltimore, MD, U.S.A.). Cell culture medium was purchased from Gibco BRL (D-MEM) or Sigma Aldrich (αMEM). HyClone bovine growth serum was from VWR and L-glutamine was from Sigma Aldrich. All other media supplements were from Gibco BRL,

including HEPES, gentamicin, penicillin/streptomycin, and geneticin. Dishes and flasks for cell culture were obtained from Sarstedt. The LIPOFECTAMINE™ 2000 Reagent and Opti-MEM I reduced serum medium used for transfection were purchased from Invitrogen Life Technologies. The anion exchange inhibitor 4,4'-dinitrostilbene-2,2'disulfonic acid (DNDS) used during acid selections was obtained from Molecular Probes.

Protein concentrations were determined using the Bio-Rad DC Protein Assay Kit, and all SDS-PAGE apparatus and the nitrocellulose membrane for Western blotting were from Bio-Rad. The anti-HA monoclonal primary antibody was purchased from Boehringer Mannheim, and the peroxidase-conjugated goat anti-mouse secondary antibody was purchased from Bio/Can. Western blots were developed using the Amersham Enhanced Chemiluminescence (ECL) Assay, exposed to film, and densitometric analysis was accomplished using NIH Image 1.63 software (National Institutes of Health, Bethesda, MD, U.S.A.). Sulpho-NHS-SS-biotin (where NHS stands for *N*-hydroxysuccinimido) and immobilized streptavidin resin used in cell surface expression experiments were purchased from Pierce Chemical Company. Reagents used for immunocytochemistry were Alexa Fluor 488-conjugated goat anti-(mouse IgG) immunoglobulin from Molecular Probes and Vectashield mounting medium with DAPI from Vector Laboratories.

To determine Na^+/H^+ exchange activity, cells were grown on glass coverslips (11x22 mm) from Thomas Scientific. The fluorescent dye used in the fluorometric assays, 2'-7'-bis(2-carboxyethyl)-5(6)-carboxyfluorescein acetoxy methyl ester (BCECF-AM), was purchased from Molecular Probes, Sigma Aldrich, or Alexis Corporation, and the nigericin used in the calibration was purchased from Sigma Aldrich. All sulfhydryl reactive reagents were purchased from Toronto Research Chemicals.

2.2 Methods

2.2.1 Plasmids and site-directed mutagenesis

The plasmid pYN4+ was used for expression of the NHE1 gene in mammalian cells. This plasmid was previously constructed in Dr. Larry Fliegel's laboratory (University of Alberta, Edmonton, Alberta) by subcloning the cDNA coding for the human NHE1 isoform with a triple hemagglutinin (HA) tag on the C-terminus of the protein into the *NotI* site of a pOPRSVICAT plasmid which had the CAT reporter removed [139]. The pYN4+ plasmid has an RSV-LTR promoter, NHE1-HA tag, TK poly(A) signal, and the neomycin resistance gene aminoglycoside 3'-phosphotransferase. To express an NHE1 protein that is devoid of cysteine residues, all ten native cysteine residues in NHE1 were

mutated to serine [140]. The resulting cysteineless-NHE1 plasmid was named pYN4-C.

pYN4-C was used as a template for mutating amino acids to cysteine, while pYN4+ was used as a template for creating mutations to all other amino acids. In addition to introducing the desired mutation, all primers were also designed to create or remove a new restriction enzyme site that could be used to screen transformants. Table 2.1 describes the oligonucleotide primers used to create the mutations in NHE1.

Mutation	Template	Primer	RE site
D172C	pYN4-C	CCGCCCATCATCCTG**tg**T<u>GCcGGC</u>TACTTCCTGCCAC	+ NaeI
A173C	pYN4-C	GCTGCCGCCCATCAT<u>tCTaGA</u>T**tgc**GGCTACTTCCTGCCAC	+ XbaI
G174C	pYN4-C	CATCATCCTGGAT<u>GCatGC</u>TACTTCCTGCCAC	+ SphI
Y175C	pYN4-C	CATCATCCTGGAT<u>GCcGGC</u>T**g**CTTCCTGCCACTGCG	+ NaeI
F176C	pYN4-C	CATCATCCTGGAT<u>GCcGGC</u>TACT**g**CCTGCCACTGCGGCAG	+ NaeI
L177C	pYN4-C	CATCATCCTGGAT<u>GCcGGC</u>TACTTC**tgc**CCACTGCGGCAGTTC	+ NaeI
D159N	pYN4+	CCCCCCTTC<u>CTGCAa</u>TCCaACGTCTTCTTCCTC	- PstI
D159Q	pYN4+	CACCCCCCTTC<u>CTGCAa</u>TCC**c**A**g**GTCTTCTTCCTCTTC	- PstI
D159E	pYN4+	CCCCCCTTC<u>CTGCAa</u>TCCGA**g**GTCTTCTTCCTCTTC	- PstI
F161A	pYN4+	CCTGCAGTCC<u>GACGT**gg**c</u>CTTCCTCTTCCTGCTG	- AatII
F161L	pYN4+	CCTGCAGTCCGACGT**gc**TCTTCCTCTTCCTGC	- AatII
F161K	pYN4+	CTGCAGTCC<u>GACGT**gaaa**</u>TTCCTCTTCCTGCTG	- AatII
D172N	pYN4+	CCGCCCATCATCCTG**a**AT<u>GCcGGC</u>TACTTCCTGCC	+ NaeI
D172Q	pYN4+	CCGCCCATCATCCTG**c**A**g**<u>GCcGGC</u>TACTTCCTGCCAC	+ NaeI
D172E	pYN4+	GCCCATCATCCTGGA**g**<u>GCcGGC</u>TACTTCCTGCC	+ NaeI

Table 2.1 Oligonucleotide primers for site-directed mutagenesis

Mutated nucleotides are in lower case letters and bold. Mutated amino acid residues are indicated using single letter notation and new or removed restriction endonuclease (RE) sites are underlined. The template with which each pair of primers was used is indicated. In each case the forward direction of the primer pair is illustrated.

Mutation	Template	Primer	RE site
P167A	pYN4+	CTTCCTCTTCCTGCTagCGCCCATCATCCTGG	+ NheI
P167G	pYN4+	CTTCCTCTTCCTGCTGggGCCCATCATtCTaGATGCGGGCTACTTC	+ XbaI
P168A	pYN4+	CCTCTTCCTGCTGCCGgCCATCATCCTGGATG	+ NaeI
P168G	pYN4+	CTCTTCCTGCTGCCGggCATCATtCTaGATGCGGGCTACTTC	+ XbaI
P178A	pYN4+	GCGGGCTACTTCCTGgCctTaaGGCAGTTCACAGAAAAC	+ AflII
F155C	pYN4-C	GGCGAGACACCCCCCTgCCTGCAaTCCGACGTCTTCTTCC	- PstI
L156C	pYN4-C	CGAGACACCCCCCTTCtgcCAGTCCGAtGTCTTCTTCCTCTTCC	- AatII
Q157C	pYN4-C	GACACCCCCCTTCCTGtgcTCCGAtGTCTTCTTCCTCTTCC	- AatII
S158C	pYN4-C	CACCCCCCTTCCTGCAaTgCGACGTCTTCTTCCTC	- PstI
D159C	pYN4-C	CACCCCCCTTCCTGCAaTCCtgCGTCTTCTTCCTCTTCC	- PstI
V160C	pYN4-C	CACCCCCCTTCCTGCAaTCCGACtgCTTCTTCCTCTTCCTGC	- PstI
F161C	pYN4-C	CCTGCAGTCCGACGTgTgCTTCCTCTTCCTGCTG	- AatII
F162C	pYN4-C	CCTGCAGTCCGACGTgTTCTgCCTCTTCCTGCTGCCG	- AatII
L163C	pYN4-C	CCTGCAGTCCGACGTgTTCTTCtgCTTCCTGCTGCCGCC	- AatII
F164C	pYN4-C	CCTGCAGTCCGACGTgTTCTTCCTCTgCCTGCTGCCGCCCATC	- AatII
L165C	pYN4-C	CCTGCAGTCCGACGTgTTCTTCCTCTTCtgtCTGCCGCCCATCATC	- AatII
L166C	pYN4-C	CCTGCAGTCCGACGTgTTCTTCCTCTTCCTGtgcCCGCCCATCATCCTG	- AatII
P167C	pYN4-C	CGTCTTCTTCCTCTTCCTGCTGtgcCCCATCATtCTaGATGCGGGCTACTTCCTGCCACTGC	+ XbaI
P168C	pYN4-C	CCTCTTCCTGCTGCCGtgcATCATtCTaGATGCGGGCTACTTCCTGC	+ XbaI
I169C	pYN4-C	CTTCCTGCTGCCGCCCtgCATtCTaGATGCGGGCTACTTCC	+ XbaI
I170C	pYN4-C	CCTGCTGCCGCCCATatgCCTGGATGCGGGCTAC	+ NdeI
L171C	pYN4-C	GCTGCCGCCCATCATatgcGATGCGGGCTACTTC	+ NdeI

Site-directed mutagenesis was used to introduce mutations into either the NHE1 gene or the cysteineless-NHE1 gene by amplification with PWO DNA polymerase followed by use of the Stratagene QuikChange™ site-directed mutagenesis kit as described below. PWO DNA polymerase (0.5 µl) was added to a 50 µl solution containing 0.75 µg of denatured template DNA, 0.25 mM dNTP's, and 1 µM each of forward and reverse primers in 1X PWO buffer + $MgSO_4$. This reaction mixture was placed in a PCR cycler set with the cycling parameters outlined in Table 2.2.

The resulting PCR product was treated with 1 µl *DpnI* for 1 hour at 37 °C to digest the template DNA, and was subsequently used to transform XL1-Blue cells by electroporation. DNA was isolated from randomly selected XL1-Blue colonies and positive colonies were identified by restriction enzyme digestion using the newly introduced or removed enzyme site. The accuracy of each mutated plasmid was confirmed by sequencing.

Segment	Cycles	Temperature	Time
1	1	95 °C	30 seconds
2	16	95 °C	30 seconds
		55 °C	1 minute
		68 °C	20 minutes

Table 2.2 Site-directed mutagenesis cycling parameters

Cycling parameters used for site-directed mutagenesis with the Stratagene QuikChange™ site-directed mutagenesis kit.

2.2.2 Cell culture and stable transfection

Two cell lines lacking an endogenous Na^+/H^+ exchanger, AP-1 and PS120, were used to examine different aspects of Na^+/H^+ exchanger expression and activity. AP-1 cells are derived from a Chinese hamster ovary cell line, while PS120 cells are derived from the Chinese hamster lung fibroblast line CCL39. Both cell lines were previously obtained by using the proton-suicide technique [21,23]. Briefly, cells were mutagenized with ethyl methane-sulfonate before being loaded with Li^+. Cells were subsequently exposed to a low external pH in the absence of Na^+. These conditions cause cells that have a functional Na^+/H^+ exchanger to extrude Li^+ in exchange for extracellular protons, resulting in a massive cytosolic acidification. This lethal cytosolic acidification will occur only in those cells that have a functional Na^+/H^+ exchanger. Thus, only cells that lack a functional Na^+/H^+ exchanger will survive this proton-suicide treatment.

AP-1 cells were grown in a humidified atmosphere containing 5% CO_2 in modified Eagle's medium (alpha modification; α-MEM) supplemented with 10% (v/v) fetal bovine serum, 40 mM HEPES, 0.25 mM glutamine, penicillin (100 U/ml), streptomycin (100 U/ml) and gentamicin (4 mg/ml). PS120 cells were grown in a humidified atmosphere containing 5% CO_2 in Dulbecco's modified Eagle's medium (D-MEM) supplemented with 10% fetal bovine serum, penicillin (100 U/ml) and streptomycin (100 U/ml).

Stable cell lines were made for all mutants by transfection with LIPOFECTAMINE™ 2000 Reagent (LF2000) according to the manufacturer's protocol. For transfection, 1×10^6 cells were seeded in a 60 mm Petri dish in 5 mL of growth media without antibiotics and grown overnight. Immediately before transfecting the cells, 10 μg of plasmid DNA was diluted into 500 μl of Opti-MEM, and 20 μl of LF2000 was diluted into a separate 500 μl aliquot of Opti-MEM. The solution containing the LF2000 was incubated at room temperature for 5 minutes, before being combined with the DNA-containing solution and incubated at room temperature for 20 minutes to allow DNA-LF2000 complexes to form. At this point, the media on the cells to be transfected was changed to media without antibiotics or fetal bovine serum. After 20 minutes, 1 ml of the solution containing the DNA-LF2000 complexes was added to the cells and mixed gently. Finally, the cells were incubated at 37 °C with 5% CO_2 for 24 hours, and were supplemented with 10% fetal bovine serum 4-6 hours after transfection.

To achieve stable expression of the protein of interest, the cells were passaged at varying dilutions from 1:10 – 1:10000 into fresh complete growth medium after 24 hours of incubation with the DNA-LF2000 complexes. The medium was changed daily for the first three days, and then every other day for 2-3 weeks, with 800 μg/μl Geneticin (G418) supplementing the medium. Once colonies began forming the G418 concentration was gradually decreased to 400

μg/μl. Single colonies were isolated, amplified, and frozen in liquid N_2 for use in future experiments. Cultures were regularly re-established from frozen stocks, and cells from passage numbers in the range 5-15 were used for experiments.

2.2.3 SDS-PAGE and immunoblotting

Expression of the NHE1 protein was confirmed by immunoblot analysis of total cell lysates. The cells were recovered from plates manually in the presence of lysis buffer consisting of 50 mM Tris, pH 7.4, 150 mM NaCl, 1% (v/v) Nonidet P-40, 0.25% (w/v) sodium deoxycholate, 0.1% (v/v) Triton X-100, 1 mM ethylene glycol-bis(β-aminoethylether)-N,N,N',N'-tetraacetic acid, 0.1 mM benzamidine, 0.1 mM phenylmethylsulfonyl fluoride, and 0.1% (v/v) protease inhibitor cocktail [141]. The cell lysates were centrifuged at 16000 *g* for 5 minutes at 4 °C in an Eppendorf Centrifuge 5415 C and the pelleted cell debris was discarded. The protein concentration of each lysate was determined using a Bio-Rad DC Protein Assay, and for each sample 100 μg of total protein was resolved on a 10% SDS-PAGE gel. The separated proteins were transferred onto a nitrocellulose membrane at 300 mA for 1 hour. The nitrocellulose membrane was blocked in 5% milk in TBS at for at least one hour before it was incubated with a 1:2000 dilution of anti-HA monoclonal antibody in 1% milk/TBS for 2 hours. The membrane was subsequently washed for 4 X 15 minutes in TBS

before being incubated with a 1:2000 dilution of peroxidase-conjugated goat anti-mouse antibody in 1% milk/TBS for 1.5 hours. Finally, the membrane was once again washed for 4 X 15 minutes in TBS prior to development with the Amersham ECL Western blotting and detection system as described by the manufacturer. Densitometric analysis of X-ray films was carried out using the NIH Image software.

2.2.4 Cell surface expression

The proportion of expressed NHE1 that was localized to the plasma membrane was measured essentially as described earlier [142]. Cells were grown to ~80% confluence in 60 mm tissue culture dishes. Initially, cells were washed with 4°C borate buffer (154 mM NaCl, 7.2 mM KCl, 1.8 mM $CaCl_2$, 10 mM boric acid, pH 9.0), and then incubated for 30 min in 3 ml of 0.5 mg/ml Sulpho-NHS-SS-Biotin in borate buffer at 4°C. After 30 minutes, the cells were washed three times with cold quenching buffer (192 mM glycine, 25 mM Tris, pH 8.3) and then solubilized on ice in 0.5 ml IP buffer containing 1% (w/v) deoxycholic acid, 1% (w/v) Triton X-100, 0.1% (w/v) SDS, 150 mM NaCl, 1 mM EDTA, 10 mM Tris/Cl, pH 7.5, 0.1 mM benzamidine, 0.1 mM phenylmethylsulfonyl fluoride, and 0.1% (v/v) protease inhibitor cocktail [141]. The samples were centrifuged at 16000 *g* for 20 minutes to remove cell debris. After centrifugation, half of the

supernatant was retained for use as the "Total" fraction in SDS-PAGE analysis while the remainder of the supernatant was gently rocked overnight at 4 °C with immobilized streptavidin resin (50 µl of 1-3 mg streptavidin/ml settled gel as a 50% v/v slurry in PBS containing 2 mM NaN_3). The following day the beads were removed by centrifuging at 8000 *g* for 2 min, and the supernatant was retained for use as the "unbound" fraction in SDS-PAGE analysis. Equivalent amounts of the total and unbound protein fractions were analyzed by SDS-PAGE and Western blotting. The amount of NHE1 on the plasma membrane was calculated by comparing both the 110 kDa and the 95 kDa species of NHE1 in the total and unbound fractions. Results are shown as mean ± SE of at least 3 trials, and statistical significance was determined with Mann-Whitney *U* test because of the small sample size.

2.2.5 Immunocytochemistry

The cellular localization was also studied using immunocytochemistry for wild-type NHE1 and the mutants of Pro167, Pro168, and Pro178. Cells grown on coverslips to 80-90% confluence were rinsed twice with 1 X PBS and then washed for 15 minutes with 1 X PBS. The cells were then fixed to the coverslips by rinsing with cold 100% methanol before being immersed in methanol at -20 °C for 15 minutes. Once the methanol fixation was complete, the coverslips were

rinsed twice with 1 X PBS and washed twice for 10 minutes with 1 X PBS. The cells were permeabilized by washing with TA-PBS (0.1% BSA, 0.2% Triton X-100 in 1 X PBS) for 15 minutes. The coverslips were subsequently washed for 3 X 10 minutes with TA-PBS before being blocked by washing with 5% (v/v) goat serum in TA-PBS for 20 minutes. The blocking solution was removed by washing the coverslips for 3 X 10 minutes with TA-PBS before incubation with the primary antibody, a 1:300 dilution of mouse monoclonal anti-HA tag antibody, in TA-PBS for 1 hour. The coverslips were once again washed for 3 X 10 minutes with TA-PBS, and were finally incubated with the secondary antibody, a 1:300 dilution of Alexa Fluor 488-conjugated goat anti-(mouse IgG) immunoglobulin in TA-PBS for 1 hour. The fluorophore attached to this secondary antibody is light sensitive; therefore the coverslips were protected from light as much as possible from this point forward. The excess secondary antibody was removed by washing the coverslips for 3 X 10 minutes in 1 X PBS. The coverslips were mounted using Vectasheild mounting media with 4′,6-diamidino-2-phenyl indole (DAPI). Coverslips were stored at -20 °C, and cells were visualized using a Zeiss Axioskop 2 fluorescent microscope.

2.2.6 Na^+/H^+ exchange activity

The ability of the wild type and mutant NHE1 proteins to exchange Na^+ and H^+ across the plasma membrane was estimated as the initial rate of Na^+-induced recovery of cytosolic pH (pH_i) after an acute acid load. Cells grown to 80-90% confluence on glass coverslips were loaded with 3 μg/ml BCECF-AM in either growth medium without serum or Na^+-normal buffer (recipes for all pH measurement buffers are given in Table 2.3). This pH indicator is membrane permeant and non-fluorescent until the acetoxy methyl ester is cleaved within the cell, at which point it becomes both membrane impermeant and fluorescent. The Na^+/H^+ exchange activity was measured using either a PTI Deltascan spectrofluorometer or a Schimadzu RF 5000 spectrofluorometer. The excitation wavelengths used were 452 and 503 nm. These excitation wavelengths were chosen because they coincide with the excitation ratios of BCECF that are pH independent and dependent, respectively [67]. The emission wavelength used was 524 nm, and the ratio of emissions at this wavelength gives a measurement of pH_i that is independent of dye concentration [143].

Solution	Contents	
Na^+-Normal buffer	135 mM	NaCl
	5 mM	KCl
	1.8 mM	$CaCl_2$
	1 mM	$MgSO_4$
	5.5 mM	Glucose
	10 mM	Hepes
	Warm to 37 °C and adjust pH to 7.3 using KOH and HCl	
Na^+-Free buffer	135 mM	N-Methyl glucamine
	5 mM	KCl
	1.8 mM	$CaCl_2$
	1 mM	$MgSO_4$
	5.5 mM	Glucose
	10 mM	Hepes
	Warm to 37 °C and adjust pH to 7.3 using KOH and HCl	
Calibration buffer	135 mM	N-Methyl glucamine
	135 mM	KCl
	1.8 mM	$CaCl_2$
	1 mM	$MgSO_4$
	5.5 mM	Glucose
	10 mM	Hepes
	Warm to 37 °C and adjust pH to 6.0, 7.0, or 8.0 using KOH and HCl	

Table 2.3 Solutions for Na^+/H^+ Exchanger Activity Assays

Recipes for Na^+-normal buffer, Na^+-free buffer, and calibration buffer used to determine the activity of the Na^+/H^+ exchanger.

To begin the assay of pH_i, the coverslip was placed in Na^+-normal buffer until a steady pH_i was obtained. The cells were then acid loaded with ammonium chloride (50 mM for 3 min in Na^+-normal buffer), followed by a brief incubation in Na^+-free buffer. The incubation in Na^+-free buffer was normally 15-20 seconds long, allowing a steady acidic pH_i to be obtained. There was no difference in the buffering capacities of the stably transfected cell lines as indicated by the degree of acidification induced by ammonium chloride. The cells were finally transferred into fresh Na^+-normal buffer and the recovery of pH_i was monitored for 3 minutes, until a stable resting pH was reached [133]. Representative activity assay traces are depicted in Figure 3.6. A three-point pH calibration was carried out for each coverslip following the recovery of the cells from the acid load. This was done using the high K^+/nigericin method by placing the cells in calibration buffers at pH 8, 7, and 6 containing 135 mM KCl in the presence of 10 μM nigericin [144]. Nigericin is a carboxylic ionophore that exchanges cations for protons with a high selectivity for K^+ [145]. The cells were incubated in each calibration buffer until a steady pH_i was obtained. A standard curve was generated using this calibration data, allowing the rate of recovery from an acid load to be calculated with final units of ΔpH/min.

Data from the first 20 seconds of linear recovery was used to determine the rate of recovery of the cells in pH change per minute. Measurements of each type of stably transfected cell were repeated on at least two independently isolated

clones of each Na^+/H^+ exchanger mutant. Results are shown as mean ± SE of at least 8 trials, and statistical significance was determined with a Mann-Whitney *U* test (sample sizes of <20) or an independent samples *t*-test (sample sizes ≥20). To calculate Na^+/H^+ exchanger activity per amount of protein present on the plasma membrane, Na^+/H^+ exchanger activity was normalized to the NHE1 expression and cell surface targeting levels that were measured as described above.

2.2.7 Reaction with sulfhydryl-reactive reagents

To determine whether any of the residues in TM IV of NHE1 are pore lining, cNHE1 and the active single-cysteine mutants were treated with sulfhydryl reactive reagents using a two-pulse assay. In this case, cells were grown on coverslips and activity was measured after an NH_4^+-induced acidification of the untreated cells as described above. However, for the two-pulse assay, after recovery the cells were incubated in Na^+-free buffer containing: 5 mM MTSEA for 8 minutes; 0.2 mM pCMBS for 2 minutes; 10 mM MTSET for 10 minutes; or 10 mM MTSES for 10 minutes. The cells were subsequently washed three times in Na^+-free buffer, and the recovery was measured after a second NH_4^+-induced acidification. To calculate residual activity the following formula was used:

$$\% \text{ residual activity} = \frac{\text{pH change after treatment}}{\text{pH change w/o treatment}} \times 100\%$$

2.2.8 Random mutagenesis using XL1-Red *E. coli* cells

Random mutations were introduced in the pYN4+/Pro167Gly mutant of NHE1 by propagating the plasmid in the XL1-Red mutator *E. coli* strain. The transformation was carried out according to the manufacturer's protocol. Briefly, the XL1-Red competent cells were thawed on ice and gently mixed by hand. For each transformation reaction, 100 µl of the XL1-Red competent cells was aliquoted into a prechilled 14-ml BD Falcon polypropylene round-bottom tube. To each aliquot 1.7 µl of 1.42 M β-mercaptoethanol was added, giving a final concentration of 25 mM. The tubes were incubated on ice for 10 minutes, with gentle swirling every 2 minutes. After 10 minutes, 50 ng of plasmid DNA was added to each aliquot of XL1-Red competent cells and swirled gently. The tubes were incubated on ice for 30 minutes, and then heat-pulsed in a 42 °C water bath for 45 seconds. Immediately following the heat pulse the tubes were incubated on ice for 2 minutes. SOC medium (0.9 ml; prewarmed to 42 °C) was added to each tube and the tubes were incubated at 37 °C for 1 hour with shaking at 225-250 rpm. The entire transformation mixture was used to inoculate 1 L of LB-Amp and the culture was incubated at 37 °C for 42 hours. These conditions will result in a mutation rate of approximately 1 in 2000 basepairs. After 42 hours the cells were harvested and the randomly mutagenized DNA was isolated using a QIAGEN Plasmid Maxiprep Kit.

2.2.9 Restriction endonuclease digestion, gel purification, and ligation of randomly mutagenized DNA

In order to have randomly introduced mutations only within the membrane domain of NHE1, an 1142 basepair fragment (corresponding to Leu171 to Leu550 in the NHE1 protein) was excised from the randomly mutagenized pYN4+/Pro167Gly (pYN4+/RandomP167G) plasmid and ligated into unmutagenized pYN4+/Pro167Gly. This was accomplished by digesting 10 µg each of pYN4+/Pro167Gly and pYN4+/RandomP167G with XbaI and AgeI for 5 hours at 37 °C. Following the digestion, the restriction enzymes in the pYN4+/Pro167Gly sample were deactivated at 65 °C for 20 minutes and the 5' phosphate group was removed from the DNA fragments by incubation with 2 µl of calf intestinal alkaline phosphatase for 1 hour at 37 °C. This step ensured that the pYN4+/Pro167Gly fragment could not self-ligate in the subsequent ligation reaction. The digested plasmid DNA was run on a 0.8% low-melt agarose gel, and the desired DNA fragment was excised. For the pYN4+/Pro167Gly digestion the fragment of interest was 6929 base pairs (7 kb vector fragment), while the fragment of interest for the pYN4+/RandomP167G was 1142 base pairs (1 kb insert fragment). The DNA fragments were extracted from the gel using either the Qiagen Qiaex II agarose gel extraction protocol as described by the manufacturer, or a squeeze technique of fragment gel purification. In this

technique, the gel slice is frozen, placed between two pieces of parafilm, and squeezed until liquid containing the fragment of interest is released. The fragment is then purified by phenol chloroform extraction and sodium acetate precipitation.

The gel purified DNA fragments were ligated overnight using T4 DNA ligase at 16 °C. The reaction mixture contained 1 μl of T4 DNA ligase, 2 μl of ligase buffer, 5 μl of the gel purified 7 kb vector fragment, and 12 μl of the gel purified 1 kb insert fragment. To ensure that the 7 kb vector fragment from pYN4+/Pro167Gly did not self ligate, a control reaction was set up containing 1 μl of T4 DNA ligase, 2 μl of ligase buffer, 5 μl of the gel purified 7 kb vector fragment, and 12 μl ddH_2O. Following the ligation reaction, the ligation products were transformed into DH5α cells by electroporation. In total, more than 20,000 colonies were obtained from the experimental ligation reaction, while less than 0.2% of this number of colonies grew from the control ligation. The plasmid DNA was isolated from 12 randomly picked colonies obtained from the experimental ligation reaction, and in each case the plasmid DNA contained both the XbaI and AgeI restriction sites, as shown by a restriction digest. Thus, the colonies obtained from transformation with the ligation product were combined and a pool of randomly mutagenized pYN4+/Pro167Gly plasmid DNA was isolated. Finally, the pooled, randomly mutagenized pYN4+/Pro167Gly was used to transfect PS120 cells, resulting in more than 4800 colonies.

2.2.10 Acid-load selection of cells

Cells that have an active Na^+/H^+ exchanger were isolated using an acid-load selection technique [146] that was modified to increase the stringency of the selection. To begin, PS120 cells transfected with either wild-type NHE1 or randomly mutagenized Pro167Gly were plated in 100 mm dishes and grown until visible colonies formed. The cells were initially washed with 1XPBS, and were subsequently incubated in 8 ml of isotonic 100 mM NH_4Cl-medium for 30 minutes at 37 °C in a nominally CO_2-free atmosphere (recipes for all acid-load selection solutions are given in Table 2.4). After 30 minutes, cells were rapidly washed twice with 4 ml of isotonic Na^+-saline medium to remove excess extracellular NH_4^+. The cells were finally incubated in 8 ml of Na^+-saline medium containing 0.1 mM DNDS [147,148] for one hour at 37 °C in a nominally CO_2-free atmosphere. After one hour the Na^+-saline medium was removed and replaced with normal culture medium. This process was repeated twice a day, every day, for five days with at least two hours between consecutive acid selections.

Solution	Contents	
100 mM NH_4^+-saline medium	100 mM	NH_4Cl
	20 mM	Choline Chloride
	5 mM	KCl
	1 mM	$MgCl_2$
	2 mM	$CaCl_2$
	5 mM	Glucose
	20 mM	HEPES
	Adjust pH to 7.4 using HCl and KOH	
	Autoclave for 40 minutes	
Na^+-saline medium	120 mM	NaCl
	5 mM	KCl
	1 mM	$MgCl_2$
	2 mM	$CaCl_2$
	5 mM	D-glucose
	20 mM	HEPES
	Adjust pH to 7.4 using HCl and KOH	
	Autoclave for 40 minutes	

Table 2.4 Solutions for Acid Load Selection of PS120 Cells

Recipes for NH_4^+-saline medium and Na^+-saline medium used to select PS120 cells expressing an active Na^+/H^+ exchanger.

2.2.11 Isolation and amplification of genomic DNA from acid-load tolerant colonies

Of the 4800 colonies obtained from the transfection with the pooled, randomly mutagenized pYN4+/Pro167Gly, approximately 225 colonies survived the acid-selection protocol outline above. Of these surviving colonies, 104 clones were propagated and all but three of these clones tested positive for NHE1 expression using the western blotting technique described in Section 2.2.3. Half of the clones expressing NHE1 were randomly chosen for screening for NHE1 activity using the fluorometric NHE1 activity assay described in Section 2.2.6. The three clones (#54, 63, and 93) with the highest activity relative to their expression were chosen and genomic DNA was isolated from these clones using the GenElute™ Mammalian Genomic DNA Miniprep Kit. The region of the NHE1 gene corresponding to Leu171 to Leu550 of the NHE1 protein sequence was amplified by PCR using the oligonucleotide primers described in Table 2.5, with either Emily 5'a or Emily 5'b used in conjunction with Emily 3'b. PCR amplification was achieved by adding PWO DNA polymerase (0.5 μl) to a 50 μl solution containing 4 μL of isolated genomic DNA, 0.25 mM dNTP's, and 1 μM each of forward and reverse primers in 1X PWO buffer + $MgSO_4$. This reaction mixture was placed in a PCR cycler set with the cycling parameters outlined in Table 2.6.

Name	Direction	Start	Primer
Emily 5'a	Forward	Ile146	GATCAAGGGTGTAGGCGAG
Emily 5'b	Forward	Val74	GTTAATCATTCCGTCACTGATC
Emily 3'b	Reverse	Ala564	CAGCTATCAGACACTTCTTCAC

Table 2.5 Oligonucleotide primers for PCR amplification

Sequence of oligonucleotide primers used to amplify the region of the NHE1 gene corresponding to amino acids Leu171 to Leu550. The direction of the primer and the location at which the primer binds in relation to the amino acid sequence are given.

Segment	Cycles	Temperature	Time (minutes)
1	1	94 °C	3
2	3	94 °C	1
		69 °C	1
		72 °C	1.5
3	3	94 °C	1
		66 °C	1
		72 °C	1.5
4	3	94 °C	1
		63 °C	1
		72 °C	1.5
5	3	94 °C	1
		60 °C	1
		72 °C	1.5
6	3	94 °C	1
		57 °C	1
		72 °C	1.5
7	15	94 °C	1
		55 °C	1
		72 °C	1.5
8	1	72 °C	10

Table 2.6 Cycling parameters for PCR amplification

Cycling parameters used for amplification of the randomly mutated segment of the NHE1 gene from genomic DNA isolated from acid-load tolerant colonies.

In the case of clones #63 and 93, the resulting PCR product was sequenced to identify any mutations that were present due to the random mutagenesis technique. In the case of clone #54, a reliable sequence was not generated directly from the PCR product. Thus, in this case, the PCR product was subcloned into the pYN4+/P167G plasmid as described in section 2.2.9, and the resulting plasmid containing the subcloned fragment was sequenced.

CHAPTER THREE:

The Role of Proline Residues in TM IV of NHE1

A version of this chapter also appears in Biochemical Journal
(2004) **379**, 31-38
Emily R. Slepkov, Signy Chow, M. Joanne Lemieux and Larry Fliegel

3.1 Introduction

As discussed in Section 1.5.1, several studies have shown that mutations in TM IV result in altered ion transport and inhibitor-binding properties of NHE1. These results provide a strong case for the importance of TM IV in the ion-binding and transport properties of NHE1. The involvement of TM IV in the mechanism of NHEI is especially interesting in light of the fact that TM IV is a proline-rich segment. Specifically, TM IV contains three proline residues (Pro167, Pro168, and Pro178) and the location of these proline residues within TM IV is highlighted in Figure 3.1. From the sequence alignment in Figure 3.2 it is evident that these proline residues are highly conserved. In particular, Pro167 and Pro168 are conserved across eight isoforms of the mammalian Na^+/H^+ exchanger, although the equivalents of Pro168 and Pro178 are not conserved in the yeast Na^+/H^+ exchanger, NHX-4 [7,9,13,14,149-153]. Conservation of Pro167 and Pro168 in the mammalian NHE isoforms suggests that these proline residues may play an important role in NHE function.

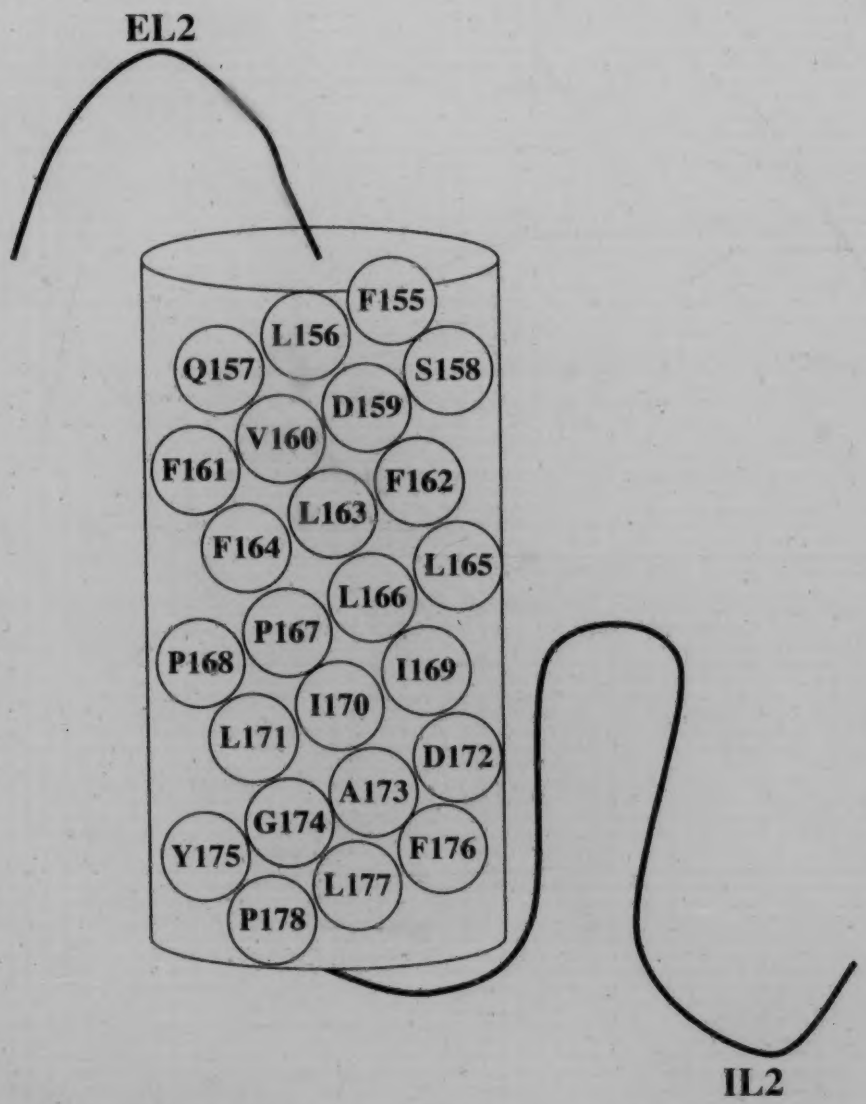

Figure 3.1 Model of TM IV

Model of TM IV of NHE1 illustrating the positions of the amino acid residues known to be important for NHE1 structure or function. Green circles represent the residues that have been previously shown to be important for NHE1 function. Yellow circles represent the conserved proline residues at positions 167, 168 and 178.

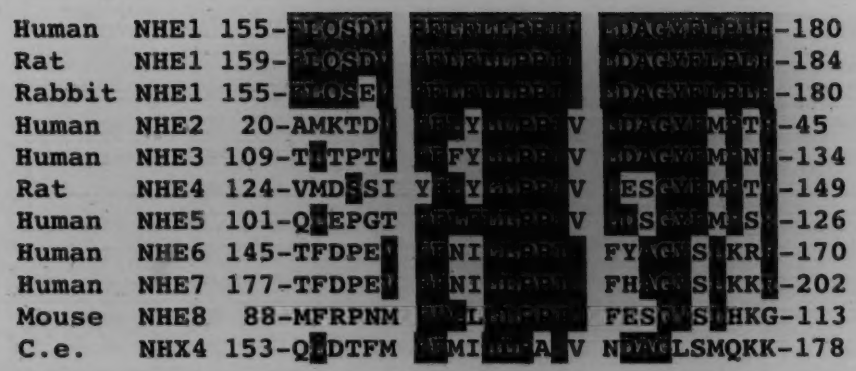
Human NHE1 155- -180
Rat NHE1 159- -184
Rabbit NHE1 155- -180
Human NHE2 20-AMKTD -45
Human NHE3 109-T -134
Rat NHE4 124-VMD -149
Human NHE5 101-Q -126
Human NHE6 145-TFDPE -170
Human NHE7 177-TFDPE -202
Mouse NHE8 88-MFRPNM -113
C.e. NHX4 153-Q -178

Figure 3.2 Sequence alignment of Na^+/H^+ exchanger isoforms

Sequence alignment of the TM IV region of mammalian Na^+/H^+ exchanger isoforms 1-8, and NHX4 of *Caenorhabditis elegans* (C.e.). Shading indicates identity with the human NHE1 isoform. References are: NHE1 [7,14]; NHE2 [149]; NHE3 [150]; NHE4 [7]; NHE5 [9]; NHE6 [151]; NHE7 [13]; NHE8 [152]; and *C. elegans* [153].

The proline residues that are in the middle of TM IV are prime candidates to be involved in the mechanism of NHE1. Proline residues are considered to be helix-breakers because they lack an amide hydrogen and because they cause a kink of ~26° in the α-helix [154-156]. These characteristics leave the *i*-4 backbone carbonyl without its normal hydrogen bond donor and prevent formation of the (*i*-3)-carbonyl-(*i*+1)-amide backbone hydrogen bond [154,156]. Thus, the characteristics of this amino acid make proline residues an interesting target for study.

In the recent X-ray structure of the glycerol-3-phosphate transporter from *E. coli* two transmembrane helices that contain two sequential prolines are present [157]. Helix IV contains two prolines and is straight, while helix V contains two prolines but is bent. Similarly, in the lactose permease of *E. coli*, some kinks in transmembrane segments are at proline residues, although others are at glycine or alanine residues [158]. Therefore it is clear that the effect of proline residues within transmembrane segments varies, that the local environment can moderate this effect, and that kinks in transmembrane segments can be induced by means other than proline residues.

The characteristics of proline residues within transmembrane segments could have several important consequences for TM IV of NHE1. Each proline introduced into an α-helix leaves two free backbone carbonyls, which could directly co-ordinate cations or interact with inhibitors [155]. A kink that is

introduced by the proline residues could also create a space to accommodate transported cations or a part of the re-entrant loop, IL2 (intracellular loop 2), which is present at the C-terminal end of TM IV in NHE1 [112,131]. Additionally, the increased flexibility in this transmembrane segment introduced by proline residues could allow for conformational changes that are required for normal exchanger function. Finally, the presence of two proline residues in helix IV may not allow the formation of an α-helix [155].

In the present study, we used site-specific mutagenesis to investigate the functional effects of mutating the conserved proline residues in TM IV. Pro178 was mutated to Ala, and Pro167 and Pro168 were mutated to Gly, Ala or Cys. These amino acids were chosen for the mutations because they differ in their α-helical tendency, backbone flexibility and their ability to cause a kink in the α-helix (Table 3.1). Mutation of Pro178 to Ala had no effect on NHE activity. In all cases, the Pro167 and Pro168 mutations caused a significant decrease in NHE activity, indicating that these proline residues are critical for normal NHE1 function.

Amino acid	α-Helical tendency	Kink	Flexibility	Free carbonyls
Proline	Strong helix breaker	Yes	Yes	Yes
Glycine	Strong helix breaker	Possibly	Yes	No
Alanine	Strong helix former	Possibly	No	No
Cysteine	Helix indifferent	No	No	No

Table 3.1 α-Helical characteristics of amino acids

The characteristics of glycine, alanine, and cysteine in were summarized in comparison to proline. The α-helical tendency, probability for the presence of a kink, flexibility introduced into the α-helix, and presence of free backbone carbonyl oxygen atoms is given for each amino acid. References are: α-Helical tendency [173]; kink [151,165]; flexibility [152, 174]; and free carbonyls [152].

3.2 Results

3.2.1 Expression of mutant NHE1 proteins

Site-directed mutagenesis was utilized to introduce the mutations Pro167Gly, Pro168Gly, Pro167Ala, Pro168Ala and Pro178Ala into wild-type NHE1, and to introduce the mutations Pro167Cys and Pro168Cys, into a cysteineless version of NHE1 (cNHE1). The constructed mutants were subsequently transfected into the Na^+/H^+ exchange-deficient AP-1 cell line, and clones that stably expressed NHE1 were selected for use in further experiments. Figure 3.3 shows the results of a Western-blot analysis using an anti-HA tag antibody to detect the expressed NHE1 via its C-terminal HA tag. A densitometric analysis was performed on this Western blot, and the levels of protein expression relative to that of NHE1 are shown beneath each lane as a percentage of wild-type NHE1 expression. From Figure 3.3, it can be seen that the mutant and wild-type exchangers displayed the same pattern of immunoreactive bands, with a larger band at approximately 110 kDa, which represents the glycosylated form of the mature NHE1, and a smaller band at approximately 95 kDa, which represents an immature form of the exchanger that is not fully glycosylated [108]. The densitometric analysis included only the larger 110 kDa species, as the 95 kDa species is retained in the endoplasmic reticulum and would not contribute to the activity of the exchanger [108].

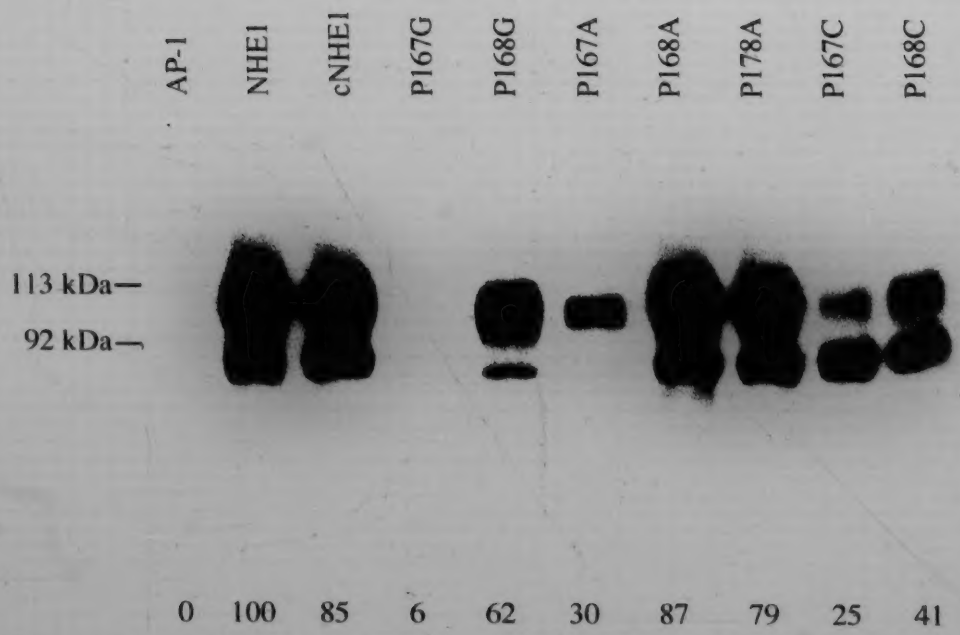

Figure 3.3 Western blot analysis of cells stably expressing Pro167, Pro168, and Pro178 mutants

Representative Western blot showing NHE1 expression in untransfectd AP-1 cells (AP-1), and AP-1 cells transfected with HA-tagged wild-type NHE1 (NHE1), cysteineless NHE1 (cNHE1) and the NHE1 mutants Pro167Gly, Pro168Gly, Pro167Ala, Pro168Ala, Pro178Ala, Pro167Cys, and Pro168Cys. In each lane 100 μg of total protein was loaded. Numbers underneath the lanes indicate the values obtained from densitometric scans of the 110 kDa band relative to wild-type NHE1 for at least three trials.

The Western blot in Figure 3.3 demonstrates that the mutants were all expressed, although Pro167Gly, Pro167Ala and Pro167Cys all have less than one-third of the expression of wild-type NHE1. In addition, the Pro167Gly, Pro167Cys and Pro168Cys mutants had more prominent bands at 95 kDa than at 110 kDa, indicating that a large portion of these mutants are not glycosylated completely, a phenomenon our lab has observed previously [133]. Western blotting of AP-1 cells that do not express NHE1 demonstrated that the antibody is specific for the expressed, tagged protein.

3.2.2 Subcellular localization of mutants and wild-type NHE1

Our lab has noted previously that mutation of some amino acids in NHE1 causes the protein to be targeted to an intracellular location [133]. We therefore examined the targeting of NHE1 by two techniques. First, to obtain a quantitative measurement of the proportion of NHE1 on the plasma membrane, cells were labeled with sulpho-NHS-SS-biotin. Cells were then lysed and solubilized, and the labeled proteins were bound to streptavidin–agarose resin. Equivalent samples of the total cell lysate and the unbound lysate were run on SDS-PAGE gels, and Western blotting with an anti-HA antibody was used to identify NHE1 protein. The fraction of labeled protein that bound to the resin (i.e. the surface NHE1) was not measured directly because of difficulties eluting the bound NHE1 from the resin. This difficulty with elution has been noted previously [142].

Figure 3.4 and Table 3.2 show examples and summaries of the results respectively. Figure 3.4 shows representative Western blots used to determine the amount of NHE1 protein present on the plasma membrane (lane T, total amount of NHE1 protein present in each sample; lane I, the fraction of NHE1 protein that did not bind to the streptavidin–agarose beads). Table 3.2 is a summary of the results in Figure 3.4 and demonstrates that wild-type NHE1, Pro167Ala, Pro168Gly, Pro168Ala, Pro168Cys and Pro178Ala are predominantly present on the plasma membrane. Less cysteineless NHE1 was present on the plasma membrane in comparison with wild-type NHE1. Both the Pro167Gly mutant and the Pro167Cys mutant were mostly present within the cell.

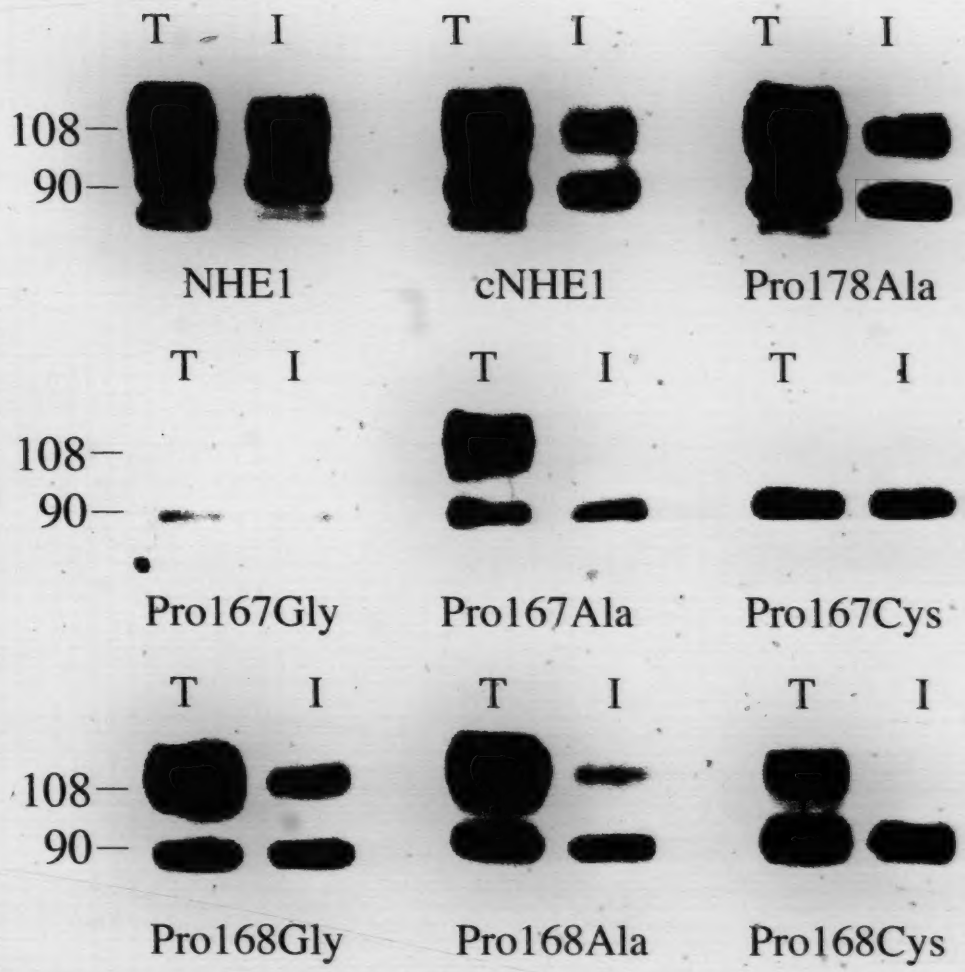

Figure 3.4 Surface expression of Pro167, Pro168, and Pro178 Mutants

Representative Western blots for measuring the subcellular localization of NHE1. Cells were treated with sulpho-NHS-SS-biotin, solubilized, and biotin-labeled proteins were bound to streptavidin-agarose beads as described in Section 2.2.4. A sample of the total cell lysate (T) and an equivalent amount of unbound lysate (I, intracellular) were run on SDS-PAGE. Western blotting with an anti-HA-tag antibody was used to identify the NHE1 protein. Results are shown for wild-type NHE1 (NHE1), cysteineless NHE1 (cNHE1) and the NHE1 mutants Pro167Gly, Pro168Gly, Pro167Ala, Pro168Ala, Pro178Ala, Pro167Cys, and Pro168Cys.

Cell line	Plasma Membrane (% of total)
NHE1	63 ± 4
Pro167Ala	67 ± 3
Pro167Gly	27 ± 12*
Pro168Ala	65± 4
Pro168Gly	57± 5
Pro178Ala	54 ± 3
cNHE1	40 ± 3*
Pro167Cys	23 ± 8*
Pro168Cys	52 ± 2

Table 3.2 Quantification of plasma membrane localization for Pro167, Pro168, and Pro178 mutants

Summary of amount of NHE1 protein localized to the plasma membrane for wild-type NHE1 (NHE1), cysteineless NHE1 (cNHE1), and mutant Na^+/H^+ exchangers. In each case the percent of the total NHE1 protein localized to the plasma membrane is indicated. The results are mean ± standard error for at least 3 determinations. * indicates mutants that have significantly less plasma membrane localization than NHE1 (Mann-Whitney *U*-test, $p < 0.05$).

Immunocytochemistry was used to visualize the localization of NHE1 within the cell. Figure 3.5 shows the immunocytochemical localization of wild-type NHE1 and the proline mutants. Control, untransfected AP-1 cells showed no fluorescence on the plasma membrane or within the cell, consistent with the fact that no HA-tagged NHE1 was expressed. Cells transfected with wild-type NHE1 or the mutants Pro168Gly, Pro168Ala, Pro168Cys, and Pro178Ala showed strong plasma-membrane localization and little intracellular localization. In contrast, in cells transfected with the mutants Pro167Gly, Pro167Ala, and Pro167Cys the bulk of the NHE1 is localized within the cell, and very little NHE1 appears to be localized to the plasma membrane.

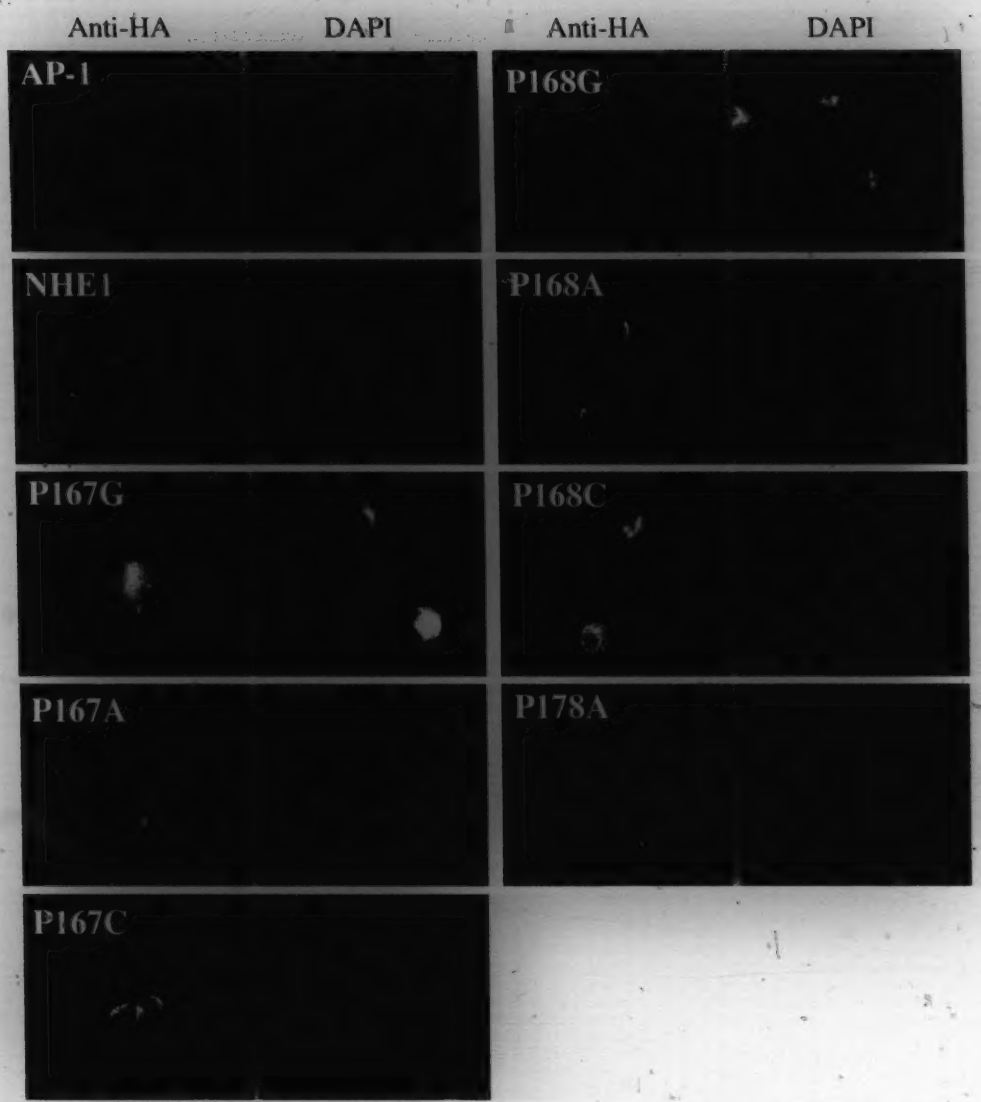

Figure 3.5 Subcellular localization of Pro167, Pro168, and Pro178 Mutants

Immunocytochemical localization of NHE1 in transfected and untransfected cells using anti-HA antibody as described in Section 2.2.5. Results are shown for untransfected AP-1 cells (AP-1) and for AP-1 cells stably transfected with wild-type NHE1 (NHE1) and the NHE1 mutants Pro167Gly, Pro167Ala, Pro167Cys, Pro168Gly, Pro168Ala, Pro168Cys and Pro178Ala. For each cell type the left panel shows the immunofluorescent staining using an anti-HA antibody and the right panel shows nuclear localization by DAPI staining.

3.2.3 Effect of mutations on NHE1 activity

A fluorescent assay was employed to compare the activities of the wild type and mutant exchangers. Figure 3.6 shows examples of the initial rate of recovery after an NH_4Cl-induced acid-load for some of the mutants. Figure 3.7 shows the mean activity (light gray bars) and the activity corrected for expression and plasma membrane targeting (dark gray bars) for wild-type NHE1 and the proline mutants as a percent of the wild-type activity. When AP-1 cells transfected with NHE1 were exposed to Na^+ after being acidified, there was an immediate and rapid increase in intracellular pH at the rate of 3.30 pH units/min. Both cNHE1 and the Pro178Ala mutant displayed essentially the same rate of recovery as wild-type NHE1. In contrast, the mutants Pro167Gly, Pro168Ala, Pro167Cys and Pro168Cys had essentially the same rate of recovery as untransfected AP-1 cells. Although the Pro167Ala and Pro168Gly mutants also had severely decreased rates of recovery, these mutants did retain significantly more activity than untransfected AP-1 cells. Because the Pro167Ala mutant was not expressed to as high a level as wild-type NHE1, the correction for the level of protein and intracellular targeting showed that it possessed 18% of wild-type activity (Figure 3.7; dark gray bars). For Pro167Gly, Pro168Ala, Pro167Cys, Pro168Cys and Pro168Gly, the decreased activity of the mutant proteins could not be accounted for by the decreased expression or intracellular targeting of the mutant exchangers.

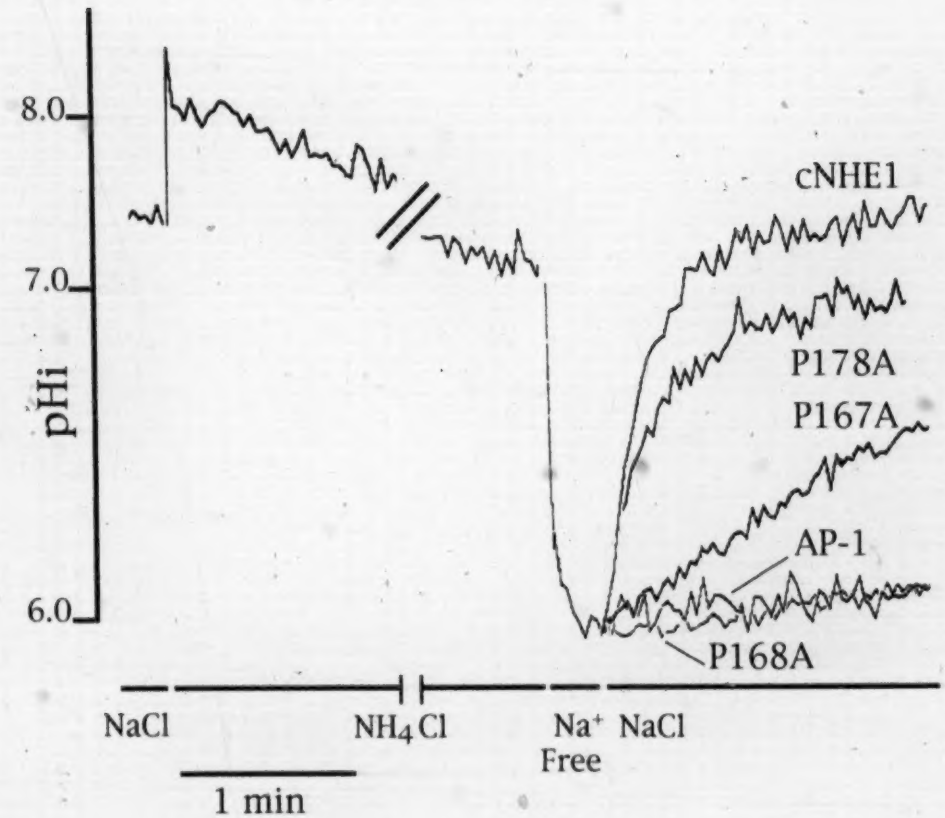

Figure 3.6 Representative rates of recovery from an acid load

Recovery from an NH_4Cl-induced acid load by cells expressing mutant Na^+/H^+ exchangers was measured as described in Section 2.2.6. One example of the entire procedure is shown along with typical rates of recovery for untransfected AP-1 cells (AP-1) and for AP-1 cells stably expressing cysteineless NHE1 (cNHE1) or the NHE1 mutants Pro167Ala, Pro168Ala or Pro178Ala. Results are typical of 10-20 determinations from two independently prepared stable cell lines.

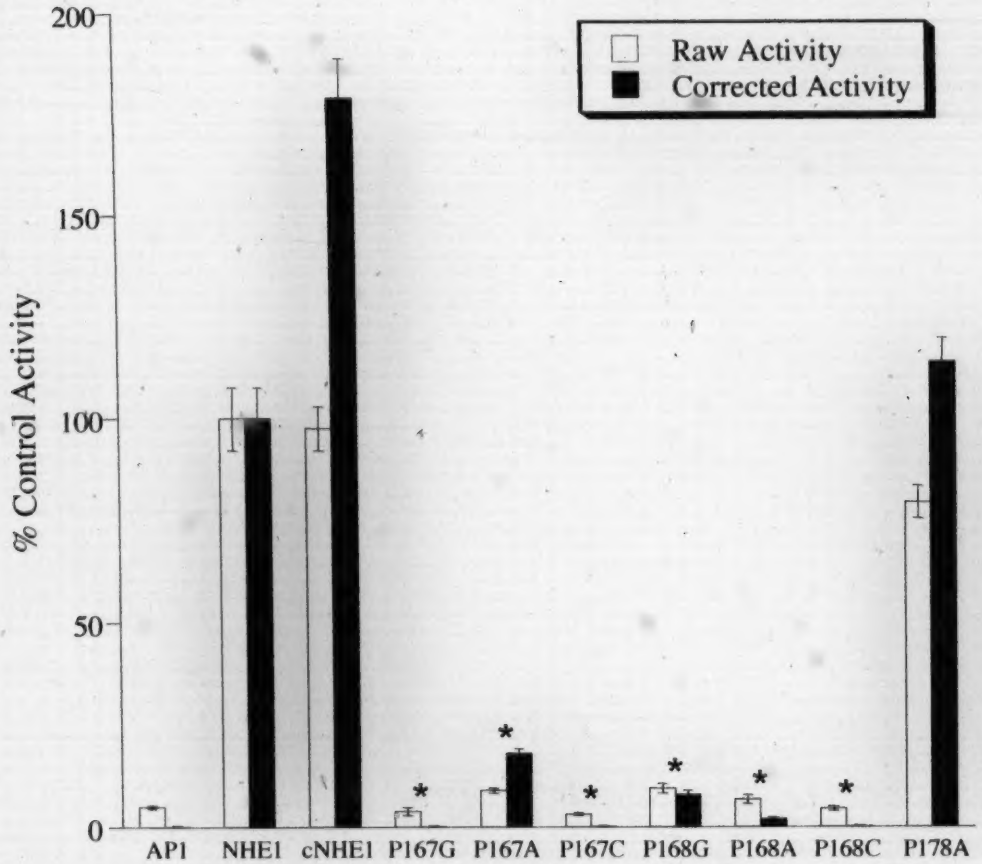

Figure 3.7 Rate of recovery from an acid load by Pro167, Pro168, and Pro178 mutants

Summary of rate of recovery from an acid load by untransfected AP-1 cells (AP1), and AP-1 cells stably transfected with wild-type NHE1 (NHE1), cysteineless NHE1 (cNHE1), and Na^+/H^+ exchanger mutants (Pro167Gly, Pro167Ala, Pro167Cys, Pro168Gly, Pro168Ala, Pro168Cys, and Pro178Ala). The activity of the cells stably transfected with NHE1 was 3.3 pH units/min, and this value was set to 100%. The results are mean ± SE of at least 10 determinations from two independently made stable cell lines. Corrected activity indicates activity normalized for amount of protein expressed and targeted to the plasma membrane after subtraction of the background activity. * indicates mutants with activity that is significantly reduced from wild-type NHE1 activity (Independent-samples t-test, $p < 0.01$).

3.2.4 Secondary-structure prediction of TM IV

It is possible to use computational analysis to predict the secondary structure for a given primary amino acid sequence. Thus, in collaboration with Dr. Joanne Lemieux (Department of Biochemistry, University of Alberta), we analyzed the structure of TM IV using the Sequence Alignment and Modeling (SAM) system [159,160]. Table 3.3 shows the results of a secondary-structure prediction of amino acids 155–177 of TM IV. The native sequence of TM IV, with proline residues 167 and 168 in the middle of the sequence, is predicted to be in an extended-strand conformation with little helical structure. In the region of the proline residues themselves, a coil is predicted instead of an α-helix. After substitution of either Pro167 or Pro168 with alanine, there was a large change in the predicted structure of the TM IV. Substitution of either of the proline residues with an alanine resulted in a helical prediction for most of the TM segment. Substitution of both native proline residues with alanine resulted in the prediction of a helical structure with a higher degree of confidence. Of course, the effect of the proline residues on the conformation of a secondary structure within a protein will vary depending on the local environment of the transmembrane segment [157]. Thus, while the secondary structure prediction may give some insight into the conformation of TM IV, it is clear that this prediction cannot substitute for high-resolution structural data.

Amino acid no.	Amino acid	Native sequence		Both Pro residues substituted with Ala		Pro^{167} substituted with Ala		Pro^{168} substituted with Ala	
		Pss	Prb	Pss	Prb	Pss	Prb	Pss	Prb
155	F	C	0.92	C	0.92	C	0.997	C	0.996
156	L	C	0.79	C	0.77	C	0.767	C	0.761
157	Q	C	0.67	C	0.55	C	0.381	C	0.415
158	S	C	0.62	H	0.61	H	0.513	H	0.423
159	D	C	0.55	H	0.75	H	0.621	H	0.537
160	V	E	0.35	H	0.86	H	0.730	H	0.652
161	F	E	0.49	H	0.89	H	0.745	H	0.686
162	F	E	0.53	H	0.93	H	0.768	H	0.719
163	L	E	0.52	H	0.94	H	0.756	H	0.671
164	F	E	0.50	H	0.93	H	0.678	H	0.609
165	L	E	0.42	H	0.93	H	0.584	H	0.569
166	L	C	0.63	H	0.94	H	0.492	H	0.467
167	**P**	C	0.71	H	0.94	H	0.484	H	0.655
168	**P**	C	0.53	H	0.92	H	0.516	H	0.637
169	I	H	0.34	H	0.89	H	0.532	H	0.619
170	I	E	0.45	H	0.84	H	0.467	H	0.547
171	L	C	0.35	H	0.79	H	0.411	H	0.491
172	D	C	0.51	H	0.64	H	0.353	H	0.425
173	A	C	0.60	H	0.51	T	0.286	H	0.316
174	G	C	0.69	C	0.66	T	0.353	T	0.356
175	Y	C	0.66	C	0.67	C	0.362	C	0.349
176	F	C	0.74	C	0.75	C	0.701	C	0.694
177	L	C	0.98	C	0.98	C	0.998	C	0.998

Table 3.3 Secondary structure analysis of transmembrane segment IV of NHE1

Amino acids 155-177 were analyzed by the sequence alignment and modeling system using the Markov model for homology sequence alignment to assist with secondary structure prediction using the DSSP program [159, 160]. The proline residues of interest are shown in bold. Pss, secondary-structure prediction of coil (C), extended strand (E), α-helix (H) or hydrogen-bonded turn (T); Prb, probability of the prediction.

3.3 Discussion

TM IV of NHE1 contains several residues that are important for ion transport and inhibitor binding [130-132]. Although their effects on membrane protein structure can vary, proline residues are required for expression and targeting to the plasma membrane in a number of membrane proteins [157,161-163]. We examined the importance of the three conserved proline residues Pro167, Pro168 and Pro178 in TM IV. Our results demonstrated that both Pro167 and Pro168 were critical for normal NHE1 activity, while Pro178 was not essential. In addition, Pro167 was critical for expression and membrane targeting of NHE1, while mutation of Pro168 did not influence targeting and had lesser effects on expression levels. As shown by our surface processing results, for both the Pro167Gly and the Pro167Cys mutants a large fraction of the NHE1 protein was retained within the cell. All of the mutations of Pro167 also caused significantly decreased levels of NHE1 protein expression.

Na^+/H^+ exchange activity was abolished by the mutations Pro167Gly and Pro167Cys, and the Pro167Ala mutant retained only 18% of the wild-type activity after correction for expression and surface processing. All of the mutants of Pro168 also had severely impaired activity, and in this case correction for expression and targeting could not account for the decreased activity of these mutants. Thus, both Pro167 and Pro168 are critical for NHE1 activity, but

Pro167 is also required for normal expression and membrane targeting of the exchanger. It is worth noting that, even though both proline residues are conserved in the mammalian NHE isoforms, Pro168 is not conserved in the yeast NHE, NHX-4 [153]. Our finding that mutation of Pro168 has lesser effects on NHE1 expression is consistent with this observation.

Why Pro167 affects the targeting and expression levels of NHE1 is not clear at present. It may be that Pro167 specifically affects TM IV conformation, causing a specific alteration in structure that does not occur at amino acids 168 and 178. The decreased expression levels of Pro167 mutants could be accounted for by protein quality control systems, consisting of chaperones and proteases that degrade mutated proteins, affecting folding and targeting [164,165]. Pro167 may be important for the conformation of helix IV or for helix–helix interactions that affect conformation. This suggestion is similar to the case of bacteriorhodopsin, where Pro50 and Pro91 contribute to the folding of the protein [166].

Several results suggest that the functional consequences of mutating Pro167 and Pro168 are probably due to specific effects on TM IV of NHE1 rather than a general effect that occurs in all proteins with mutation of proline residues. First, the effects of mutating Pro167 and Pro168 are specific to these particular proline residues in TM IV, because Pro178 could be mutated to alanine without affecting NHE1 activity. Second, it was shown previously that the mutation Pro239Ala in TM VI of NHE1 also had no effect on NHE activity [133]. Third,

proline residues in transmembrane helices of other membrane proteins can be mutated and do not always affect protein function [162,167,168].

Our findings of important functional roles for prolines 167 and 168 are in keeping with the results of previous studies on some other integral membrane proteins. Proline residues are frequently found in the transmembrane α-helices of multi-spanning integral membrane proteins, and over the past two decades the importance of transmembrane prolines has been confirmed in numerous integral membrane proteins [169,170]. Mutation of any of the proline residues in the transmembrane helices of the Ca^{2+}-ATPase of the sarcoplasmic reticulum decreased the activity of the transporter [171]. In this protein, mutation of Pro308 or Pro803 reduced affinity for Ca^{2+}, while mutation of Pro312 abolished Ca^{2+} transport [171]. Similarly, both of the proline residues in the transmembrane region of the 5-HT_3-receptor are necessary for the function of this protein [172]. In the human glucose transporter GLUT1 the mutation of proline residues in TM X to either glutamine or isoleucine caused a significant decrease in 2-deoxy-D-glucose uptake [163,173]. Finally, several proline residues are required for normal function of the lactose permease of *Escherichia coli*. Replacement of Pro28 in lactose permease with glycine or alanine abolishes lactose transport, and replacement of Pro280 with glutamine, leucine, or methionine causes defective lactose transport [167,174].

There are several mechanisms by which alterations in Pro167 and Pro168 could affect the conformation of NHE1. Proline residues allow free backbone carbonyls at the *i*-3 and *i*-4 position of α-helices, and their presence causes a steric clash between the proline ring and the backbone carbonyl group at position *i*-4 [169,175]. This induces flexibility in the region and can cause kinks in TM helices [168]. A recent analysis of the distribution of proline residues within TM helices of proteins with known structure revealed that proline residues occur with a relatively high frequency in the middle of TM helices [175]. This induces a hinge region prior to the proline residue [175]. In this analysis of proline residues within TM helices, the effect of adjacent proline residues was not examined, but these would presumably cause even greater alterations in the structure of a TM segment. Thus, changes to this type of unusual double proline structure would probably influence the structure of the Na^+/H^+ exchanger, in addition to affecting its activity. Our prediction of the structure of TM IV (Table 3.3) agrees with the suggestion that Pro167 and Pro168 significantly affect the structure of this segment. Substitution of alanine for either Pro167 or Pro168 resulted in marked changes in the prediction of the structure of TM IV. This result agrees with our experiments showing that other residues were unable to substitute effectively for a proline residue regardless of their character. Glycine, alanine and cysteine residues vary in their α-helical propensity and flexibility [176,177]. However, neither a glycine, alanine nor cysteine residue could effectively substitute for the

proline residue at either position 167 or 168. Thus, the tendency to either be flexible or break an α-helix was not the critical determinant for NHE1 function. An alanine residue was capable of substituting for Pro167 to a small degree. It is not clear why an alanine residue allowed partial NHE1 activity to remain. It may be that packing constraints allowed the retention of an appropriate conformation only in the presence of the alanine residue. Further studies on the conformation of this transmembrane segment are necessary to understand how these small mutations could have such major effects on the expression and targeting of NHE1.

In conclusion, both Pro167 and Pro168 in TM IV of NHE1 are required for normal NHE1 activity, while Pro178 is not essential. In addition, mutation of Pro167 causes decreased expression and membrane targeting of the exchanger, suggesting that this residue may be important for NHE1 to be properly folded and targeted. Thus, both Pro167 and Pro168 are strictly required for NHE1 function and may play critical roles in the structure of TM IV of the Na^+/H^+ exchanger.

CHAPTER FOUR:

Structural and Functional Characterization of TM IV of NHE1

A version of this chapter also appears in The Journal of Biological Chemistry (2005) **280**, 17863-17872

Emily R. Slepkov, Jan K. Rainey, Xiuju Li, Yongsheng Liu, Florence Cheng, Darrin A. Lindhout, Brian D. Sykes, and Larry Fliegel

4.1 Introduction

Although the activity of NHE1 has been extensively examined in many tissues, only recently is information starting to be elucidated on how this antiporter actually binds and transports Na^+ ions and protons. While transmembrane segment four appears to be involved in the ion transport and inhibitor binding properties of NHE1, the specific amino acids in TM IV that line the ion-transport pore remain elusive [130-132,140]. Unfortunately, membrane proteins such as NHE1 are notoriously difficult to express, purify, and crystallize. Thus, other methods have been developed to probe their three-dimensional structure without the necessity for overexpression and purification. One such method, cysteine-scanning mutagenesis, takes advantage of the fact that the sulfhydryl moiety is the most reactive functional group in a protein [178,179]. Cysteine-scanning mutagenesis involves mutating all native cysteine residues in a protein to an unreactive amino acid such as serine, and then individually introducing cysteine residues at each position in a putative TM segment in the cysteineless background. The single-cysteine mutants are then expressed, and the reaction of the substituted cysteine with small, charged, sulfhydryl-specific reagents is assessed. In many cases, the reaction of a reagent with the cysteine residue results in an irreversible alteration in the function of the protein [180]. This method often provides a distinct pattern of inhibition, with residues that lie

on one face of an α-helix being susceptible to inhibition by sulfhydryl reagents when they are mutated to cysteine [181-183]. Figure 4.1 depicts the molecular structures of sulfhydryl-reactive reagents commonly used in pore-lining studies: *p*-chloromercuribenzosulfonate (pCMBS), a membrane impermeant, hydrophilic sulfhydryl-reactive agent; 2-aminoethylmethane thiosulfonate (MTSEA), a membrane permeant, partially charged primary amine; 2-trimethylammonioethylmethane thiosulfonate (MTSET), a membrane impermeant, permanently charged quaternary amine; and 2-sulfonatoethylmethane thiosulfonate (MTSES), a membrane impermeant, permanently charged sulfonate [180,184,185]. Cysteine-scanning mutagenesis has been used to determine pore-lining residues in numerous membrane proteins [185,186], including the Na^+/Ca^{2+} exchanger [187,188], the acetylcholine receptor [181], the glucose transporter Glut1 [189-192], the anion exchanger AE1 [183], and the lactose permease of *E. coli* [182,193,194].

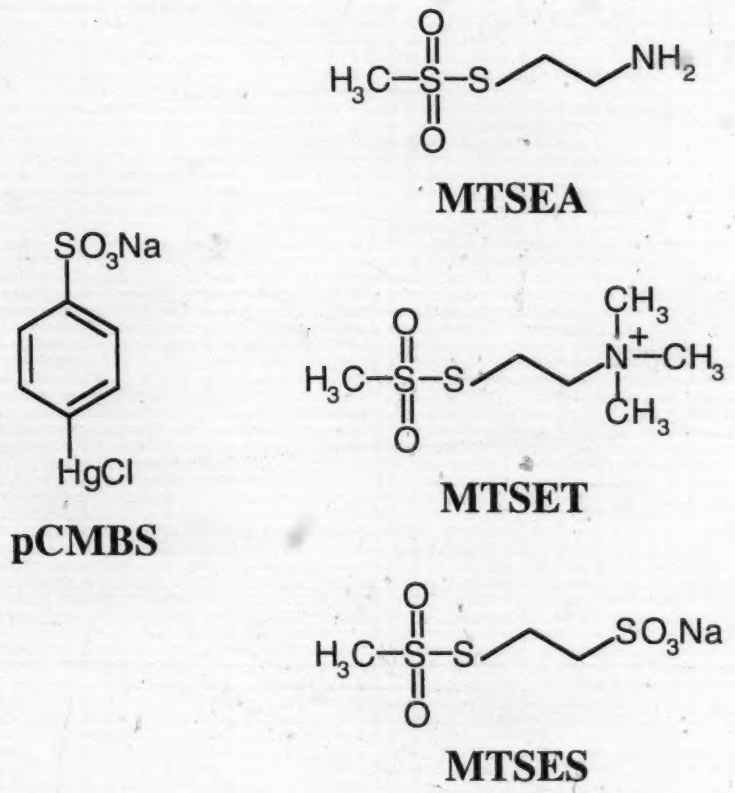

Figure 4.1 Molecular structures of sulfhydryl-reactive reagents

Structures of sulfhydryl-reactive reagents for use in determining pore-lining residues are shown. pCMBS, *p*-chloromercuribenzosulfonate; MTSEA, 2-aminoethylmethane thiosulfonate; MTSET, 2-trimethylammonioethylmethane thiosulfonate; MTSES, 2-sulfonatoethylmethane thiosulfonate.

The use of cysteine-scanning mutagenesis involves several assumptions [181]. First, it is assumed that residues lining the ion-transport pore constitute a portion of the water-accessible surface of the protein. Second, it is assumed that if the introduced cysteines line the ion-transport pore they will be accessible to sufficiently small, charged reagents. Third, it is assumed that the addition of a charged group to a pore-lining residue will alter the activity of the transporter. Last, it is assumed that residues in the membrane-spanning segments that are not exposed in the pore will remain inaccessible to charged, lipophobic reagents.

Cysteine-scanning mutagenesis has proven to be extremely useful for examining the three-dimensional structure of membrane proteins. However, there are some shortcomings to this method. For example, if a large number of cysteine-substituted mutants of a membrane protein cannot be expressed or are not active, this will limit the structural conclusions that can be drawn [195]. A second shortcoming to this method involves the interpretation of negative results. For mutants in which activity is not affected by treatment with sulfhydryl-reactive reagents, the lack of an effect could be due to either toleration of the modification or a genuine lack of reaction due to inaccessibility [180,186]. Unfortunately, experiments that rely on an altered activity cannot distinguish between these two categories of negative results. Finally, the failure of a cysteine residue to react could be due to factors other than the true accessibility of the cysteine. For example, reactivity depends on the acid dissociation of the Cys-SH, the steric

constraints on formation of an activated complex, and, for charged reagents, the electric field along the path to the residue [180].

Despite the shortcomings that are sometimes associated with the use of cysteine-scanning mutagenesis the structural information obtained using this technique shows very high fidelity to known crystal structures of membrane proteins. For example, in the recent crystal structure of the *E. coli* Na^+/H^+ antiporter, NhaA, the residue Asp133 was located at the middle of the plane of the lipid bilayer, facing the pore of the protein, a finding that is consistent with previous cysteine accessibility analysis [107,196]. In addition, in the 4 Å resolution electron microscopy model of the acetylcholine receptor all residues that were found to be exposed in the channel lumen using cysteine accessibility were indeed facing the lumen of the pore [197,198]. Finally, the results of biochemical studies including cysteine-scanning mutagenesis experiments were used to create a three-dimensional structural model of the lactose permease of *E. coli*, and the recently determined crystal structure of this protein is highly consistent with the proposed model [158,193,199].

In this study we used cysteine-scanning mutagenesis to examine both functional and structural aspects of TM IV of NHE1. This technique allowed us to not only identify numerous amino acids in TM IV that are important for NHE1 function, but also to identify Phe161 as a pore-lining residue in TM IV. In addition, based on the structure of TM IV in a membrane-mimetic solvent we

chose to further investigate the importance of two aspartic acid residues in TM IV. Based on our results from mutating each of these aspartic acid residues to glutamic acid, asparagine, or glutamine we further suggest that Asp159 may be a pore-lining residue.

4.2 Results

4.2.1 Expression of NHE1 Mutants

We used the substituted-cysteine accessibility method to identify pore-lining amino acids in TM IV of the Na^+/H^+ exchanger. To begin, we created a Na^+/H^+ exchanger that was devoid of cysteine residues (cysteineless NHE1; cNHE1). Subsequently, each residue in TM IV of cNHE1 was individually mutated to a cysteine, resulting in the creation of 23 single-cysteine mutants. These mutants were expressed in AP-1 cells, a cell line that is deficient in Na^+/H^+ exchange activity.

Figure 4.2 illustrates a Western blot of total cell extracts from AP-1 cells stably expressing the single-cysteine mutants. Both the mutant and wild-type exchangers displayed the same pattern of immunoreactive bands, with a larger band at 110 kDa that represents the glycosylated form of the mature Na^+/H^+ exchanger and a smaller band at 95 kDa that represents an immature form of the exchanger that is not fully glycosylated [108]. Both wild-type NHE1 and cysteineless NHE1 showed strong immunoreactive bands at 110 kDa, representing mature NHE1, and a weaker band at 95 kDa, representing immature NHE1.

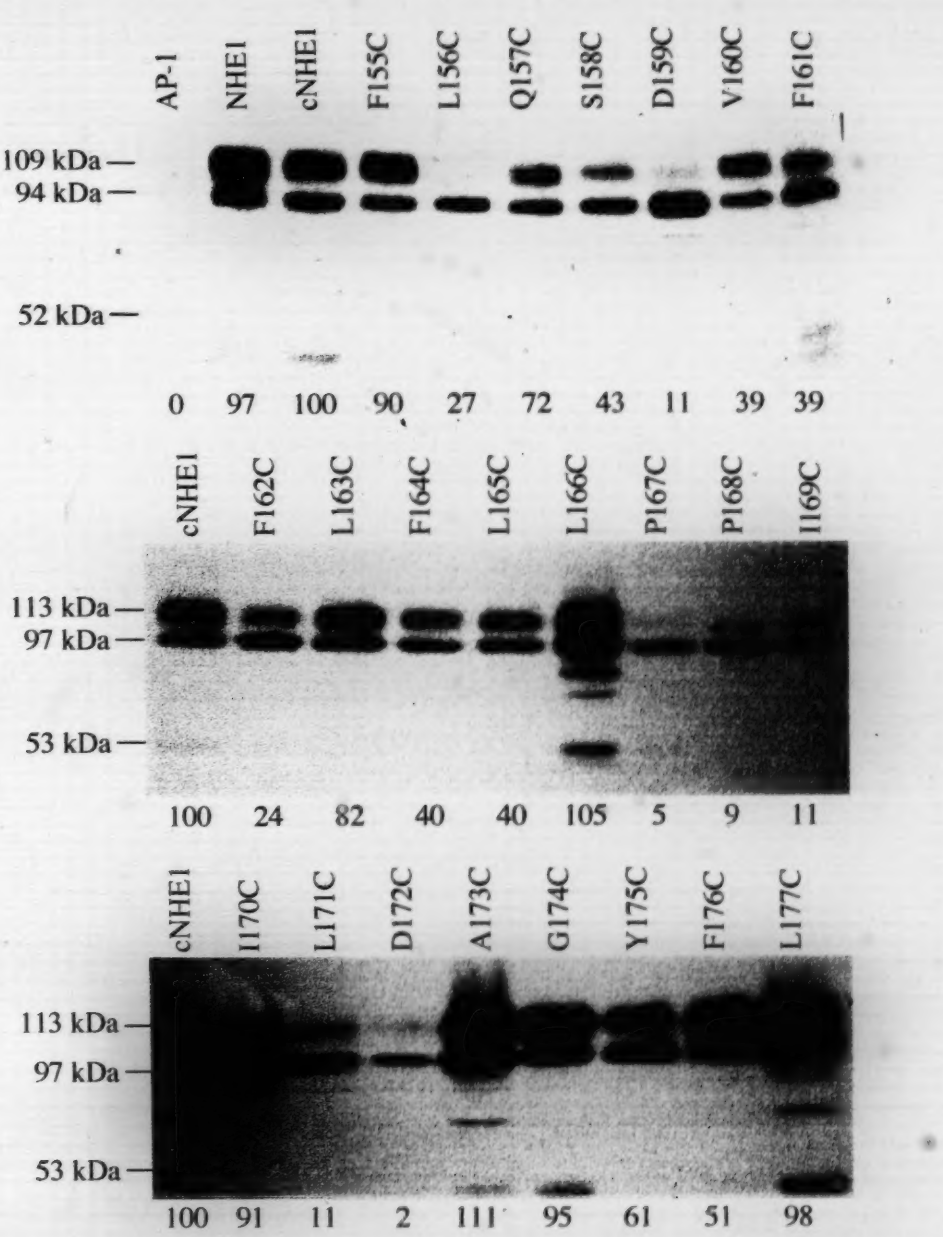

Figure 4.2 Western blot analysis of cells expressing single-cysteine mutants

Representative Western blots of cell extracts prepared from control (AP-1) cells and from cells stably transfected with cDNA coding for HA-tagged wild-type NHE1 (NHE1), cysteineless NHE1 (cNHE1), and single-cysteine NHE1 mutants. 100 μg of total protein was loaded in each lane. Results are typical of at least two experiments. Numbers below the lanes indicate the values obtained from densitometric scans of the 110 kDa band relative to cNHE1.

The amount of mature 110 kDa NHE1 relative to cNHE1 is quantified below each lane in Figure 4.2. All of the mutants were expressed, and several mutants have relatively normal levels of expression relative to cNHE1, including F155C, Q157C, S158C, L163C, L166C, I170C, A173C, G174C, Y175C, F176C, and L177C. On the other hand, there were also numerous mutants that were expressed but that had much less of the mature NHE1. These mutants included L156C, D159C, V160C, F161C, F162C, F164C, L165C, P167C, P168C, I169C, L171C, and D172C. Of the mutants with impaired expression, many had a high proportion of the immature 95 kDa form of the exchanger, including L156C, D159C, F161C, F162C, P167C, P168C, I169C, and L171C.

4.2.2 Subcellular localization of single-cysteine mutants

Our earlier studies found that mutation of some amino acids in the Na^+/H^+ exchanger can cause the protein to be targeted to an intracellular location [133,140]. We therefore used a surface-processing assay to quantify the amount of NHE1 targeted to the plasma membrane within AP-1 cells. Cells were treated with sulpho-NHS-SS-biotin and then lysed and solubilized, and labeled proteins were bound to streptavidin-agarose beads. An equal amount of the total cell lysate and unbound lysate was separated by size using SDS-PAGE followed by Western blotting with anti-HA antibody to identify tagged NHE1 protein.

Figure 4.3 illustrates examples of the results, and Table 4.1 summarizes the results quantitatively. In Figure 4.3, the total lanes (*T*) represent the total cell lysate, and the intracellular lanes (*I*) illustrate the fraction of the Na^+/H^+ exchanger that did not bind to the streptavidin-agarose beads. Approximately 50% of the cysteineless NHE1 protein was present on the plasma membrane, and most of the mutant exchanger proteins did not have significantly less plasma membrane targeting than cNHE1. However, two Na^+/H^+ exchanger mutants, D159C and D172C, did have significantly reduced plasma membrane targeting as compared to cNHE1.

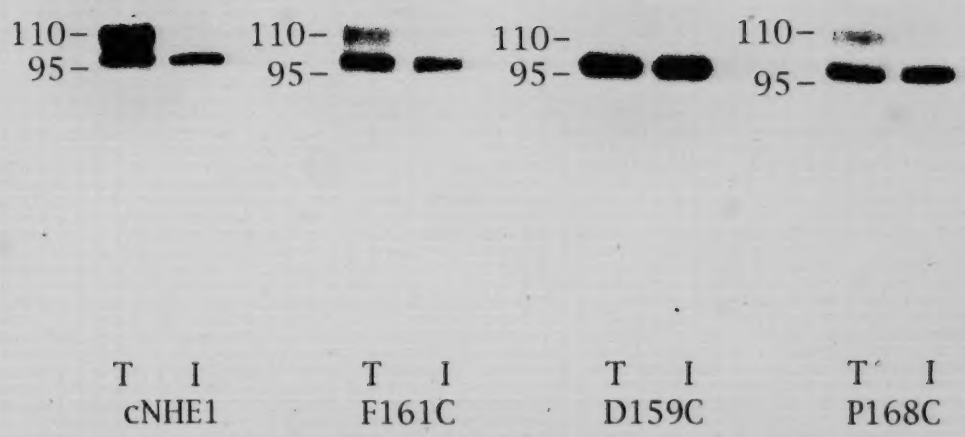

Figure 4.3 Example Western blots for determination of plasma membrane targeting of single-cysteine mutants

Sulpho-NHS-SS-biotin-treated cells were lysed, and solubilized proteins were bound to streptavidin-agarose beads as described in Section 2.2.4. Equivalent samples of total cell lysate (T) and unbound lysate (I, intracellular) were run on SDS-PAGE. Western blotting with anti-HA-tag antibody identified the NHE1 protein. cNHE1, cysteineless NHE1 (cNHE1); representative mutants are Phe161Cys, Asp159Cys, and Pro168Cys.

Cell line	Plasma Membrane (% of total)
NHE1	77 ± 5
cNHE1	51 ± 7
F155C	69 ± 5
L156C	48 ± 1
Q157C	61 ± 2
S158C	65 ± 2
D159C	17 ± 4*
V160C	55 ± 4
F161C	42 ± 3
F162C	27 ± 8
L163C	48 ± 5
F164C	61 ± 1
L165C	48 ± 9
L166C	38 ± 4
P167C	28 ± 10
P168C	47 ± 5
I169C	37 ± 7
I170C	36 ± 2
L171C	64 ± 4
D172C	15 ± 1*
A173C	42 ± 6
G174C	53 ± 10
Y175C	47 ± 2
F176C	54 ± 4
L177C	54 ± 7

Table 4.1 Summary of plasma membrane localization for single-cysteine mutants

Plasma membrane targeting of the Na^+/H^+ exchanger in AP-1 cells transfected with wild-type NHE1 (NHE1), cysteineless NHE1 (cNHE1), and the single-cysteine mutants was determined as described in Section 2.2.4. The percent of the total NHE1 protein localized to the plasma membrane is indicated. The results are mean ± standard error for at least 3 determinations. * indicates significantly reduced plasma membrane targeting in comparison to cNHE1 (Mann-Whitney *U*-test, $p < 0.05$).

4.2.3 Activity of NHE1 single-cysteine mutants

Before the accessibility of the introduced cysteine residues to sulfhydryl-reactive reagents could be assessed, initial experiments were required to examine whether the single-cysteine mutants were active. Surprisingly, we found that TM IV is exceptionally sensitive to mutation. Figure 4.4 shows both the uncorrected activity (black bars) and the activity corrected for surface processing (gray bars) relative to cNHE1 for the TM IV single-cysteine mutants. Substitution of any of the amino acids in TM IV with cysteine results in a significant reduction in the measurable activity of the exchanger ($p < 0.05$). Correcting the activity for plasma membrane targeting did not greatly affect the activity results for the single-cysteine mutants. For example, even after correction for surface processing, the activity of the mutants Asp159Cys and Asp172Cys that had significantly decreased plasma membrane targeting (Table 4.1) remained at less than half of the activity of cNHE1 (Figure 4.4, gray bars). In particular, the mutants Phe155Cys, Leu156Cys, Ser158Cys, Asp159Cys, Phe162Cys, Phe164Cys, Pro167Cys, Pro168Cys, Asp172Cys, Tyr175Cys, and Phe176Cys retained less than 20% of cNHE1 activity. Thus, these single-cysteine mutants were not used in subsequent cysteine-accessibility studies because their activity was deemed too low to be reliably further inhibited.

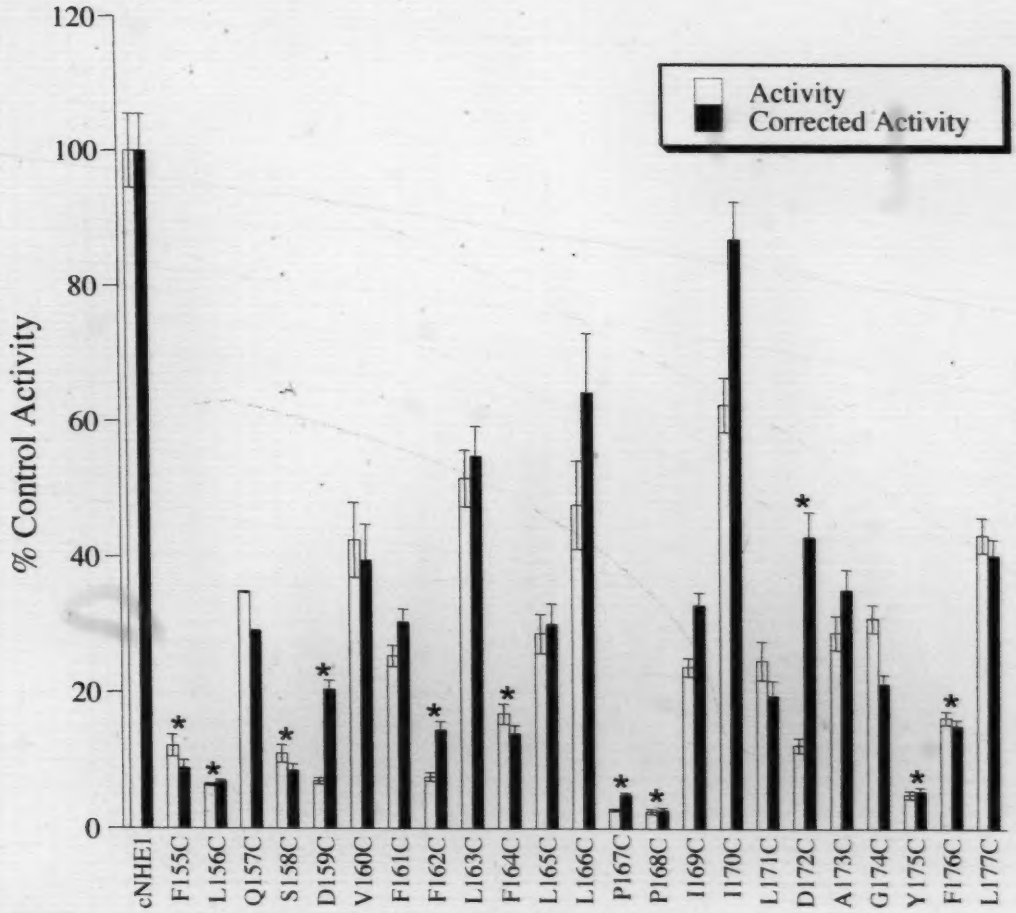

Figure 4.4 Activity of single-cysteine NHE1 mutants

Summary of the rate of recovery from an acid load by AP-1 cells stably transfected with cysteineless NHE1 (cNHE1), and the single-cysteine Na^+/H^+ exchanger mutants (Phe155 to Leu177 individually changed to Cys). The rate of recovery from a transient acid load of cells stably transfected with cNHE1 was 3.2 pH units/min, and this value was set to 100%. The results are mean ± SE for at least 10 determinations from two independently made stable cell lines. Results are shown for uncorrected activity (light gray) and activity corrected for surface processing (dark gray). * indicates mutants with uncorrected activity that is less than 20% of cNHE1.

4.2.4 Cysteine-accessibility analysis of NHE1 mutants

We examined the sensitivity of the active single-cysteine mutants of the Na^+/H^+ exchanger to sulfhydryl-reactive reagents. Initial experiments using the reagents MTSEA and pCMBS were unsuccessful because MTSEA caused the AP-1 cells to detach from the glass coverslip, and pCMBS inhibited cysteineless NHE1 (Figure 4.5). Fortunately, a ten minute incubation with either 10 mM MTSET or 10 mM MTSES did not inhibit cNHE1. Thus, we used these reagents to determine the accessibility of the introduced cysteine residues by comparing the activity of the single-cysteine mutants before and after treatment with these reagents.

Figure 4.6 shows the effect of MTSET (light gray bars) or MTSES (dark gray bars) treatment on the activity of cNHE1 and the single-cysteine mutants. Of the twelve active single-cysteine mutants only F161C was significantly inhibited by treatment the sulfhydryl reactive reagents. Specifically, incubation of the F161C mutant with 10 mM MTSET resulted in a 60% decrease in activity, and incubation with 10 mM MTSES resulted in an 80% decrease in activity.

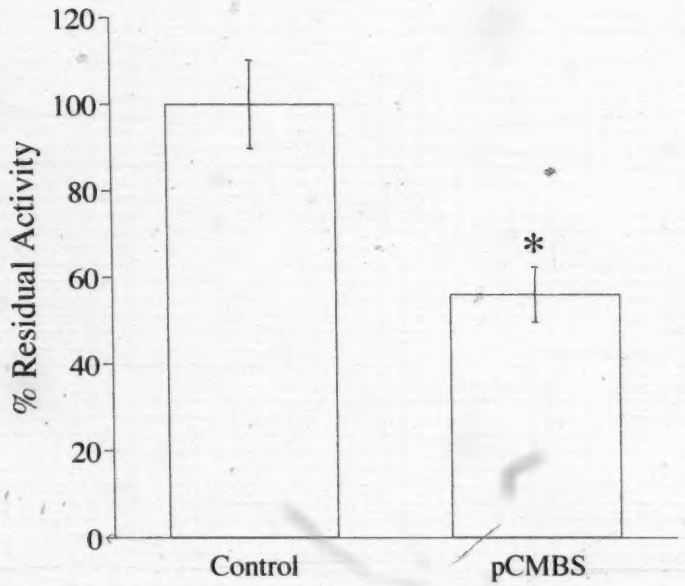

Figure 4.5 Effect of pCMBS on cysteineless NHE1 activity

The rate of recovery from an acid load by AP-1 cells stably transfected with cysteineless NHE1 was measured after treatment with either Na^+-free buffer (Control) or 0.2 mM pCMBS in Na^+-free buffer (pCMBS) for 2 minutes. The rate of recovery of the control cells was 4.3 pH units/min, and this value was set to 100%. The results are mean ± SE for at least 12 determinations. * indicates a significantly lower rate of recovery compared to control cells (Mann-Whitney *U* test; $p < 0.05$).

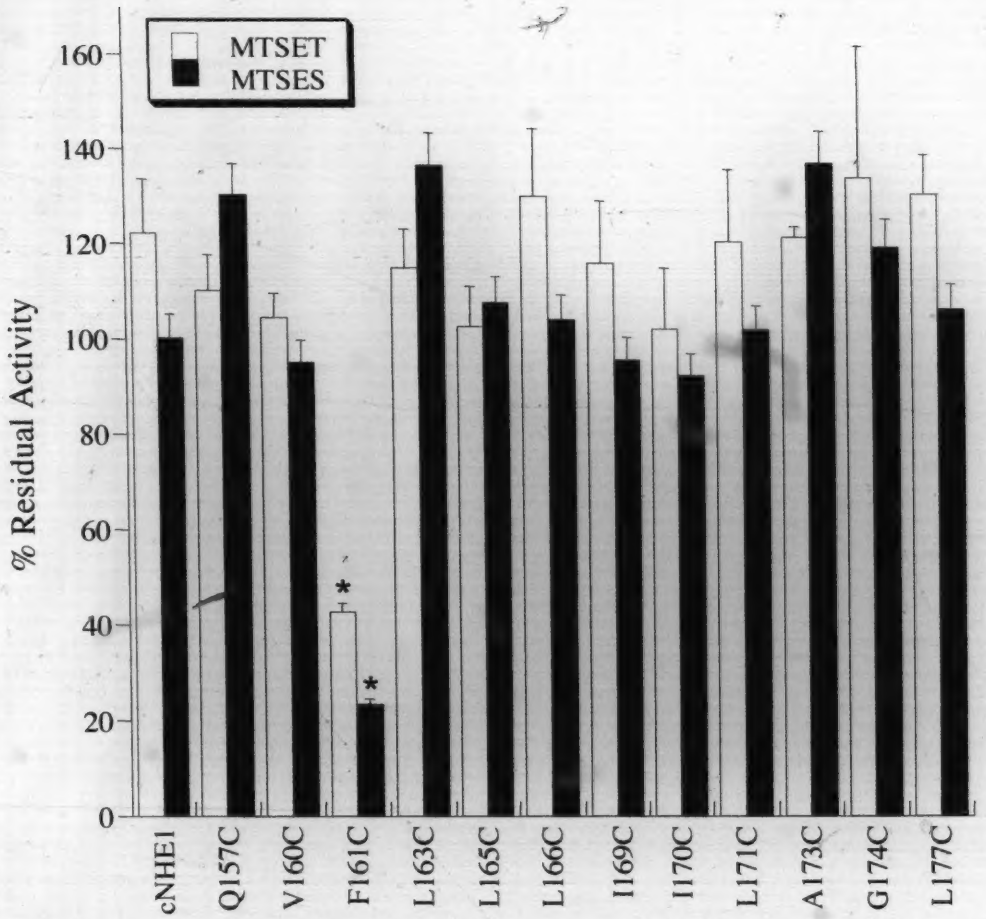

Figure 4.6 Effect of MTSET and MTSES on activity of cNHE1 and single-cysteine NHE1 mutants

Na^+/H^+ exchange activity was measured after transient induction with an acid load as described in Section 2.2.7. Cells were subsequently treated with 10 mM MTSET (light gray bars) or 10 mM MTSES (dark gray bars) for 10 minutes before a second transient acidification and recovery. Illustrated results represent the % activity remaining after the second acid load in comparison to the activity after the first acid load. The results are mean ± SE for at least 4 determinations. * indicates that the second recovery was significantly lower than the first (Mann-Whitney *U* test; $p < 0.01$).

4.2.5 Solution structure of TM IV

Our laboratory has expressed and purified TM IV, and determined its structure in a membrane mimetic environment in collaboration with the laboratory of Dr. Brian Sykes. While I was not directly involved in this aspect of the project, this structure is extremely relevant to my research. Accordingly, I will present the general results of this structural study here but refer the reader to Slepkov *et al.* 2005 [200] for a detailed description of the methods and results associated with this structure.

The structure of TM IV in D_3OH:$CDCl_3$:H_2O at 30 °C is shown in Figure 4.7, where Panel A is a schematic of TM IV illustrating convergent structured stretches and Panel B is a stick diagram representation of TM IV. From this NMR structure it is clear that TM IV does not resemble a canonical transmembrane α-helix. In fact, TM IV does not, as a whole, assume a single conformation. Rather, sections within TM IV have distinct structural characteristics. Specifically, TM IV is composed of three sections of four to nine residues that converge structurally: Asp159-Leu163 form a series of β-turns; Leu165-Pro168 has an extended structure; and Ile169-Pre176 form an α-helix. These three structured regions rotate quite freely with respect to each other at swivel points that are located at Phe164 and Pro168/Ile169 (Figure 4.7, Panel A, *black*). The N- and C-termini of the segment are flexible and are represented by dashed lines in Figure 4.7.

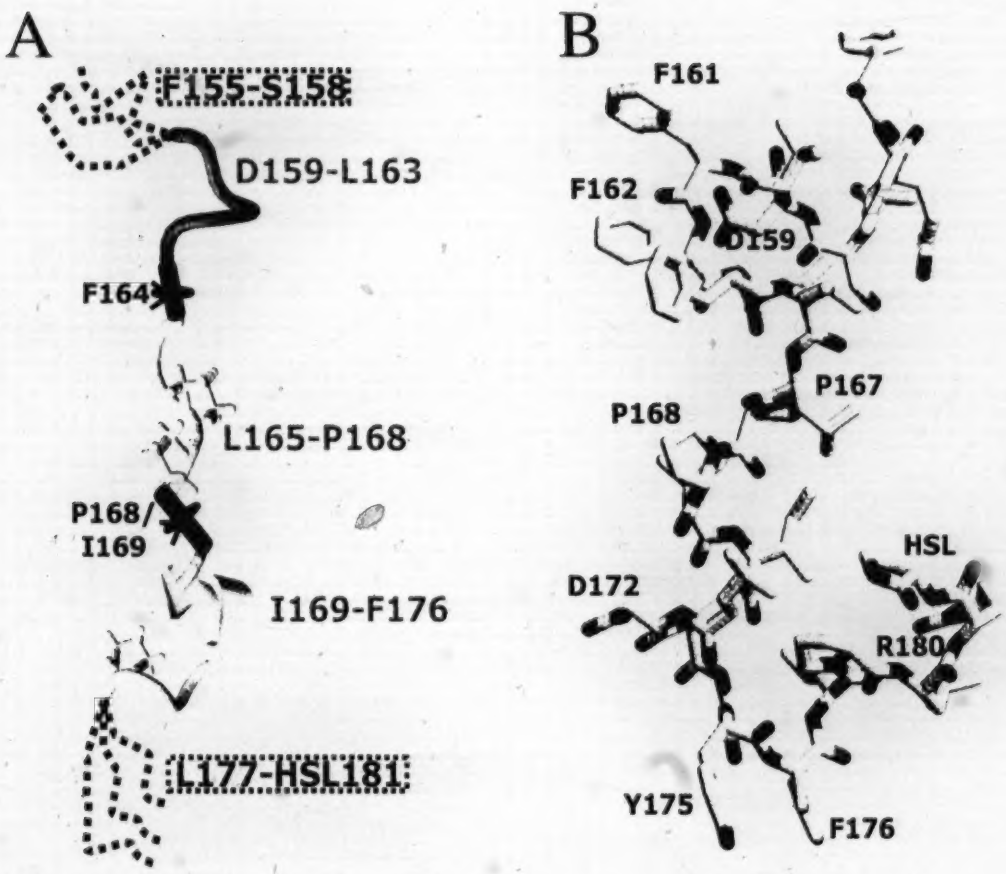

Figure 4.7 Structure of the TM IV peptide in CD_3OH:$CDCl_3$:H_2O at 30 °C

A) Schematic illustrating convergent stretches (gray) of residues D159-L163, L165-P168, and I169-F176 in relation to pivot residues F164 and P168/I169 (black). The flexible N- and C-termini are represented by dashed lines. Note that only the proline side chains are drawn. B) Stick diagram of a single conformational structure (*i.e.* the flexible linkers and termini have assumed a discrete configuration), demonstrating the overall extended nature of the TM IV peptide. Asp159 lies on the same face of the structure as Phe161.

Within the structure of TM IV the side chain of the pore-lining residue Phe161 is fully exposed. Unfortunately, because the structurally convergent sections can rotate with respect to each other, it is not possible to determine which other residues face the pore C-terminal of the Phe164 swivel point. However, within the convergent stretch of Asp159-Leu163 the Asp159 side chain is uniformly observed on the same face as Phe161. Thus, the Asp159 side chain likely protrudes into the pore.

4.2.6 Further characterization of Phe161, Asp159, and Asp172

Based on our knowledge that Phe161 lines the ion transport pore of NHE1 and that Asp159 faces the same way as Phe161, we decided to further investigate the importance of these pore-lining residues. In addition, we introduced new mutations at Asp172, a residue that inactivated the exchanger when mutated to cysteine, to investigate whether this residue might be pore-lining as well. Specifically, in the wild-type NHE1 background we mutated Phe161 to alanine, leucine, and lysine, and we mutated each aspartic acid residue to glutamic acid, asparagine, and glutamine.

Figure 4.8 is a Western blot of total cell extracts from AP-1 cells stably expressing the mutants of Phe161, Asp159, and Asp172. The mutant and wild-type exchangers displayed the same pattern of immunoreactive bands, with a larger band at 110 kDa that represents the glycosylated form of the mature Na^+/H^+ exchanger and a smaller band at 95 kDa that represents an immature form of the exchanger that is not fully glycosylated [108]. The amount of mature 110 kDa NHE1 relative to the wild type is quantified below each lane in Figure 4.8. All of the mutants were expressed as mostly mature NHE1, and only the Phe161Lys and Asp172Glu mutants had substantially decreased expression of mature NHE1. We also studied the plasma membrane targeting of the Phe161, Asp159, and Asp172 mutants. Table 4.2 quantitatively summarizes the results of our surface processing studies. The majority of the wild-type NHE1 protein was present on the plasma membrane, and most of the mutant exchanger proteins did not have significantly less plasma membrane targeting than wild-type NHE1. However, three of the Na^+/H^+ exchanger mutants, Phe161Ala, Phe161Lys, and Asp172Asn, did have significantly reduced plasma membrane targeting as compared to wild-type NHE1.

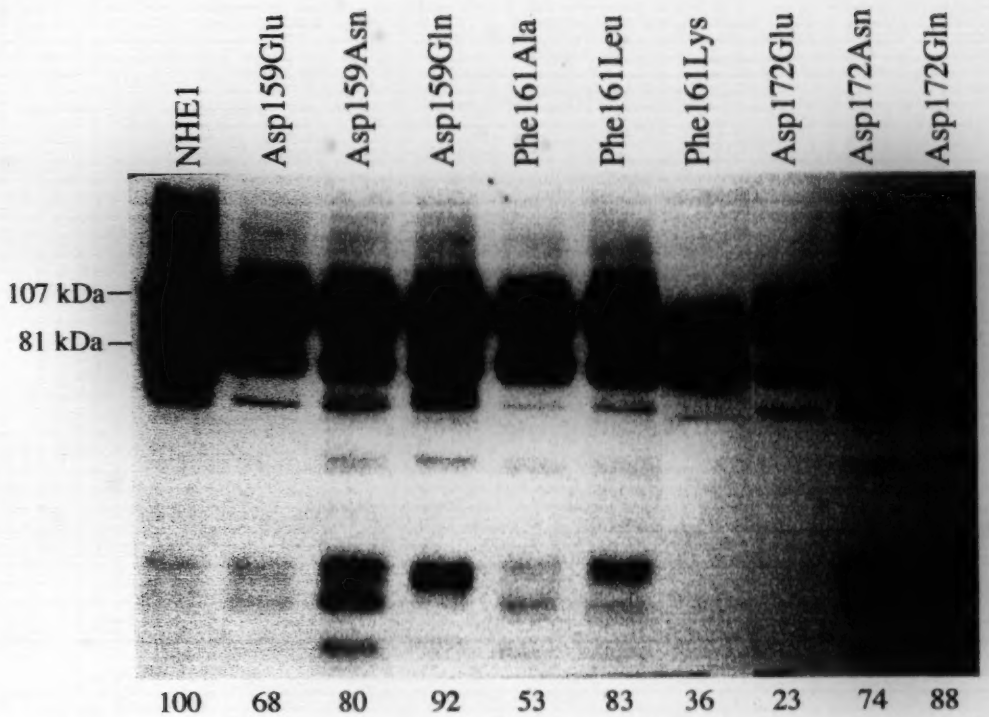

Figure 4.8 Western blot analysis of cells stably expressing Asp159, Phe161, and Asp172 mutants of NHE1

Representative Western blot showing NHE1 expression in AP-1 cells transfected with HA-tagged wild-type NHE1 (NHE1) and the NHE1 mutants Asp159Glu, Asp159Asn, Asp159Gln, Phe161Ala, Phe161Leu, Phe161Lys, Asp172Glu, Asp172Asn, and Asp172Gln. In each lane 100 μg of total protein was loaded. Numbers underneath the lanes indicate the mean values obtained from densitometric scans of the 110 kDa band relative to wild-type NHE1 for at least three trials.

Cell line	Plasma Membrane (% of total)
NHE1	77 ± 5
D159E	71 ± 7
D159N	79 ± 4
D159Q	67 ± 2
F161A	43 ± 8*
F161L	86 ± 3
F161K	47 ± 6*
D172E	87 ± 4
D172N	53 ± 3*
D172Q	63 ± 2

Table 4.2 Summary of plasma membrane localization for Asp159, Phe161, and Asp172 NHE1 mutants

Plasma membrane targeting of the Na^+/H^+ exchanger in AP-1 cells transfected with wild-type NHE1 (NHE1) and the mutants Asp159Glu, Asp159Asn, Asp159Gln, Phe161Ala, Phe161Leu, Phe161Lys, Asp172Glu, Asp172Asn, and Asp172Gln was determined as described in Section 2.2.4. The percent of the total NHE1 protein localized to the plasma membrane is indicated. The results are mean ± standard error for at least 4 determinations. * indicates significantly reduced plasma membrane targeting in comparison to NHE1 (Mann-Whitney *U*-test, $p < 0.05$).

Once we confirmed that the Phe161, Asp159, and Asp172 mutants were at least partially expressed and targeted to the plasma membrane, we examined the activity of the mutant exchangers. Figure 4.9 shows both the uncorrected activity (light gray bars) and the activity corrected for expression and surface processing (dark gray bars) relative to wild-type NHE1 for the Phe161, Asp159, and Asp172 mutants. The mutants Asp159Glu, Phe161Ala, Phe161Lys, Asp172Glu, and Asp172Asn had significantly decreased activity relative to wild-type NHE1. However, correction for expression and plasma membrane targeting is able to account for the decreased activity for all of the mutants other than Asp159Glu. Surprisingly, the mutations Asp159Gln and Phe161Leu resulted in increased exchanger activity, and this increase in activity was not due to increased expression and plasma membrane targeting of the exchanger.

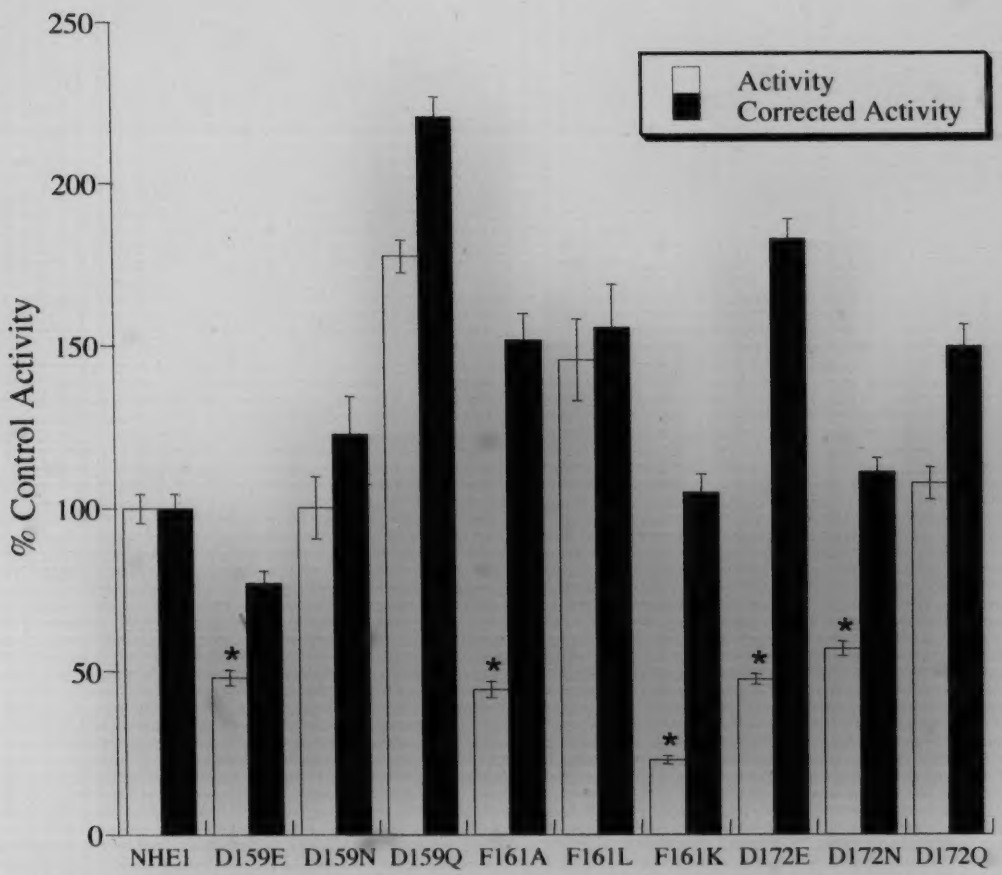

Figure 4.9 Activity of Asp159, Phe161, and Asp172 mutants of NHE1

Rate of recovery from an acid load by AP-1 cells stably transfected with wild-type NHE1 (NHE1) and the Na^+/H^+ exchanger mutants Asp159Glu, Asp159Asn, Asp159Gln, Phe161Ala, Phe161Leu, Phe161Lys, Asp172Glu, Asp172Asn, and Asp172Gln. The activity of cells stably transfected with NHE1 was 1.7 pH units/min, and this value was set to 100%. The results are mean ± SE for at least 8 determinations from two independently made stable cell lines. Corrected activity indicates activity normalized for amount of protein expressed and targeted to the plasma membrane. * indicates mutants with uncorrected activity that is significantly reduced from wild-type NHE1 activity (Mann-Whitney *U* test, $p < 0.05$).

4.3 Discussion

One method to determine the functional role of individual amino acids in a transmembrane segment of a membrane protein is cysteine-scanning mutagenesis in combination with reaction with sulfhydryl-reactive reagents. Cysteine-scanning mutagenesis can be used to determine the accessibility of amino acid side chains by taking advantage of the fact that the sulfhydryl moiety is the most reactive functional group in a protein. The sulfhydryl-reactive reagents that are commonly used in these studies are small, hydrophilic compounds and as such, they cannot reach residues within the hydrophobic bilayer but can react with pore-lining residues that are in an aqueous environment (Figure 4.1)[184,195,201].

We began our cysteine-scanning mutagenesis study of TM IV by individually substituting each of the amino acids in TM IV with cysteine in a cysteineless NHE1 background. We found that TM IV was exceptionally sensitive to mutation. Each of the introduced single-cysteine mutations results in a significant decrease in exchanger activity, and almost half of the single-cysteine mutants had less than 20% of the activity of the control cNHE1. Western blotting revealed that in some cases the reduction in activity was due to a lower level of expression of the mature NHE1 protein (Figure 4.2). Several of the mutants were expressed mainly as the immature form of NHE1 that is not fully glycosylated, and many but not all of these had greatly reduced activity. In addition, we

determined whether the mutations affected the surface targeting of the exchanger. Only two of the mutants, Asp159Cys and Asp172Cys had significantly less surface NHE1 than the wild type, and even for these two mutants the decreased plasma membrane targeting could not account for their decreased activity (Figure 4.4, dark gray bars).

Our finding that many of the single-cysteine mutations in TM IV affected the expression and/or activity of NHE1 are similar to the results found with the human anion exchanger (AE1) and with TM XI of lactose permease [182,183]. However, our results suggest that TM IV of NHE1 is especially sensitive to mutation as compared with the results for TM VIII of AE1 or TM XI of lactose permease. In TM VIII of AE1 there were three single-cysteine mutants that had greatly impaired anion exchange function, and in TM XI of lactose permease there were four single-cysteine mutants with had decreased lactose uptake function, and one mutant that was not expressed. In other membrane proteins such as the tetracycline-resistant transporter of *E. coli* [202] and P-glycoprotein [203], all the amino acids in a TM segment can be individually mutated to cysteine and the protein will still retain appreciable activity. The susceptibility to mutation appears to vary not only between proteins, but also within different transmembrane segments of the same protein. While TM XI of lactose permease had several sensitive amino acids [182], TM XII only had one [194]. This property could be reflective of both the importance of the residues in the

particular segment, and of the importance of the segment itself to the structure and function of the protein. In our case, it was clear that there was a strict requirement for many of the amino acids of TM IV, and this could be indicative of precise structural and functional roles. Specifically, the fact that so many of the mutants had impaired activity suggests that amino acids on all faces of TM IV are important for activity, indicating that in addition to lining the ion transport pore this TM segment is likely involved in many interactions with other parts of the NHE1 protein, rather than simply facing the lipid bilayer.

We examined the sensitivity of the active single-cysteine mutants of the Na^+/H^+ exchanger to sulfhydryl-reactive reagents. Of the reagents that we tested, only the membrane impermeant reagents MTSET and MTSES were suitable for use in our system. The membrane permeant reagent MTSEA caused the transfected AP-1 cells to detach from the glass coverslip, a result that we cannot explain but that has also been observed in other laboratories (Colin Josephson and John Orlowski, personal communication). The membrane impermeant, hydrophilic reagent pCMBS inhibited cNHE1, even when used at the relatively low concentrations that have been used in other cysteine-scanning studies [183]. Although we do not know why pCMBS would inhibit cysteineless NHE1, it is possible that this reagent reacts with and affects another protein that interacts with NHE1. Alternatively, pCMBS could be reacting with cNHE1 at residues other than cysteine. Treatment with either positively charged MTSET or negatively

charged MTSES had no effect on cNHE1 activity but caused a significant reduction in the activity of Phe161Cys (Figure 4.6). These results indicate that Phe161 is accessible to these sulfhydryl-reactive reagents, and the most likely explanation for this accessibility is that Phe161 resides at a site that lines the ion translocation pore. Thus, when either MTSET or MTSES reacts, the covalently attached reagent at least partially blocks the pore of the exchanger and therefore inhibits ion transport. Therefore, we conclude that Phe161 in TM IV is the first residue in a transmembrane segment to be unambiguously identified as lining the ion transport pore of NHE1.

The NMR structure of TM IV was determined in CD3OH:CDCl3:H2O, a membrane mimetic solution that has a low dielectric constant and mimics both a lipid bilayer and a protein interior. As with many peptides studied by NMR [204,205] the TM IV segment does not, as a whole, assume a single conformation. Rather, sections within the peptide converge structurally. Consideration of these sections relative to each other then provides insight into the overall structure of TM IV. Of course, it must be presumed that in the entire NHE1 protein the interaction of TM IV with other TM segments could affect the conformation of TM IV. However, this structure is likely to be a good representation of the TM IV conformation because studies have demonstrated a strong correspondence between structures of peptides or transmembrane protein

segments obtained in membrane mimetic solvents and their structures in the entire protein [206,207].

The most easily noticed feature of the TM IV structure is that it certainly does not resemble a canonical transmembrane α-helix. Rather, three core regions of four to nine residues converge structurally: Asp159-Leu163 constitutes a series of β-turns, Leu165-Pro168 appears to be quite extended, and Ile169-Phe176 provides the only appreciable α-helical character over the entire transmembrane segment. It is possible that the overall conformation of TM IV is not as extended as the one shown in Figure 4.7B. However, given that the segment must span a membrane with the width on the order of 25–35 Å, a relatively extended structure is likely more representative of the expected biological configuration than one that curls back on itself. In addition the extended nature of the TM IV peptide corresponds well with our secondary-structure prediction of TM IV (Section 3.2.4), which predicts that the native sequence of TM IV will adopt an extended-strand conformation.

Similar experimental resolution in NMR studies has been achieved using micelles in aqueous solution, an environment that would surround the TM IV peptide with hydrophobic detergent tails and serve to stabilize the conformation of the peptide [208]. However, in its natural setting, TM IV of the NHE1 protein would likely contact lipid tail groups, surrounding polypeptide segments, and a pore region that has a relatively high dielectric constant. Thus, although in the

micellar state the rotations about Phe164 and Pro168/Ile169 would probably be greatly reduced, this may actually be an artificial constraint upon the peptide structure relative to the solvent setting. Accordingly, we feel that the present structure in a mixture of solvents representing a variety of dielectrics provides a reliable representation of the best-structured regions of the TM IV segment.

In light of the structural data, plausible explanations for the loss in activity observed for some of the most detrimental single-cysteine mutants can be advanced. Mutations to P167C and P168C abolish all exchanger activity, and, as seen in Chapter 3, mutation of these prolines to other residues did not allow for a return to a normally functioning Na^+/H^+ exchanger [140]. In the case of these proline residues, mutation from an imino to a much freer amino acid moiety would be expected to modify the observed structural motif. Given the loss of activity upon mutation of these proline residues, it is likely that the extended structural nature of this motif is crucial for NHE1 activity. Indeed, in the crystal structure of NhaA, a unique assembly of two pairs of short helices connected by crossed, extended chains are thought to be imperative in allowing alternating access of the substrate-binding site to either the intracellular or extracellular space (see Figure 1.5). Our structure of TM IV in NHE1 is quite reminiscent of the structure of TM IV in NhaA, although in our structure the N-terminal region is defined by a series of β-turns rather than an α-helix. Thus, the general structure

of the extended chain could certainly be a common element between these two proteins.

We created and studied additional NHE1 mutants in the wild-type background based on our new knowledge about the structure and function of TM IV. First, we mutated Phe161 to alanine, leucine, or lysine. The mutations to Phe161 show that this pore-lining residue is not required for NHE1 activity. The mutation Phe161Leu caused an increase in NHE1 activity, and the mutations Phe161Ala and Phe161Lys each caused a decrease in activity, but this decrease could be fully accounted for by correction for expression and surface processing. Thus, Phe161 can be mutated to smaller and/or charged amino acids without decreasing NHE1 activity. A previous study found that the mutant Phe165Tyr in hamster NHE1 sequence (corresponding to Phe161 in the human sequence) causes a 3- to 4-fold decrease in Na^+ transport rate [130]. When taken together with our finding that Phe161 is pore-lining but not required for transport, this result suggests that the addition of a hydroxyl group to the Phe161 side chain may slow down transport due to its increased interaction with transported cations.

Examination of the structure of the TM IV peptide with the knowledge that Phe161 faces the ion-transport pore provides a very interesting revelation. Within this structure, over the convergent stretch of Asp159–Leu163, the Asp159 side chain is often observed to be on the same face of the peptide as Phe161. Therefore, it is possible that the anionic Asp159 side chain might also face into

the pore of the exchanger. Our laboratory has previously found that polar residues within transmembrane segments of the Na^+/H^+ exchanger are important in cation coordination and transport [119,133], and our finding that the mutation Asp159Cys affects the expression and activity of the exchanger is consistent with this. Accordingly, we mutated Asp159 to glutamic acid, asparagine, or glutamine. We found that the mutation Asp159Glu decreases the activity of the exchanger by approximately 20%, that the mutation Asp159Asn does not affect the activity of the exchanger, and that the mutation Asp159Gln increases the activity of the exchanger nearly 2-fold. Thus, our results indicate that Asp159 is not essential for the activity of NHE1, and that a negative charge is not required at this position. However, they do support the possibility that Asp159 faces the ion-transport pore. Mutation of Asp159 to the longer glutamic acid side chain results in a decrease in activity. This could be due to an increased interaction between the transported cations and the negatively charged side chain that is protruding further into the pore.

Because rotation of the structurally convergent sections is observed about Phe164 and Pro168/Ile169, it was not possible to determine which other C-terminal amino acids face the translocation pore. However, because the mutant Asp172Cys was inactive and other acidic residues in NHE1 are important for function [133], we further investigated the importance of Asp172 by mutating it to glutamic acid, asparagine, and glutamine. The mutation Asp172Gln did not

affect NHE1 activity, and the mutations Asp172Glu and Asp172Asn each caused a decrease in activity that was fully accounted for by correction for expression and surface processing. Thus, Asp172 is not required for NHE1 transport activity, and we have no indication that it lines the ion transport pore.

Our study has given the first detailed structural and functional information on TM IV of the NHE1 isoform of the Na^+/H^+ exchanger. TM IV is extremely sensitive to alterations in its amino acid sequence. The structure of TM IV in a membrane mimetic environment indicates that it is well structured, but its conformation is uniquely different from a typical α-helix. This unique structure may reflect its pivotal role in cation binding and transport, and is reminiscent of the conformation of TM IV in the NhaA structure. The residue Phe161 was unambiguously found to line the ion transport pore of NHE1, and our results support the suggestion that the side chain of Asp159 also faces into the pore of NHE1.

CHAPTER FIVE:

Identification of Second-site Revertant Mutations of Pro167Gly using Random Mutagenesis

5.1 Introduction

The Na^+/H^+ exchanger and other membrane proteins are notoriously difficult to express, purify, and crystallize. Thus, little is known about the three-dimensional structure of NHE1, and specifically there is nearly no information available about which transmembrane segments within the exchanger are in close contact with each other. One method that has been used to discover interactions between transmembrane segments is the identification of second-site revertant mutations that rescue inactive or pharmacologically altered mutants. This method allows for the identification of long-range interactions within a membrane protein without the necessity for overexpression and purification that is required to obtain a high-resolution structure. The principle behind this method is that if a mutation in transmembrane segment Y renders a membrane protein inactive, and a subsequent mutation in transmembrane segment Z restores activity, then transmembrane segments Y and Z must be within close proximity for this effect to occur.

Accurate predictions regarding long-range interactions have been generated using second-site revertant data for membrane proteins including the ATP synthase and Na^+/H^+ antiporter NhaA of *E. coli*. In the *E. coli* ATP synthase, a Pro64Leu mutation in TM II inactivates the enzyme, and a second site Ala20Pro mutation in TM I restores partial activity, suggesting that Pro64 may

reside close to Ala20 [209]. The proximity of these residues was confirmed when the high resolution structure of this enzyme was published, as it showed that TM I and II form a hairpin structure with Ala20 and Pro64 lying adjacent to each other [206]. In addition, the structure of the double mutant Ala20Pro/Pro64Ala showed how introducing a proline at position 20 caused a kink in TM I that was able to compensate for the loss of the kink in TM II due to the removal of Pro64 [210]. In the *E. coli* Na^+/H^+ antiporter NhaA, a Gly338Ser mutation in TM XI abolishes the pH control of the antiporter such that it remains fully active from pH 7 to 9, and is 70% active at pH 6 [211]. Three second-site mutations restored pH regulation in NhaA such that it was mostly inactive between pH 6 and 6.5. These revertant mutations clustered in TM IV of the antiporter, suggesting that TM XI and TM IV may interact. Indeed, the recent crystal structure of NhaA confirmed that these TM segments do interact, with TM segments IV and XI forming a unique assembly at the binding site that undergoes pH dependent a conformational change that allows transport to occur [107].

Second-site revertant mutations have also previously been identified in the mammalian Na^+/H^+ exchanger. Wakabayashi *et al.* used random mutagenesis at Cys8 and its surrounding residues in the cytosolic N-terminal tail. They identified that a second-site revertant mutation in the N-terminal tail of the exchanger was able to rescue a Tyr454Cys mutant showing defective surface expression, suggesting that N-terminal tail of NHE1 may interact directly with the region of

TM XI containing Tyr454 [135]. In another study on NHE1, Touret *et al.* identified second-site revertants of a Phe162Ser mutation in TM IV [132]. The original mutation resulted in a Na^+/H^+ exchanger with low affinities for cariporide and Na^+, and mutants having the second-site mutations Ile169Ser or Ile170Thr had restored Na^+ affinity but remained resistant to cariporide. In this case, because the second-site mutations were clustered within the same TM segment as the original mutation, the authors hypothesized that the second-site revertant mutations allowed for restoration of a geometrically constrained binding site that is crucial for cation binding.

The goal of our study was to identify second-site revertant mutations that could rescue the inactive NHE1 mutant Pro167Gly in TM IV. As presented in Chapter 3, this mutant does not show any Na^+/H^+ exchange activity, and has defective expression and surface processing in AP-1 cells. We used a unique method for identifying second-site mutations that eliminated the possibility of isolating clones that had reverted back to the original wild-type sequence, and we selected for clones that were able to survive an intense acid-load selection protocol that requires that cells have an active Na^+/H^+ exchanger to survive. We sequenced the mutated segment of the NHE1 gene in the three clones that survived the acid load selection protocol and showed high Na^+/H^+ exchange activity, and found that none of these clones possessed a second-site revertant mutation.

5.2 Results

5.2.1 Random mutagenesis

Random mutations were introduced in the pYN4+/Pro167Gly mutant of NHE1 by propagating the plasmid in the XL1-Red mutator *E. coli* strain. This technique for introducing mutations will result in a mutation rate of approximately 1 in 2000 basepairs, and the mutations may be introduced at any location within the plasmid. As depicted in Figure 5.1, in order to have mutations only within the membrane domain of NHE1, an 1142 basepair fragment (corresponding to Leu171 to Leu550 in the NHE1 protein) was excised from the randomly mutagenized pYN4+/Pro167Gly plasmid pool and ligated into the original pYN4+/Pro167Gly vector. The resulting pool of plasmids contained random mutations only within the membrane domain (TM IV-TM XII) and the proximal region of the cytoplasmic tail. Transformation of the ligation product containing the randomly mutagenized DNA into *E. coli* cells resulted in more than 20,000 colonies. Transformation with a control ligation product to ensure that the original pYN4+/Pro167Gly did not self ligate resulted in less than 0.2% of this number of colonies.

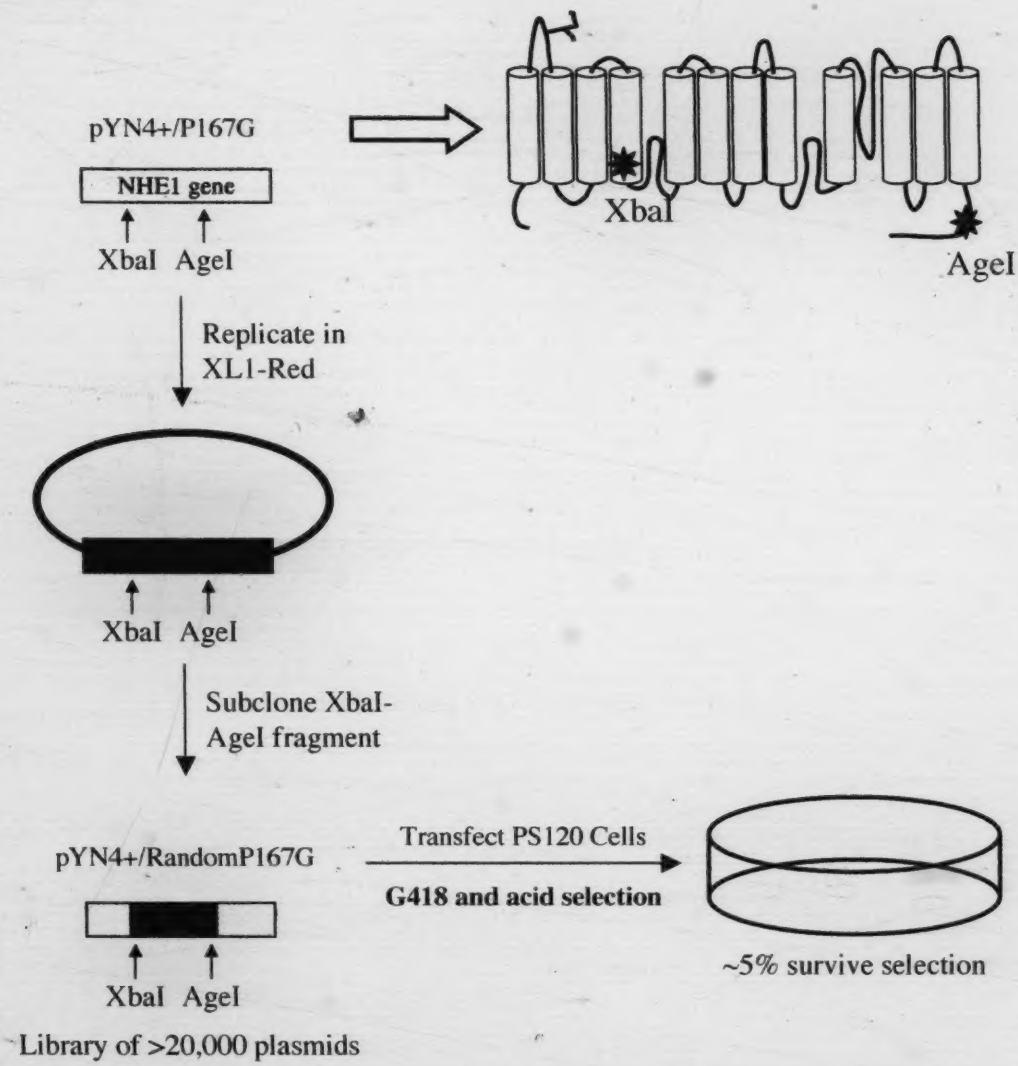

Figure 5.1 Strategy for identification of Pro167Gly second-site revertants

The plasmid encoding the Pro167Gly (P167G) NHE1 mutant with unique XbaI and AgeI restriction endonuclease sites was propagated in the XL1-Red mutator *E. coli* strain. The location of the XbaI and AgeI sites with respect to the NHE1 protein is shown. The XbaI-AgeI fragment from the plasmids constituting the pool of randomly mutagenized plasmids was subcloned back into the original pYN4+/P167G vector to create the pYN4+/RandomP167G library of plasmids. This library was used to transfect PS120, and cells expressing a functional Na^+/H^+ exchanger were selected.

5.2.2 Isolation of acid-load tolerant cells

The colonies obtained from transformation with the ligation product were combined and a pool of pYN4+/Pro167Gly plasmid DNA containing random mutations in the DNA sequence corresponding to Leu171 to Leu550 was isolated. This pool of randomly mutagenized pYN4+/Pro167Gly (referred to as pYN4+/RandomPro167Gly) was used to transfect Na^+/H^+ exchange deficient PS120 cells, resulting in more than 4800 colonies. We chose to use PS120 cells rather than AP-1 cells for the acid selection of second-site revertants because preliminary experiments showed that PS120 were killed more efficiently by acid load selection than were AP-1 cells.

Following transfection with pYN4+/RandomPro167Gly and selection with geneticin, cells that had an active Na^+/H^+ exchanger were isolated using a high-stringency acid-load selection technique [146]. Of the 4800 colonies obtained from the transfection using pYN4+/RandomPro167Gly, approximately 225 colonies (4.7%) survived the acid-selection protocol. Control PS120 cells had a survival rate of 0.1%, and PS120 cells transfected with wild-type NHE1 had a survival rate of 8.7%. Of the colonies transfected with RandomPro167Gly, 104 clones were propagated and tested for NHE1 expression. We found that NHE1 was expressed in 101 of the clones tested.

5.2.3 Na^+/H^+ exchange activity of acid-load tolerant colonies

To screen for mutants with a potential second site revertant mutation that allows the Pro167Gly mutant to regain function we measured the Na^+/H^+ exchange activity of the clones that expressed NHE1. Figure 5.2 illustrates the uncorrected Na^+/H^+ exchange activity of PS120 cells transfected with wild-type NHE1, the Pro167Gly mutant, and the RandomPro167Gly clones as a percent of the wild type activity. When PS120 cells transfected with wild-type NHE1 were exposed to Na^+ after being acidified, there was an immediate and rapid increase in intracellular pH at the rate of 1.16 pH units/min. We were surprised to find that PS120 cells transfected with the Pro167Gly mutant showed an increase in intracellular pH at the rate of 0.40 pH units/min, an activity that is approximately 40% of the wild-type NHE1 activity. This is a significant increase in activity as compared to Pro176Gly expressed in AP-1 cells (Chapter 3), and we believe that the difference in activity is due to the expression of this clone in a different cell line. Of the fifty-two RandomPro167Gly clones that were tested, only clones 6, 17, 35, 45, 50, 54, 63, 68, 92, and 93 had significantly more activity than Pro167Gly.

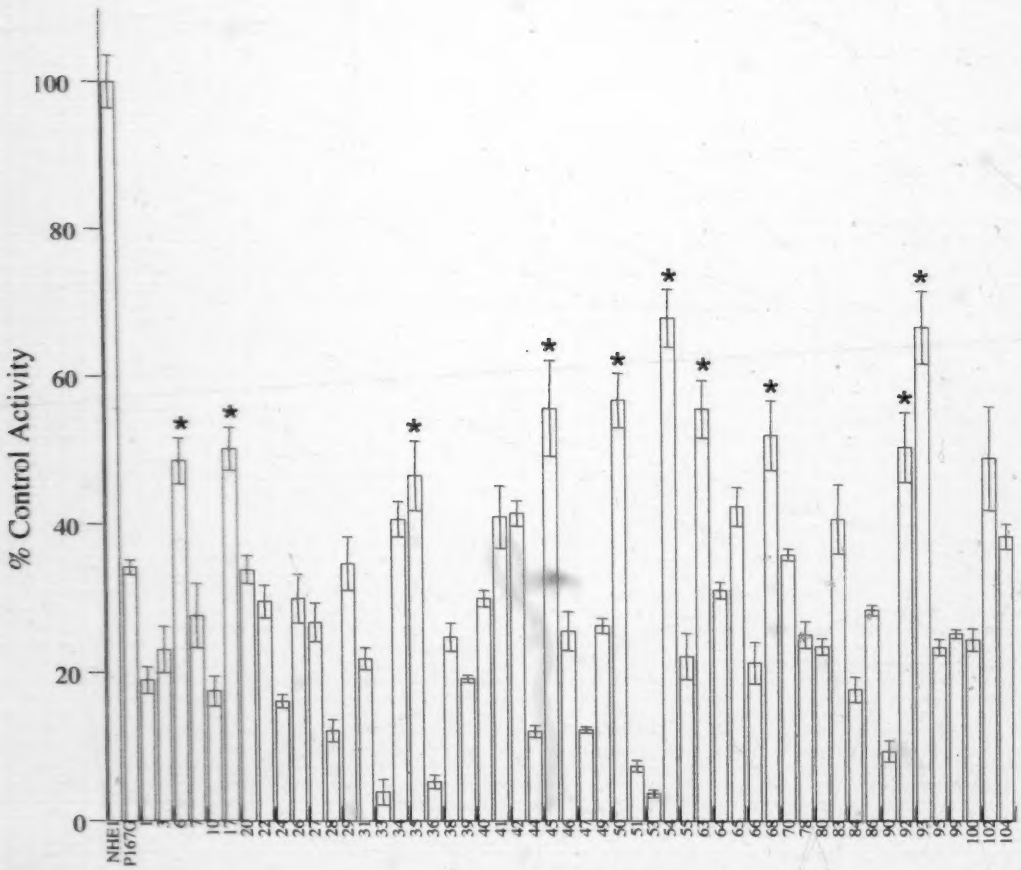

Figure 5.2 Uncorrected activity of RandomPro167Gly clones

Summary of the rate of recovery from an acid load by PS120 cells stably transfected with wild-type NHE1, the Pro167Gly mutant, and with RandomPro167Gly mutants. The rate of recovery from a transient acid load of cells stably transfected with NHE1 was 1.16 pH units/min, and this value was set to 100%. The results are mean ± SE for at least 3 determinations. * indicates mutants with uncorrected activity that is significantly higher than the activity of the Pro167Gly mutant (Mann-Whitney *U*-test, $p < 0.05$).

5.2.4 NHE1 expression in acid-load tolerant colonies having high Na^+/H^+ exchange activity

The expression of the RandomPro167Gly clones that had significantly higher activity than the Pro167Gly mutant was quantified by Western blotting. Figure 5.3 shows a Western blot of total cell extracts from PS120 cells stably transfected with wild-type NHE1, Pro167Gly, and the RandomPro167Gly clones. The amount of mature 110 kDa NHE1 relative to wild-type NHE1 is quantified below each lane in Figure 5.3. The wild-type and mutant exchangers displayed the same pattern of immunoreactive bands, with a larger band at 110 kDa that represents the fully glycosylated form of the mature Na^+/H^+ exchanger and a smaller band at 95 kDa that represents an immature form of the exchanger that is not fully glycosylated [108]. The Pro167Gly mutant had approximately 60% as much mature Na^+/H^+ exchanger expressed as compared to wild-type NHE1. All of the RandomPro167Gly clones had at least as much mature NHE1 expressed as the Pro167Gly control, and in most cases the RandomPro167Gly clones had expression that was similar to wild-type NHE1.

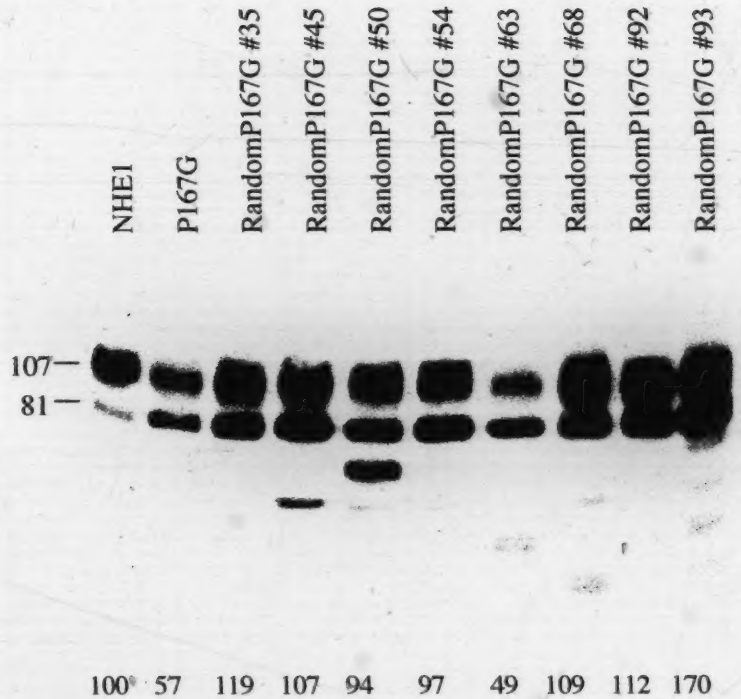

Figure 5.3 Expression of RandomPro167Gly mutants

Representative Western blot showing NHE1 expression in PS120 cells stably transfected with wild-type NHE1, the Pro167Gly mutant (P167G), and with RandomP167G mutants. In each lane 100 μg of total protein was loaded. Numbers underneath the lanes indicate the values obtained from densitometric scans of the 110 kDa band relative to wild-type NHE1.

To account for the differences in expression between wild-type NHE1, Pro167Gly, and the RandomPro167Gly clones, the activity of these proteins was normalized to their expression levels. Figure 5.4 shows the corrected activity of the RandomPro167Gly clones as compared to wild-type NHE1 and the Pro167Gly mutant. As seen in Figure 5.4, after correction for expression only the clones 54, 63, and 93 had higher activity than the Pro167Gly mutant.

5.2.5 Identification of second-site mutations

Genomic DNA was isolated from the three clones (#54, 63, and 93) that had higher corrected activity than the control Pro167Gly mutant, and the region of the NHE1 gene potentially containing random mutations was amplified by PCR using a high fidelity DNA polymerase. In the case of clones #63 and 93, the resulting PCR product was sequenced directly. In the case of clone #54, a reliable sequence was not generated directly from the PCR product. Thus, for clone #54, the PCR product was subcloned into the pYN4+/P167G plasmid for sequencing. Upon sequencing, no mutations were found in the section of the NHE1 gene that was submitted to random mutagenesis for either clone 63 or 93. In clone 54, a single guanidine to adenine mutation was found, but this mutation was silent and would not affect the amino acid sequence of the NHE1 protein.

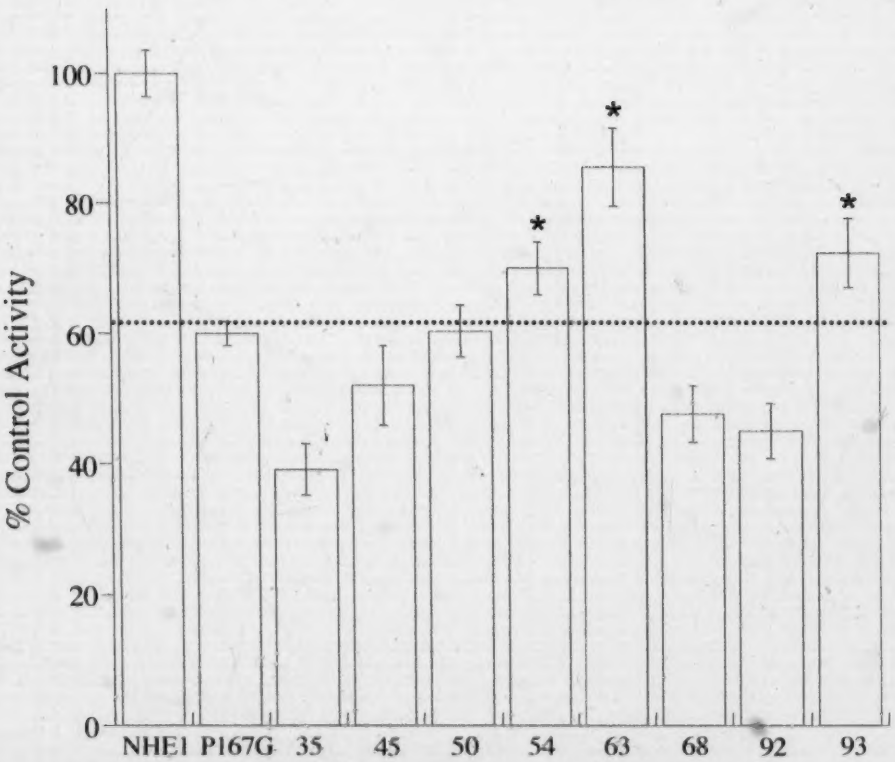

Figure 5.4 Corrected activity of RandomPro167Gly mutants

Summary of rate of recovery from an acid load after correction for protein expression by PS120 cells stably transfected with wild-type NHE1, the Pro167Gly mutant, and RandomPro167Gly clones 35, 45, 50, 54, 63, 68, 92, and 93. The activity of the cells stably transfected with wild-type NHE1 was 1.16 pH units/min, and this value was set to 100%. The results are mean ± SE of at least 4 determinations. * indicates clones that have higher activity than the Pro167Gly mutant after correction for expression (Mann-Whitney *U*-test, $p < 0.05$).

5.3 Discussion

We attempted to identify second-site revertant mutations that could rescue the inactive NHE1 mutant Pro167Gly in TM IV. In AP-1 cells, this mutant does not show any Na^+/H^+ exchange activity, and has defective expression and surface processing. Unfortunately, we were unable to isolate a clone having a second-site revertant mutation to rescue the Pro167Gly mutant. We believe that the major reason that we did not identify any second-site revertant mutations lies in the fact that we used PS120 cells rather than AP-1 cells for our experiments. We chose to use the PS120 cell line because this cell line was more susceptible to acid selection than the AP-1 cell line. However, we had not characterized the Pro167Gly mutant in this cell line prior to beginning our random mutagenesis and acid load selection protocol. Thus, when we first tested the expression and activity of the acid load tolerant colonies and the Pro167Gly mutant, we were surprised to find that when this mutant is expressed in PS120 cells it has 60% of the expression of wild-type NHE1, and retains over 30% of the wild-type activity. At this time it is not clear why the Pro167Gly mutant is expressed at higher levels and is more active in PS120 cells than in AP-1 cells. However, it does indicate that processing and activity of NHE1 mutants can vary between cell lines, and that Pro167 is not absolutely essential for NHE1 expression and activity. Nevertheless, taking into account the significant activity of the Pro167Gly mutant,

it is not surprising that we were not able to isolate any second-site revertant mutants as acid load selection would not be an effective selection method if the background mutation displays enough Na^+/H^+ exchange activity to be protective.

While our attempts to isolate a second-site revertant mutant of Pro167Gly was not successful, the unique method that we used for isolating second-site mutations may be useful to find second-site revertants of other NHE1 mutants. The method that we used involved subjecting the plasmid encoding the Pro167Gly NHE1 mutant to random mutagenesis, and subsequently subcloning a portion of the NHE1 gene encoding Leu171 to Leu550 back into the original plasmid. This method is superior to methods using an entire plasmid that has been subjected to random mutagenesis because it eliminates the possibility of isolating clones that have reverted back to the original wild-type sequence. Thus, a similar strategy would be appropriate for use with other inactive NHE1 mutants such as Glu262Gln and Asp267Asn in TM VII, assuming that control experiments transfecting these mutant NHE1 proteins into PS120 cells proves that they are not active in this cell line.

Although we did not identify any second-site revertant mutations in the three clones that had significantly higher activity than the Pro167Gly mutant after correction for expression, we did find other clones that may be of interest for study. Of note, clones #33, 36, and 53 retained significantly less Na^+/H^+ exchange acid activity than the Pro167Gly mutant, although they did have enough

Na^+/H^+ exchange activity to survive the acid selection protocol. While we did not study these clones beyond characterizing their activity, because of their decreased activity we speculate that they may have second site mutations that cause a decrease in Na^+/H^+ exchange activity. Thus, in the future our laboratory will further characterize these clones with respect to their expression to ensure that their decreased activity is not due to decreased expression. If the decreased activity of these clones cannot be accounted for by decreased expression, we will sequence the randomly mutagenized portion of the NHE1 gene from these clones in an attempt to identify detrimental second site mutations.

CHAPTER SIX:

Conclusions and Future Directions

6.1 Conclusions

Although NHE1 has been studied extensively, the mechanism by which it transports cations remains unknown, and there is little structural information available about this protein. Thus, the objective of my thesis was to identify specific amino acids that are important for the function of NHE1, and to elucidate structural and functional information about NHE1 using biochemical experiments. My work focused on transmembrane segment IV of NHE1, with the goal of identifying residues that were important for NHE1 function, identifying pore-lining residues within this TM segment, and by identifying long-range interactions between TM IV and other transmembrane segments in NHE1.

The first goal of my thesis was to investigate the importance three highly conserved proline residues in TM IV that were previously suggested to be involved in the structure and function of NHE1, and were thought to allow for conformational changes within this transmembrane segment [112,131]. We used site-specific mutagenesis to mutate Pro167 and Pro168 to glycine, alanine, or cysteine, and to mutate Pro178 to alanine. We found that Pro167 and Pro168 are essential for NHE1 activity, and that mutation of Pro167 also affects the expression and membrane targeting of the exchanger in the AP-1 cell line. In contrast, Pro178 could be mutated without effect. Therefore, we conclude that the proline residues Pro167 and Pro168 in the middle of TM IV are critical for normal

NHE1 function, and may be required to directly interact with transported cations, or to allow TM IV to assume a unique structure or undergo a conformational change that is required for NHE1 activity.

The second goal of my thesis was to increase our knowledge about the structure of NHE1 by identifying residues that line the ion transport pore. Because numerous amino acids in TM IV (including Pro167 and Pro168) are important for NHE1 function, we chose to base our study on this TM segment. We used cysteine-scanning mutagenesis in combination with reaction with sulfhydryl reactive reagents to identify pore-lining residues in TM IV. This technique requires that each of the amino acids in TM IV be individually mutated to cysteine in a cysteineless NHE1 background. Before we began to identify pore-lining residues we characterized the mutant exchangers with respect to their activity, expression, and surface targeting. We found that TM IV was exceptionally sensitive to mutation, with all introduced single-cysteine mutations resulting in a significant decrease in exchanger activity. In addition, twelve out of twenty-three mutants had decreased expression, and two of the mutants showed reduced surface targeting. Thus, many of the residues in TM IV may potentially be involved in cation binding and transport, or may be required for TM IV to remain in a structural conformation that is appropriate for function. In most membrane proteins, mutation to cysteine is very well tolerated and the introduction of a cysteine side chain that faces the lipid bilayer has little or no

effect on activity [180,212]. Thus, the fact that there were so many single-cysteine mutants in TM IV that had impaired activity suggests that this TM segment lines the ion transport pore and is involved in many interactions with other parts of the NHE1 protein, rather than simply facing the lipid bilayer.

We went on to react the active single-cysteine mutants with sulfhydryl reactive reagents to identify pore-lining residues. Of the twelve single-cysteine mutants that retained at least 20% of the activity of the cysteineless control, only the activity of Phe161 was inhibited by reaction with sulfhydryl reactive reagents. Therefore, we were able to conclude that Phe161 in TM IV lines the ion transport pore of NHE1. Based on the fact that Phe161 is a pore-lining residue and on the structure of TM IV in a membrane-mimetic solvent, we chose to further investigate the importance of Phe161 and two aspartic acid residues in TM IV: Asp159 and Asp172. We used site-directed mutagenesis to mutate Phe161 to alanine, leucine, and lysine, and to mutate each aspartic acid residue to glutamic acid, asparagine, and glutamine. After correction for expression and plasma membrane targeting, the only mutant that had decreased activity was Asp159Glu. Therefore, we conclude that the residues Asp159, Phe161, and Asp172 are not essential for NHE1 activity. In addition, we conclude that Asp159 may face the pore of NHE1, as the Asp159Glu mutation that increases the length of the side chain, thereby causing the acidic functional group to protrude into the pore, results in a reduction in transport.

The final goal of my thesis was to identify long-range interactions between TM IV and other transmembrane segments in NHE1 by isolating and identifying second-site revertant mutations of an inactive Na^+/H^+ exchanger that has a mutation in TM IV. We chose to identify second-site revertant mutations that could rescue the inactive NHE1 mutant Pro167Gly in TM IV using a unique method for identifying second-site mutations that eliminated the possibility of isolating clones that had reverted back to the original wild-type sequence. We generated a library of over 20,000 plasmids, transfected the plasmid library into PS120 cells and obtained over 4800 colonies, subjected the colonies to an acid-load selection protocol that eliminated over 95% of the colonies, and finally isolated 104 clones that were able to survive the intense acid-load selection protocol and thus should have an active Na^+/H^+ exchanger. Unfortunately, when we sequenced the mutated segment of NHE1 gene in the three clones having the highest Na^+/H^+ exchange activity, and we found that none of these clones possessed a second-site revertant mutation. Therefore, we were unable to isolate a clone having a second-site revertant mutation to rescue the Pro167Gly mutant. We believe that the major reason that we did not identify any second-site revertant mutations is that, as opposed to the results in the AP-1 cell line where the Pro167Gly mutant is inactive, in the PS120 cell line the Pro167Gly mutant retains over 30% of the wild-type activity. Thus, the background activity of the Pro167Gly mutant was high enough to be protective against our acid load

selection technique, and precluded us from being able to select for second-site revertants.

6.2 Future Directions

Although advances have been made in our understanding of the structure and function of NHE1, many unanswered questions still remain. For example, while our research has demonstrated that Phe161 and possibly Asp159 line the ion transport pore of NHE1, no other residues in the TM segments of NHE1 are known to be pore lining. Thus, further cysteine scanning mutagenesis studies to identify pore-lining residues in other TM segments of NHE1 are required to provide us with a better understanding of which TM segments are likely involved in ion transport. Accordingly, our laboratory is now using cysteine-scanning mutagenesis in combination with reaction with sulfhydryl reactive reagents to identify pore-lining residues in TM VII and TM IX.

If pore-lining residues are identified in TM segments other than TM IV, another option for use in elucidating structural information about the exchanger would be the use of site-directed chemical cross-linking experiments. In recent years, the three-dimensional structures of many polytopic membrane proteins have been probed using a combination of cysteine mutagenesis and oxidative cross-linking [213-217]. This approach requires the introduction of individual cysteine residues within two different TM segments in a cysteineless background. The two cysteine residues can be treated with cross-linking reagents, the cross-linked protein can be cleaved at an introduced protease site, and the presence of a

cross-link can subsequently be detected using SDS-PAGE and immunoblotting. This technique provides information about the distance between the α-carbons of the two cross-linked residues and indicates that the cross-linked residues must be on facing sides of two helices [218]. Thus, site-directed chemical cross-linking experiments would provide us with further information about the tertiary structure of NHE1, and if we identify numerous pore-lining residues and cross-links between them, the information can be used to develop a model for the arrangement of TM segments [199,214].

Further studies are also needed to increase our knowledge about the location at which inhibitors bind to NHE1. It is currently known that mutation of specific residues alters inhibitor binding, but the exact location of inhibitor binding remains elusive. A simple experiment using the Phe161Cys NHE1 mutant may add valuable information to our knowledge about the inhibitor-binding site, as mutation of Phe161 is known to affect inhibitor binding [130]. The first step to this experiment would be treating the Phe161Cys mutant with an NHE1 inhibitor such as cariporide, measuring the Na^+/H^+ exchange activity, washing away the cariporide, and ensuring that normal Na^+/H^+ exchange activity returns. Once the control experiment is successfully completed, a subsequent experiment would then treat NHE1 with a sulfhydryl reactive reagent such as MTSET while it is inhibited by cariporide, then measure the activity after removal of the cariporide and of the excess sulfhydryl reagent. In this case, if the activity

returns to normal, the cariporide has blocked the MTSET from reacting, indicating that the cariporide binding site does include Phe161. In addition to studying the role of Phe161 in inhibitor binding we are also interested in examining the effects of mutating Asp159 and Asp172 on NHE1 inhibition. The role of these residues in inhibitor binding has never been studied before, so these experiments may reveal new interactions between NHE1 and inhibitors.

Our attempt to isolate a second-site revertant mutant of Pro167Gly was not successful, but the method that we used for isolating second-site mutations may be useful to find second-site revertants of other NHE1 mutants. In the future, our lab may use a similar strategy to identify second-site revertant mutations of other inactive NHE1 mutants such as Glu262Gln and Asp267Asn in TM VII. This would potentially indicate interactions between TM VII and other TM segments in NHE1. A second area of interest for continued study with our second-site revertant project would be the study of clones that retained significantly less Na^+/H^+ exchange acid activity than the Pro167Gly mutant. In this case we might be able to identify unique mutations that are detrimental to NHE1 activity, and this might implicate new TM segments as being important for NHE1 function.

Finally, a major goal in the field of Na^+/H^+ exchanger research is the elucidation of high-resolution structural information about NHE1. Work to obtain the structure of peptides of other TM segments is currently underway in our

laboratory in collaboration with the laboratory of Dr. Brian Sykes. Specifically, we are working on the structures of peptides of TM VII and TM IX, and we are also attempting to express and purify larger sections of the NHE1 protein that encompass several TM segments. The structures of larger sections of the NHE1 protein may be especially useful for understanding our biochemical studies because interactions between the TM segments may limit rotation within the TM segments, allowing the segments to adopt the conformation that they have in full-length NHE1. Finally, we await the structure of full-length NHE1, which will allow us to understand at a molecular level how this protein binds and transports cations and interacts with inhibitors.

CHAPTER SEVEN:

References

1. Hoffmann, E. K., and Simonsen, L. O. (1989) Membrane mechanisms in volume and pH regulation in vertebrate cells. *Physiol. Rev.* **69**(2), 315-382

2. Grinstein, S., Rotin, D., and Mason, M. J. (1989) Na^+/H^+ exchange and growth factor-induced cytosolic pH changes. Role in cellular proliferation. *Biochim. Biophys. Acta.* **988**(1), 73-97

3. Orlowski, J., and Grinstein, S. (2004) Diversity of the mammalian sodium/proton exchanger SLC9 gene family. *Pflügers Arch.* **447**(5), 549-565

4. Nakamura, N., Tanaka, S., Teko, Y., Mitsui, K., and Kanazawa, H. (2005) Four Na^+/H^+ exchanger isoforms are distributed to Golgi and post-Golgi compartments and are involved in organelle pH regulation. *J. Biol. Chem.* **280**(2), 1561-1572

5. Khadilkar, A., Iannuzzi, P., and Orlowski, J. (2001) Identification of sites in the second exomembrane loop and ninth transmembrane helix of the mammalian Na^+/H^+ exchanger important for drug recognition and cation translocation. *J. Biol. Chem.* **276**(47), 43792-43800

6. Karmazyn, M., Gan, X. T., Humphreys, R. A., Yoshida, H., and Kusumoto, K. (1999) The myocardial Na^+/H^+ exchange: Structure, regulation, and its role in heart disease. *Circ. Res.* **85**(9), 777-786

7. Orlowski, J., Kandasamy, R. A., and Shull, G. E. (1992) Molecular cloning of putative members of the Na^+/H^+ exchanger gene family. cDNA cloning, deduced amino acid sequence, and mRNA tissue expression of the rat Na^+/H^+ exchanger NHE-1 and two structurally related proteins. *J. Biol. Chem.* **267**(13), 9331-9339

8. Noel, J., Roux, D., and Pouyssegur, J. (1996) Differential localization of Na^+/H^+ exchanger isoforms (NHE1 and NHE3) in polarized epithelial cell lines. *J. Cell Sci.* **109**(Pt 5), 929-939

9. Baird, N. R., Orlowski, J., Szabo, E. Z., Zaun, H. C., Schultheis, P. J., Menon, A. G., and Shull, G. E. (1999) Molecular cloning, genomic organization, and functional expression of Na^+/H^+ exchanger isoform 5 (NHE5) from human brain. *J. Biol. Chem.* **274**(7), 4377-4382

10. Attaphitaya, S., Park, K., and Melvin, J. E. (1999) Molecular cloning and functional expression of a rat Na^+/H^+ exchanger (NHE5) highly expressed in brain. *J. Biol. Chem.* **274**(7), 4383-4388

11. Szabo, E. Z., Numata, M., Shull, G. E., and Orlowski, J. (2000) Kinetic and pharmacological properties of human brain Na^+/H^+ exchanger isoform 5 stably expressed in Chinese hamster ovary cells. *J. Biol. Chem.* **275**(9), 6302-6307

12. Brett, C. L., Wei, Y., Donowitz, M., and Rao, R. (2002) Human Na^+/H^+ exchanger isoform 6 is found in recycling endosomes of cells, not in mitochondria. *Am. J. Physiol. Cell Physiol.* **282**(5), C1031-1041

13. Numata, M., and Orlowski, J. (2001) Molecular cloning and characterization of a novel $(Na^+,K^+)/H^+$ exchanger localized to the trans-Golgi network. *J. Biol. Chem.* **276**(20), 17387-17394

14. Sardet, C., Franchi, A., and Pouyssegur, J. (1989) Molecular cloning, primary structure, and expression of the human growth factor-activatable Na^+/H^+ antiporter. *Cell* **56**(2), 271-280

15. Sardet, C., Counillon, L., Franchi, A., and Pouyssegur, J. (1990) Growth factors induce phosphorylation of the Na^+/H^+ antiporter, glycoprotein of 110 kD. *Science* **247**(4943), 723-726

16. Haworth, R. S., Frohlich, O., and Fliegel, L. (1993) Multiple carbohydrate moieties on the Na^+/H^+ exchanger. *Biochem. J.* **289**(Pt 3), 637-640

17. Wakabayashi, S., Fafournoux, P., Sardet, C., and Pouyssegur, J. (1992) The Na^+/H^+ antiporter cytoplasmic domain mediates growth factor signals and controls "H^+-sensing". *Proc. Natl. Acad. Sci. U.S.A.* **89**(6), 2424-2428

18. Orlowski, J., and Grinstein, S. (1997) Na^+/H^+ exchangers of mammalian cells. *J. Biol. Chem.* **272**(36), 22373-22376

19. Pedersen, S. F., O'Donnell M, E., Anderson, S. E., and Cala, P. M. (2006) Physiology and pathophysiology of Na^+/H^+ exchange and Na^+-K^+-$2Cl^-$ cotransport in the heart, brain, and blood. *Am. J. Physiol. Regul. Integr. Comp. Physiol.* **291**(1), R1-25

20. Masereel, B., Pochet, L., and Laeckmann, D. (2003) An overview of inhibitors of Na^+/H^+ exchanger. *Eur. J. Med. Chem.* **38**(6), 547-554

21. Pouyssegur, J., Sardet, C., Franchi, A., L'Allemain, G., and Paris, S. (1984) A specific mutation abolishing Na^+/H^+ antiport activity in hamster fibroblasts precludes growth at neutral and acidic pH. *Proc. Natl. Acad. Sci. U.S.A.* **81**(15), 4833-4837

22. Shrode, L. D., Cabado, A. G., Goss, G. G., and Grinstein, S. (1996) Role of the Na^+/H^+ antiporter isoforms in cell volume regulation. In: *The Na^+/H^+ Exchanger*. Fliegel, L. (ed.), R.G. Landes Company, Austin, TX, U.S.A., pp. 101-122

23. Rotin, D., and Grinstein, S. (1989) Impaired cell volume regulation in Na^+/H^+ exchange-deficient mutants. *Am. J. Physiol.* **257**(6 Pt 1), C1158-C1165

24. Grinstein, S., Rothstein, A., and Cohen, S. (1985) Mechanism of osmotic activation of Na^+/H^+ exchange in rat thymic lymphocytes. *J. Gen. Physiol.* **85**(5), 765-787

25. Bianchini, L., Kapus, A., Lukacs, G., Wasan, S., Wakabayashi, S., Pouyssegur, J., Yu, F. H., Orlowski, J., and Grinstein, S. (1995) Responsiveness of mutants of NHE1 isoform of Na^+/H^+ antiport to osmotic stress. *Am. J. Physiol.* **269**(4 Pt 1), C998-1007

26. Putney, L. K., and Barber, D. L. (2003) Na^+-H^+ exchange-dependent increase in intracellular pH times G2/M entry and transition. *J. Biol. Chem.* **278**(45), 44645-44649

27. Wang, H., Singh, D., and Fliegel, L. (1997) The Na^+/H^+ antiporter potentiates growth and retinoic acid-induced differentiation of P19 embryonal carcinoma cells. *J. Biol. Chem.* **272**(42), 26545-26549

28. Rao, G. N., Sardet, C., Pouyssegur, J., and Berk, B. C. (1992) Na^+/H^+ antiporter gene expression increases during retinoic acid-induced granulocytic differentiation of HL60 cells. *J. Cell. Physiol.* **151**(2), 361-366

29. Yang, W., Dyck, J. R., and Fliegel, L. (1996) Regulation of NHE1 expression in L6 muscle cells. *Biochim. Biophys. Acta.* **1306**(1), 107-113

30. Wu, K. L., Khan, S., Lakhe-Reddy, S., Jarad, G., Mukherjee, A., Obejero-Paz, C. A., Konieczkowski, M., Sedor, J. R., and Schelling, J. R. (2004) The NHE1 Na^+/H^+ exchanger recruits ezrin/radixin/moesin proteins to regulate Akt-dependent cell survival. *J. Biol. Chem.* **279**(25), 26280-26286

31. Wu, K. L., Khan, S., Lakhe-Reddy, S., Wang, L., Jarad, G., Miller, R. T., Konieczkowski, M., Brown, A. M., Sedor, J. R., and Schelling, J. R. (2003) Renal tubular epithelial cell apoptosis is associated with caspase cleavage of the NHE1 Na^+/H^+ exchanger. *Am. J. Physiol. Renal Physiol.* **284**(4), F829-839

32. Rich, I. N., Worthington-White, D., Garden, O. A., and Musk, P. (2000) Apoptosis of leukemic cells accompanies reduction in intracellular pH after targeted inhibition of the Na^+/H^+ exchanger. *Blood* **95**(4), 1427-1434

33. Khaled, A. R., Moor, A. N., Li, A., Kim, K., Ferris, D. K., Muegge, K., Fisher, R. J., Fliegel, L., and Durum, S. K. (2001) Trophic factor withdrawal: p38 mitogen-activated protein kinase activates NHE1, which induces intracellular alkalinization. *Mol. Cell. Biol.* **21**(22), 7545-7557

34. Fliegel, L., Sardet, C., Pouyssegur, J., and Barr, A. (1991) Identification of the protein and cDNA of the cardiac Na^+/H^+ exchanger. *FEBS Lett.* **279**(1), 25-29

35. Avkiran, M. (2003) Basic biology and pharmacology of the cardiac sarcolemmal sodium/hydrogen exchanger. *J. Card. Surg.* **18**(Suppl 1), 3-12

36. Cross, H. R., Lu, L., Steenbergen, C., Philipson, K. D., and Murphy, E. (1998) Overexpression of the cardiac Na^+/Ca^{2+} exchanger increases susceptibility to ischemia/reperfusion injury in male, but not female, transgenic mice. *Circ. Res.* **83**(12), 1215-1223

37. Karmazyn, M., Sostaric, J. V., and Gan, X. T. (2001) The myocardial Na^+/H^+ exchanger: a potential therapeutic target for the prevention of myocardial ischaemic and reperfusion injury and attenuation of postinfarction heart failure. *Drugs* **61**(3), 375-389

38. Gumina, R. J., Buerger, E., Eickmeier, C., Moore, J., Daemmgen, J., and Gross, G. J. (1999) Inhibition of the Na^+/H^+ exchanger confers greater cardioprotection against 90 minutes of myocardial ischemia than ischemic preconditioning in dogs. *Circulation* **100**(25), 2519-2526

39. Spitznagel, H., Chung, O., Xia, Q., Rossius, B., Illner, S., Jahnichen, G., Sandmann, S., Reinecke, A., Daemen, M. J., and Unger, T. (2000) Cardioprotective effects of the Na^+/H^+-exchange inhibitor cariporide in infarct-induced heart failure. *Cardiovasc. Res.* **46**(1), 102-110

40. Chen, L., Chen, C. X., Gan, X. T., Beier, N., Scholz, W., and Karmazyn, M. (2004) Inhibition and reversal of myocardial infarction-induced hypertrophy and heart failure by NHE-1 inhibition. *Am. J. Physiol. Heart Circ. Physiol.* **286**(1), H381-387

41. Baartscheer, A., Schumacher, C. A., van Borren, M. M., Belterman, C. N., Coronel, R., Opthof, T., and Fiolet, J. W. (2005) Chronic inhibition of Na^+/H^+-exchanger attenuates cardiac hypertrophy and prevents cellular remodeling in heart failure. *Cardiovasc. Res.* **65**(1), 83-92

42. Wang, Y., Meyer, J. W., Ashraf, M., and Shull, G. E. (2003) Mice with a null mutation in the NHE1 Na^+-H^+ exchanger are resistant to cardiac ischemia-reperfusion injury. *Circ. Res.* **93**(8), 776-782

43. Theroux, P., Chaitman, B. R., Danchin, N., Erhardt, L., Meinertz, T., Schroeder, J. S., Tognoni, G., White, H. D., Willerson, J. T., and Jessel, A. (2000) Inhibition of the sodium-hydrogen exchanger with cariporide to prevent myocardial infarction in high-risk ischemic situations. Main results of the GUARDIAN trial. *Circulation* **102**(25), 3032-3038

44. Zeymer, U., Suryapranata, H., Monassier, J. P., Opolski, G., Davies, J., Rasmanis, G., Linssen, G., Tebbe, U., Schroder, R., Tiemann, R., Machnig, T., and Neuhaus, K. L. (2001) The Na^+/H^+ exchange inhibitor eniporide as an adjunct to early reperfusion therapy for acute myocardial infarction. Results of the evaluation of the safety and cardioprotective effects of eniporide in acute myocardial infarction (ESCAMI) trial. *J. Am. Coll. Cardiol.* **38**(6), 1644-1650

45. Rupprecht, H. J., vom Dahl, J., Terres, W., Seyfarth, K. M., Richardt, G., Schultheibeta, H. P., Buerke, M., Sheehan, F. H., and Drexler, H. (2000) Cardioprotective effects of the Na^+/H^+ exchange inhibitor cariporide in patients with acute anterior myocardial infarction undergoing direct PTCA. *Circulation* **101**(25), 2902-2908

46. Mentzer, R. M. (2003) Effects of Na^+/H^+ exchange inhibition by cariporide on death and nonfatal myocardial infarction in patients undergoing coronary artery bypass graft surgery: The Expedition study. *Circulation* **108**, 2723 (Abstract)

47. Kusumoto, K., Haist, J. V., and Karmazyn, M. (2001) Na^+/H^+ exchange inhibition reduces hypertrophy and heart failure after myocardial infarction in rats. *Am. J. Physiol. Heart Circ. Physiol.* **280**(2), H738-745

48. Chen, L., Gan, X. T., Haist, J. V., Feng, Q., Lu, X., Chakrabarti, S., and Karmazyn, M. (2001) Attenuation of compensatory right ventricular hypertrophy and heart failure following monocrotaline-induced pulmonary vascular injury by the Na^+-H^+ exchange inhibitor cariporide. *J. Pharmacol. Exp. Ther.* **298**(2), 469-476

49. Ennis, I. L., Escudero, E. M., Console, G. M., Camihort, G., Dumm, C. G., Seidler, R. W., Camilion de Hurtado, M. C., and Cingolani, H. E. (2003) Regression of isoproterenol-induced cardiac hypertrophy by Na^+/H^+ exchanger inhibition. *Hypertension* **41**(6), 1324-1329

50. Kevelaitis, E., Qureshi, A. A., Mouas, C., Marotte, F., Kevelaitiene, S., Avkiran, M., and Menasche, P. (2005) Na^+/H^+ exchange inhibition in hypertrophied myocardium subjected to cardioplegic arrest: an effective cardioprotective approach. *Eur. J. Cardiothorac. Surg.* **27**(1), 111-116

51. Rotin, D., Steele-Norwood, D., Grinstein, S., and Tannock, I. (1989) Requirement of the Na^+/H^+ exchanger for tumor growth. *Cancer Res.* **49**(1), 205-211

52. Cardone, R. A., Casavola, V., and Reshkin, S. J. (2005) The role of disturbed pH dynamics and the Na^+/H^+ exchanger in metastasis. *Nat. Rev. Cancer* **5**(10), 786-795

53. Harguindey, S., Orive, G., Luis Pedraz, J., Paradiso, A., and Reshkin, S. J. (2005) The role of pH dynamics and the Na^+/H^+ antiporter in the etiopathogenesis and treatment of cancer. Two faces of the same coin--one single nature. *Biochim. Biophys. Acta.* **1756**(1), 1-24

54. Reshkin, S. J., Bellizzi, A., Caldeira, S., Albarani, V., Malanchi, I., Poignee, M., Alunni-Fabbroni, M., Casavola, V., and Tommasino, M. (2000) Na^+/H^+ exchanger-dependent intracellular alkalinization is an early event in malignant transformation and plays an essential role in the development of subsequent transformation-associated phenotypes. *FASEB J.* **14**(14), 2185-2197

55. Cardone, R. A., Bagorda, A., Bellizzi, A., Busco, G., Guerra, L., Paradiso, A., Casavola, V., Zaccolo, M., and Reshkin, S. J. (2005) Protein kinase A gating of a pseudopodial-located RhoA/ROCK/p38/NHE1 signal module regulates invasion in breast cancer cell lines. *Mol. Biol. Cell* **16**(7), 3117-3127

56. Reshkin, S. J., Bellizzi, A., Cardone, R. A., Tommasino, M., Casavola, V., and Paradiso, A. (2003) Paclitaxel induces apoptosis via protein kinase A- and p38 mitogen-activated protein-dependent inhibition of the Na^+/H^+ exchanger (NHE) NHE isoform 1 in human breast cancer cells. *Clin. Cancer Res.* **9**(6), 2366-2373

57. Wong, P., Kleemann, H. W., and Tannock, I. F. (2002) Cytostatic potential of novel agents that inhibit the regulation of intracellular pH. *Br. J. Cancer* **87**(2), 238-245

58. Grinstein, S., Woodside, M., Sardet, C., Pouyssegur, J., and Rotin, D. (1992) Activation of the Na^+/H^+ antiporter during cell volume regulation. Evidence for a phosphorylation-independent mechanism. *J. Biol. Chem.* **267**(33), 23823-23828

59. Denker, S. P., Huang, D. C., Orlowski, J., Furthmayr, H., and Barber, D. L. (2000) Direct binding of the Na^+-H^+ exchanger NHE1 to ERM proteins regulates the cortical cytoskeleton and cell shape independently of H^+ translocation. *Mol. Cell* **6**(6), 1425-1436

60. Karmazyn, M., Sawyer, M., and Fliegel, L. (2005) The Na^+/H^+ exchanger: a target for cardiac therapeutic intervention. *Curr. Drug Targets Cardiovasc. Haematol. Disord.* **5**(4), 323-335

61. Denker, S. P., and Barber, D. L. (2002) Cell migration requires both ion translocation and cytoskeletal anchoring by the Na^+-H^+ exchanger NHE1. *J. Cell Biol.* **159**(6), 1087-1096

62. Putney, L. K., Denker, S. P., and Barber, D. L. (2002) The changing face of the Na^+/H^+ exchanger, NHE1: structure, regulation, and cellular actions. *Annu. Rev. Pharmacol. Toxicol.* **42**, 527-552

63. Baumgartner, M., Patel, H., and Barber, D. L. (2004) Na^+/H^+ exchanger NHE1 as plasma membrane scaffold in the assembly of signaling complexes. *Am. J. Physiol. Cell Physiol.* **287**(4), C844-850

64. Avkiran, M., and Haworth, R. S. (2003) Regulatory effects of G protein-coupled receptors on cardiac sarcolemmal Na^+/H^+ exchanger activity: signaling and significance. *Cardiovasc. Res.* **57**(4), 942-952

65. Sardet, C., Fafournoux, P., and Pouyssegur, J. (1991) Alpha-thrombin, epidermal growth factor, and okadaic acid activate the Na^+/H^+ exchanger, NHE-1, by phosphorylating a set of common sites. *J. Biol. Chem.* **266**(29), 19166-19171

66. Haworth, R. S., McCann, C., Snabaitis, A. K., Roberts, N. A., and Avkiran, M. (2003) Stimulation of the plasma membrane Na^+/H^+ exchanger NHE1 by sustained intracellular acidosis. Evidence for a novel mechanism mediated by the ERK pathway. *J. Biol. Chem.* **278**(34), 31676-31684

67. Moor, A. N., and Fliegel, L. (1999) Protein kinase-mediated regulation of the Na^+/H^+ exchanger in the rat myocardium by mitogen-activated protein kinase-dependent pathways. *J. Biol. Chem.* **274**(33), 22985-22992

68. Wang, H., Silva, N. L., Lucchesi, P. A., Haworth, R., Wang, K., Michalak, M., Pelech, S., and Fliegel, L. (1997) Phosphorylation and regulation of the Na^+/H^+ exchanger through mitogen-activated protein kinase. *Biochemistry* **36**(30), 9151-9158

69. Snabaitis, A. K., Yokoyama, H., and Avkiran, M. (2000) Roles of mitogen-activated protein kinases and protein kinase C in alpha(1A)-adrenoceptor-mediated stimulation of the sarcolemmal Na^+-H^+ exchanger. *Circ. Res.* **86**(2), 214-220

70. Takahashi, E., Abe, J., and Berk, B. C. (1997) Angiotensin II stimulates p90rsk in vascular smooth muscle cells. A potential Na^+-H^+ exchanger kinase. *Circ. Res.* **81**(2), 268-273

71. Takahashi, E., Abe, J., Gallis, B., Aebersold, R., Spring, D. J., Krebs, E. G., and Berk, B. C. (1999) p90(RSK) is a serum-stimulated Na^+/H^+ exchanger isoform-1 kinase. Regulatory phosphorylation of serine 703 of Na^+/H^+ exchanger isoform-1. *J. Biol. Chem.* **274**(29), 20206-20214

72. Tominaga, T., Ishizaki, T., Narumiya, S., and Barber, D. L. (1998) p160ROCK mediates RhoA activation of Na^+-H^+ exchange. *EMBO J.* **17**(16), 4712-4722

73. Yan, W., Nehrke, K., Choi, J., and Barber, D. L. (2001) The Nck-interacting kinase (NIK) phosphorylates the Na^+-H^+ exchanger NHE1 and regulates NHE1 activation by platelet-derived growth factor. *J. Biol. Chem.* **276**(33), 31349-31356

74. Fliegel, L., Walsh, M. P., Singh, D., Wong, C., and Barr, A. (1992) Phosphorylation of the C-terminal domain of the Na^+/H^+ exchanger by Ca^{2+}/calmodulin-dependent protein kinase II. *Biochem. J.* **282**(Pt 1), 139-145

75. Kusuhara, M., Takahashi, E., Peterson, T. E., Abe, J., Ishida, M., Han, J., Ulevitch, R., and Berk, B. C. (1998) p38 Kinase is a negative regulator of angiotensin II signal transduction in vascular smooth muscle cells: effects on Na^+/H^+ exchange and ERK1/2. *Circ. Res.* **83**(8), 824-831

76. Haworth, R. S., Sinnett-Smith, J., Rozengurt, E., and Avkiran, M. (1999) Protein kinase D inhibits plasma membrane Na^+/H^+ exchanger activity. *Am. J. Physiol.* **277**(6 Pt 1), C1202-1209

77. Sauvage, M., Maziere, P., Fathallah, H., and Giraud, F. (2000) Insulin stimulates NHE1 activity by sequential activation of phosphatidylinositol 3-kinase and protein kinase C zeta in human erythrocytes. *Eur. J. Biochem.* **267**(4), 955-962

78. Misik, A. J., Perreault, K., Holmes, C. F., and Fliegel, L. (2005) Protein phosphatase regulation of Na^+/H^+ exchanger isoform I. *Biochemistry* **44**(15), 5842-5852

79. Bertrand, B., Wakabayashi, S., Ikeda, T., Pouyssegur, J., and Shigekawa, M. (1994) The Na^+/H^+ exchanger isoform 1 (NHE1) is a novel member of the calmodulin-binding proteins. Identification and characterization of calmodulin-binding sites. *J. Biol. Chem.* **269**(18), 13703-13709

80. Wakabayashi, S., Bertrand, B., Ikeda, T., Pouyssegur, J., and Shigekawa, M. (1994) Mutation of calmodulin-binding site renders the Na^+/H^+ exchanger (NHE1) highly H^+-sensitive and Ca^{2+} regulation-defective. *J. Biol. Chem.* **269**(18), 13710-13715

81. Li, X., Ding, J., Liu, Y., Brix, B. J., and Fliegel, L. (2004) Functional analysis of acidic amino acids in the cytosolic tail of the Na^+/H^+ exchanger. *Biochemistry* **43**(51), 16477-16486

82. Lin, X., and Barber, D. L. (1996) A calcineurin homologous protein inhibits GTPase-stimulated Na^+-H^+ exchange. *Proc. Natl. Acad. Sci. U.S.A.* **93**(22), 12631-12636

83. Pang, T., Hisamitsu, T., Mori, H., Shigekawa, M., and Wakabayashi, S. (2004) Role of calcineurin B homologous protein in pH regulation by the Na^+/H^+ exchanger 1: tightly bound Ca^{2+} ions as important structural elements. *Biochemistry* **43**(12), 3628-3636

84. Pang, T., Su, X., Wakabayashi, S., and Shigekawa, M. (2001) Calcineurin homologous protein as an essential cofactor for Na^+/H^+ exchangers. *J. Biol. Chem.* **276**(20), 17367-17372

85. Pang, T., Wakabayashi, S., and Shigekawa, M. (2002) Expression of calcineurin B homologous protein 2 protects serum deprivation-induced cell death by serum-independent activation of Na^+/H^+ exchanger. *J. Biol. Chem.* **277**(46), 43771-43777

86. Mailander, J., Muller-Esterl, W., and Dedio, J. (2001) Human homolog of mouse tescalcin associates with Na^+/H^+ exchanger type-1. *FEBS Lett.* **507**(3), 331-335

87. Li, X., Liu, Y., Kay, C. M., Muller-Esterl, W., and Fliegel, L. (2003) The Na^+/H^+ exchanger cytoplasmic tail: structure, function, and interactions with tescalcin. *Biochemistry* **42**(24), 7448-7456

88. Li, X., Liu, Y., Alvarez, B. V., Casey, J. R., and Fliegel, L. (2006) A novel carbonic anhydrase II binding site regulates NHE1 activity. *Biochemistry* **45**(7), 2414-2424

89. Li, X., Alvarez, B., Casey, J. R., Reithmeier, R. A., and Fliegel, L. (2002) Carbonic anhydrase II binds to and enhances activity of the Na^+/H^+ exchanger. *J. Biol. Chem.* **277**(39), 36085-36091

90. Lehoux, S., Abe, J., Florian, J. A., and Berk, B. C. (2001) 14-3-3 Binding to Na^+/H^+ exchanger isoform-1 is associated with serum-dependent activation of Na^+/H^+ exchange. *J. Biol. Chem.* **276**(19), 15794-15800

91. Silva, N. L., Haworth, R. S., Singh, D., and Fliegel, L. (1995) The carboxyl-terminal region of the Na^+/H^+ exchanger interacts with mammalian heat shock protein. *Biochemistry* **34**(33), 10412-10420

92. Aharonovitz, O., Zaun, H. C., Balla, T., York, J. D., Orlowski, J., and Grinstein, S. (2000) Intracellular pH regulation by Na^+/H^+ exchange requires phosphatidylinositol 4,5-bisphosphate. *J. Cell Biol.* **150**(1), 213-224

93. Fliegel, L. (2001) Regulation of myocardial Na^+/H^+ exchanger activity. *Basic Res. Cardiol.* **96**(4), 301-305

94. Dyck, J. R., Lopaschuk, G. D., and Fliegel, L. (1992) Identification of a small Na^+/H^+ exchanger-like message in the rabbit myocardium. *FEBS Lett.* **310**(3), 255-259

95. Gan, X. T., Chakrabarti, S., and Karmazyn, M. (1999) Modulation of Na^+/H^+ exchange isoform 1 mRNA expression in isolated rat hearts. *Am. J. Physiol.* **277**(3 Pt 2), H993-998

96. Sandmann, S., Yu, M., Kaschina, E., Blume, A., Bouzinova, E., Aalkjaer, C., and Unger, T. (2001) Differential effects of angiotensin AT1 and AT2 receptors on the expression, translation and function of the Na^+-H^+ exchanger and Na^+-$HCO3^-$ symporter in the rat heart after myocardial infarction. *J. Am. Coll. Cardiol.* **37**(8), 2154-2165

97. Dyck, J. R., Silva, N. L., and Fliegel, L. (1995) Activation of the Na^+/H^+ exchanger gene by the transcription factor AP-2. *J. Biol. Chem.* **270**(3), 1375-1381

98. Yang, W., Dyck, J. R., Wang, H., and Fliegel, L. (1996) Regulation of NHE-1 promoter in mammalian myocardium. *Am. J. Physiol.* **270**(1 Pt 2), H259-266

99. Rieder, C. V., and Fliegel, L. (2003) Transcriptional regulation of Na^+/H^+ exchanger expression in the intact mouse. *Mol. Cell. Biochem.* **243**(1-2), 87-95

100. Yang, W., Wang, H., and Fliegel, L. (1996) Regulation of Na^+/H^+ exchanger gene expression. Role of a novel poly(dA.dT) element in regulation of the NHE1 promoter. *J. Biol. Chem.* **271**(34), 20444-20449

101. Fernandez-Rachubinski, F., and Fliegel, L. (2001) COUP-TFI and COUP-TFII regulate expression of the NHE through a nuclear hormone responsive element with enhancer activity. *Eur. J. Biochem.* **268**(3), 620-634

102. Slepkov, E., and Fliegel, L. (2004) Regulation of expression of the Na^+/H^+ exchanger by thyroid hormone. *Vitam. Horm.* **69**, 249-269

103. Li, X., Misik, A. J., Rieder, C. V., Solaro, R. J., [illegible] A., and Fliegel, L. (2002) Thyroid hormone receptor alpha 1 regulates expression of the Na^+/H^+ exchanger (NHE1). *J. Biol. Chem.* **277**(32), 28656-28662

104. Counillon, L., Scholz, W., Lang, H. J., and Pouyssegur, J. (1993) Pharmacological characterization of stably transfected Na^+/H^+ antiporter isoforms using amiloride analogs and a new inhibitor exhibiting anti-ischemic properties. *Mol. Pharmacol.* **44**(5), 1041-1045

105. Harris, C., and Fliegel, L. (1999) Amiloride and the Na^+/H^+ exchanger protein: mechanism and significance of inhibition of the Na^+/H^+ exchanger. *Int. J. Mol. Med.* **3**(3), 315-321

106. Kleyman, T. R., and Cragoe, E. J., Jr. (1988) Amiloride and its analogs as tools in the study of ion transport. *J. Membr. Biol.* **105**(1), 1-21

107. Hunte, C., Screpanti, E., Venturi, M., Rimon, A., Padan, E., and Michel, H. (2005) Structure of a Na^+/H^+ antiporter and insights into mechanism of action and regulation by pH. *Nature* **435**(7046), 1197-1202

108. Counillon, L., Pouyssegur, J., and Reithmeier, R. A. (1994) The Na^+/H^+ exchanger NHE-1 possesses N- and O-linked glycosylation restricted to the first N-terminal extracellular domain. *Biochemistry* **33**(34), 10463-10469

109. Fliegel, L., Haworth, R. S., and Dyck, J. R. (1993) Characterization of the placental brush border membrane Na^+/H^+ exchanger: identification of thiol-dependent transitions in apparent molecular size. *Biochem. J.* **289**, 101-107

110. Fafournoux, P., Noel, J., and Pouyssegur, J. (1994) Evidence that Na^+/H^+ exchanger isoforms NHE1 and NHE3 exist as stable dimers in membranes with a high degree of specificity for homodimers. *J. Biol. Chem.* **269**(4), 2589-2596

111. Hisamitsu, T., Pang, T., Shigekawa, M., and Wakabayashi, S. (2004) Dimeric interaction between the cytoplasmic domains of the Na^+/H^+ exchanger NHE1 revealed by symmetrical intermolecular cross-linking and selective co-immunoprecipitation. *Biochemistry* **43**(34), 11135-11143

112. Wakabayashi, S., Pang, T., Su, X., and Shigekawa, M. (2000) A novel topology model of the human Na^+/H^+ exchanger isoform 1. *J. Biol. Chem.* **275**(11), 7942-7949

113. Meyer, S., and Dutzler, R. (2006) Crystal structure of the cytoplasmic domain of the chloride channel ClC-0. *Structure* **14**(2), 299-307

114. Li, Y., Fanning, A. S., Anderson, J. M., and Lavie, A. (2005) Structure of the conserved cytoplasmic C-terminal domain of occludin: identification of the ZO-1 binding surface. *J. Mol. Biol.* **352**(1), 151-164

115. Gulbis, J. M., Zhou, M., Mann, S., and MacKinnon, R. (2000) Structure of the cytoplasmic beta subunit-T1 assembly of voltage-dependent K^+ channels. *Science* **289**(5476), 123-127

116. Zhang, D., Kiyatkin, A., Bolin, J. T., and Low, P. S. (2000) Crystallographic structure and functional interpretation of the cytoplasmic domain of erythrocyte membrane band 3. *Blood* **96**(9), 2925-2933

117. Gebreselassie, D., Rajarathnam, K., and Fliegel, L. (1998) Expression, purification, and characterization of the carboxyl-terminal region of the Na^+/H^+ exchanger. *Biochem. Cell Biol.* **76**(5), 837-842

118. Padan, E., Tzubery, T., Herz, K., Kozachkov, L., Rimon, A., and Galili, L. (2004) NhaA of *Escherichia coli*, as a model of a pH-regulated Na^+/H^+ antiporter. *Biochim. Biophys. Acta.* **1658**(1-2), 2-13

119. Dibrov, P., and Fliegel, L. (1998) Comparative molecular analysis of Na^+/H^+ exchangers: a unified model for Na^+/H^+ antiport? *FEBS Lett.* **424**(1-2), 1-5

120. Wiebe, C. A., DiBattista, E. R., and Fliegel, L. (2001) Functional role of polar amino acid residues in Na^+/H^+ exchangers. *Biochem. J.* **357**(Pt 1), 1-10

121. Dutzler, R., Campbell, E. B., Cadene, M., Chait, B. T., and MacKinnon, R. (2002) X-ray structure of a ClC chloride channel at 3.0 Å reveals the molecular basis of anion selectivity. *Nature* **415**(6869), 287-294

122. Khademi, S., O'Connell, J., Remis, J., Robles-Colmenares, Y., Miercke, L. J., and Stroud, R. M. (2004) Mechanism of ammonia transport by Amt/MEP/Rh: structure of AmtB at 1.35 Å. *Science* **305**(5690), 1587-1594

123. Kinsella, J. L., Heller, P., and Froehlich, J. P. (1998) Na^+/H^+ exchanger: proton modifier site regulation of activity. *Biochem. Cell Biol.* **76**(5), 743-749

124. Wakabayashi, S., Hisamitsu, T., Pang, T., and Shigekawa, M. (2003) Mutations of Arg440 and Gly455/Gly456 oppositely change pH sensing of Na^+/H^+ exchanger 1. *J. Biol. Chem.* **278**(14), 11828-11835

125. Gerchman, Y., Rimon, A., Venturi, M., and Padan, E. (2001) Oligomerization of NhaA, the Na^+/H^+ antiporter of *Escherichia coli* in the membrane and its functional and structural consequences. *Biochemistry* **40**(11), 3403-3412

126. Vinothkumar, K. R., Smits, S. H., and Kuhlbrandt, W. (2005) pH-induced structural change in a sodium/proton antiporter from *Methanococcus jannaschii*. *EMBO J.* **24**(15), 2720-2729

127. Orlowski, J., and Kandasamy, R. A. (1996) Delineation of transmembrane domains of the Na^+/H^+ exchanger that confer sensitivity to pharmacological antagonists. *J. Biol. Chem.* **271**(33), 19922-19927

128. Yun, C. H., Little, P. J., Nath, S. K., Levine, S. A., Pouyssegur, J., Tse, C. M., and Donowitz, M. (1993) Leu143 in the putative fourth membrane spanning domain is critical for amiloride inhibition of an epithelial Na^+/H^+ exchanger isoform (NHE-2). *Biochem. Biophys. Res. Commun.* **193**(2), 532-539

129. Wang, D., Balkovetz, D. F., and Warnock, D. G. (1995) Mutational analysis of transmembrane histidines in the amiloride-sensitive Na^+/H^+ exchanger. *Am. J. Physiol.* **269**(2 Pt 1), C392-C402

130. Counillon, L., Franchi, A., and Pouyssegur, J. (1993) A point mutation of the Na^+/H^+ exchanger gene (NHE1) and amplification of the mutated allele confer amiloride resistance upon chronic acidosis. *Proc. Natl. Acad. Sci. U.S.A.* **90**(10), 4508-4512

131. Counillon, L., Noel, J., Reithmeier, R. A., and Pouyssegur, J. (1997) Random mutagenesis reveals a novel site involved in inhibitor interaction within the fourth transmembrane segment of the Na^+/H^+ exchanger-1. *Biochemistry* **36**(10), 2951-2959

132. Touret, N., Poujeol, P., and Counillon, L. (2001) Second-site revertants of a low-sodium-affinity mutant of the Na^+/H^+ exchanger reveal the participation of TM4 into a highly constrained sodium-binding site. *Biochemistry* **40**(16), 5095-5101

133. Murtazina, R., Booth, B. J., Bullis, B. L., Singh, D. N., and Fliegel, L. (2001) Functional analysis of polar amino-acid residues in membrane associated regions of the NHE1 isoform of the mammalian Na^+/H^+ exchanger. *Eur. J. Biochem.* **268**(17), 4674-4685

134. Noel, J., Germain, D., and Vadnais, J. (2003) Glutamate 346 of human Na^+-H^+ exchanger NHE1 is crucial for modulating both the affinity for Na^+ and the interaction with amiloride derivatives. *Biochemistry* **42**(51), 15361-15368

135. Wakabayashi, S., Pang, T., Su, X., and Shigekawa, M. (2000) Second mutations rescue point mutant of the Na^+/H^+ exchanger NHE1 showing defective surface expression. *FEBS Lett.* **487**(2), 257-261

136. Wakabayashi, S., Hisamitsu, T., Pang, T., and Shigekawa, M. (2003) Kinetic dissection of two distinct proton binding sites in Na^+/H^+ exchangers by measurement of reverse mode reaction. *J. Biol. Chem.* **278**(44), 43580-43585

137. Su, X., Pang, T., Wakabayashi, S., and Shigekawa, M. (2003) Evidence for involvement of the putative first extracellular loop in differential volume sensitivity of the Na^+/H^+ exchangers NHE1 and NHE2. *Biochemistry* **42**(4), 1086-1094

138. Dibrov, P., Murtazina, R., Kinsella, J., and Fliegel, L. (2000) Characterization of a histidine rich cluster of amino acids in the cytoplasmic domain of the Na^+/H^+ exchanger. *Biosci. Rep.* **20**(3), 185-197

139. Wang, H., Singh, D., and Fliegel, L. (1998) Functional role of cysteine residues in the Na^+/H^+ exchanger effects of mutation of cysteine residues on targeting and activity of the Na^+/H^+ exchanger. *Arch. Biochem. Biophys.* **358**(1), 116-124

140. Slepkov, E. R., Chow, S., Lemieux, M. J., and Fliegel, L. (2004) Proline residues in transmembrane segment IV are critical for activity, expression and targeting of the Na^+/H^+ exchanger isoform 1. *Biochem. J.* **379**(Pt 1), 31-38

141. Michalak, M., Fliegel, L., and Wlasichuk, K. (1990) Isolation and characterization of calcium binding glycoproteins of cardiac sarcolemmal vesicles. *J. Biol. Chem.* **265**(10), 5869-5874

142. Sterling, D., and Casey, J. R. (1999) Transport activity of AE3 chloride/bicarbonate anion-exchange proteins and their regulation by intracellular pH. *Biochem. J.* **344**(Pt 1), 221-229

143. Chaillet, J. R., and Boron, W. F. (1985) Intracellular calibration of a pH-sensitive dye in isolated, perfused salamander proximal tubules. *J. Gen. Physiol.* **86**(6), 765-794

144. Thomas, J. A., Buchsbaum, R. N., Zimniak, A., and Racker, E. (1979) Intracellular pH measurements in Ehrlich ascites tumor cells utilizing spectroscopic probes generated in situ. *Biochemistry* **18**(11), 2210-2218

145. Pressman, B. C. (1976) Biological applications of ionophores. *Annu. Rev. Biochem.* **45**, 501-530

146. Franchi, A., Perucca-Lostanlen, D., and Pouyssegur, J. (1986) Functional expression of a human Na^+/H^+ antiporter gene transfected into antiporter-deficient mouse L cells. *Proc. Natl. Acad. Sci. U.S.A.* **83**(24), 9388-9392

147. Tang, X. B., and Casey, J. R. (1999) Trapping of inhibitor-induced conformational changes in the erythrocyte membrane anion exchanger AE1. *Biochemistry* **38**(44), 14565-14572

148. Cabantchik, Z. I., and Greger, R. (1992) Chemical probes for anion transporters of mammalian cell membranes. *Am. J. Physiol.* **262**(4 Pt 1), C803-827

149. Ghishan, F. K., Knobel, S. M., and Summar, M. (1995) Molecular cloning, sequencing, chromosomal localization, and tissue distribution of the human Na^+/H^+ exchanger (SLC9A2). *Genomics* **30**(1), 25-30

150. Brant, S. R., Yun, C. H., Donowitz, M., and Tse, C. M. (1995) Cloning, tissue distribution, and functional analysis of the human Na^+/H^+ exchanger isoform, NHE3. *Am. J. Physiol.* **269**(1 Pt 1), C198-206

151. Numata, M., Petrecca, K., Lake, N., and Orlowski, J. (1998) Identification of a mitochondrial Na^+/H^+ exchanger. *J. Biol. Chem.* **273**(12), 6951-6959

152. Goyal, S., Vanden Heuvel, G., and Aronson, P. S. (2003) Renal expression of novel Na^+/H^+ exchanger isoform NHE8. *Am. J. Physiol. Renal Physiol.* **284**(3), F467-473

153. Nehrke, K., and Melvin, J. E. (2002) The NHX family of Na^+-H^+ exchangers in *Caenorhabditis elegans*. *J. Biol. Chem.* **277**(32), 29036-29044

154. Barlow, D. J., and Thornton, J. M. (1988) Helix geometry in proteins. *J. Mol. Biol.* **201**(3), 601-619

155. Sansom, M. S. (1992) Proline residues in transmembrane helices of channel and transport proteins: a molecular modeling study. *Protein Eng.* **5**(1), 53-60

156. von Heijne, G. (1991) Proline kinks in transmembrane alpha-helices. *J. Mol. Biol.* **218**(3), 499-503

157. Huang, Y., Lemieux, M. J., Song, J., Auer, M., and Wang, D. N. (2003) Structure and mechanism of the glycerol-3-phosphate transporter from *Escherichia coli*. *Science* **301**(5633), 616-620

158. Abramson, J., Smirnova, I., Kasho, V., Verner, G., Kaback, H. R., and Iwata, S. (2003) Structure and mechanism of the lactose permease of *Escherichia coli*. *Science* **301**(5633), 610-615

159. Karplus, K., Barrett, C., and Hughey, R. (1998) Hidden Markov models for detecting remote protein homologies. *Bioinformatics* **14**(10), 846-856

160. Kabsch, W., and Sander, C. (1983) Dictionary of protein secondary structure: pattern recognition of hydrogen-bonded and geometrical features. *Biopolymers* **22**(12), 2577-2637

161. Lin, Z., Itokawa, M., and Uhl, G. R. (2000) Dopamine transporter proline mutations influence dopamine uptake, cocaine analog recognition, and expression. *FASEB J.* **14**(5), 715-728

162. Hong, S., Ryu, K. S., Oh, M. S., Ji, I., and Ji, T. H. (1997) Roles of transmembrane prolines and proline-induced kinks of the lutropin/choriogonadotropin receptor. *J. Biol. Chem.* **272**(7), 4166-4171

163. Wellner, M., Monden, I., Mueckler, M. M., and Keller, K. (1995) Functional consequences of proline mutations in the putative transmembrane segments 6 and 10 of the glucose transporter GLUT1. *Eur. J. Biochem.* **227**(1-2), 454-458

164. Bross, P., Corydon, T. J., Andresen, B. S., Jorgensen, M. M., Bolund, L., and Gregersen, N. (1999) Protein misfolding and degradation in genetic diseases. *Hum. Mutat.* **14**(3), 186-198

165. Gregersen, N., Bross, P., Andrese, B. S., Pedersen, C. B., Corydon, T. J., and Bolund, L. (2001) The role of chaperone-assisted folding and quality control in inborn errors of metabolism: protein folding disorders. *J. Inherit. Metab. Dis.* **24**(2), 189-212

166. Lu, H., Marti, T., and Booth, P. J. (2001) Proline residues in transmembrane alpha helices affect the folding of bacteriorhodopsin. *J. Mol. Biol.* **308**(2), 437-446

167. Consler, T. G., Tsolas, O., and Kaback, H. R. (1991) Role of proline residues in the structure and function of a membrane transport protein. *Biochemistry* **30**(5), 1291-1298

168. Shelden, M. C., Loughlin, P., Tierney, M. L., and Howitt, S. M. (2001) Proline residues in two tightly coupled helices of the sulphate transporter, SHST1, are important for sulphate transport. *Biochem. J.* **356**(Pt 2), 589-594

169. Brandl, C. J., and Deber, C. M. (1986) Hypothesis about the function of membrane-buried proline residues in transport proteins. *Proc. Natl. Acad. Sci. U.S.A.* **83**(4), 917-921

170. von Heijne, G., and Gavel, Y. (1988) Topogenic signals in integral membrane proteins. *Eur. J. Biochem.* **174**(4), 671-678

171. Vilsen, B., Andersen, J. P., Clarke, D. M., and MacLennan, D. H. (1989) Functional consequences of proline mutations in the cytoplasmic and transmembrane sectors of the Ca^{2+}-ATPase of sarcoplasmic reticulum. *J. Biol. Chem.* **264**(35), 21024-21030

172. Deane, C. M., and Lummis, S. C. (2001) The role and predicted propensity of conserved proline residues in the 5-HT_3 receptor. *J. Biol. Chem.* **276**(41), 37962-37966

173. Tamori, Y., Hashiramoto, M., Clark, A. E., Mori, H., Muraoka, A., Kadowaki, T., Holman, G. D., and Kasuga, M. (1994) Substitution at Pro385 of GLUT1 perturbs the glucose transport function by reducing conformational flexibility. *J. Biol. Chem.* **269**(4), 2982-2986

174. Lolkema, J. S., Puttner, I. B., and Kaback, H. R. (1988) Site-directed mutagenesis of Pro327 in the *lac* permease of *Escherichia coli*. *Biochemistry* **27**(22), 8307-8310

175. Cordes, F. S., Bright, J. N., and Sansom, M. S. (2002) Proline-induced distortions of transmembrane helices. *J. Mol. Biol.* **323**(5), 951-960

176. Chou, P. Y., and Fasman, G. D. (1978) Prediction of the secondary structure of proteins from their amino acid sequence. *Adv. Enzymol. Relat. Areas Mol. Biol.* **47**, 45-148

177. Blaber, M., Zhang, X. J., and Matthews, B. W. (1993) Structural basis of amino acid alpha helix propensity. *Science* **260**(5114), 1637-1640

178. Mattson, G., Conklin, E., Desai, S., Nielander, G., Savage, M. D., and Morgensen, S. (1993) A practical approach to crosslinking. *Mol. Biol. Rep.* **17**(3), 167-183

179. Kenyon, G. L., and Bruice, T. W. (1977) Novel sulfhydryl reagents. *Methods Enzymol.* **47**, 407-430

180. Karlin, A., and Akabas, M. H. (1998) Substituted-cysteine accessibility method. *Methods Enzymol.* **293**, 123-145

181. Akabas, M. H., Stauffer, D. A., Xu, M., and Karlin, A. (1992) Acetylcholine receptor channel structure probed in cysteine- substitution mutants. *Science* **258**(5080), 307-310

182. Dunten, R. L., Sahin-Toth, M., and Kaback, H. R. (1993) Cysteine scanning mutagenesis of putative helix XI in the lactose permease of *Escherichia coli*. *Biochemistry* **32**(47), 12644-12650

183. Tang, X. B., Kovacs, M., Sterling, D., and Casey, J. R. (1999) Identification of residues lining the translocation pore of human AE1, plasma membrane anion exchange protein. *J. Biol. Chem.* **274**(6), 3557-3564

184. Holmgren, M., Liu, Y., Xu, Y., and Yellen, G. (1996) On the use of thiol-modifying agents to determine channel topology. *Neuropharmacology* **35**(7), 797-804

185. Yan, R. T., and Maloney, P. C. (1995) Residues in the pathway through a membrane transporter. *Proc. Natl. Acad. Sci. U.S.A.* **92**(13), 5973-5976

186. Slotboom, D. J., Konings, W. N., and Lolkema, J. S. (2001) Cysteine-scanning mutagenesis reveals a highly amphipathic, pore-lining membrane-spanning helix in the glutamate transporter GltT. *J. Biol. Chem.* **276**(14), 10775-10781

187. Doering, A. E., Nicoll, D. A., Lu, Y., Lu, L., Weiss, J. N., and Philipson, K. D. (1998) Topology of a functionally important region of the cardiac Na^+/Ca^{2+} exchanger. *J. Biol. Chem.* **273**(2), 778-783

188. Nicoll, D. A., Ottolia, M., Lu, L., Lu, Y., and Philipson, K. D. (1999) A new topological model of the cardiac sarcolemmal Na^+-Ca^{2+} exchanger. *J. Biol. Chem.* **274**(2), 910-917

189. Hruz, P. W., and Mueckler, M. M. (1999) Cysteine-scanning mutagenesis of transmembrane segment 7 of the GLUT1 glucose transporter. *J. Biol. Chem.* **274**(51), 36176-36180

190. Hruz, P. W., and Mueckler, M. M. (2000) Cysteine-scanning mutagenesis of transmembrane segment 11 of the GLUT1 facilitative glucose transporter. *Biochemistry* **39**(31), 9367-9372

191. Mueckler, M., and Makepeace, C. (1999) Transmembrane segment 5 of the Glut1 glucose transporter is an amphipathic helix that forms part of the sugar permeation pathway. *J. Biol. Chem.* **274**(16), 10923-10926

192. Olsowski, A., Monden, I., Krause, G., and Keller, K. (2000) Cysteine scanning mutagenesis of helices 2 and 7 in GLUT1 identifies an exofacial cleft in both transmembrane segments. *Biochemistry* **39**(10), 2469-2474

193. Frillingos, S., Sahin-Toth, M., Wu, J., and Kaback, H. R. (1998) Cys-scanning mutagenesis: a novel approach to structure function relationships in polytopic membrane proteins. *FASEB J.* **12**(13), 1281-1299

194. He, M. M., Sun, J., and Kaback, H. R. (1996) Cysteine-scanning mutagenesis of transmembrane domain XII and the flanking periplasmic loop in the lactose permease of *Escherichia coli*. *Biochemistry* **35**(39), 12909-12914

195. Liu, J., and Siegelbaum, S. A. (2000) Change of pore helix conformational state upon opening of cyclic nucleotide-gated channels. *Neuron* **28**(3), 899-909

196. Galili, L., Rothman, A., Kozachkov, L., Rimon, A., and Padan, E. (2002) Trans membrane domain IV is involved in ion transport activity and pH regulation of the NhaA-Na^+/H^+ antiporter of *Escherichia coli*. *Biochemistry* **41**(2), 609-617

197. Akabas, M. H., Kaufmann, C., Archdeacon, P., and Karlin, A. (1994) Identification of acetylcholine receptor channel-lining residues in the entire M2 segment of the alpha subunit. *Neuron* **13**(4), 919-927

198. Miyazawa, A., Fujiyoshi, Y., and Unwin, N. (2003) Structure and gating mechanism of the acetylcholine receptor pore. *Nature* **423**(6943), 949-955

199. Sorgen, P. L., Hu, Y., Guan, L., Kaback, H. R., and Girvin, M. E. (2002) An approach to membrane protein structure without crystals. *Proc. Natl. Acad. Sci. U.S.A.* **99**(22), 14037-14040

200. Slepkov, E. R., Rainey, J. K., Li, X., Liu, Y., Cheng, F. J., Lindhout, D. A., Sykes, B. D., and Fliegel, L. (2005) Structural and functional characterization of transmembrane segment IV of the NHE1 isoform of the Na^+/H^+ exchanger. *J. Biol. Chem.* **280**(18), 17863-17872

201. Stauffer, D. A., and Karlin, A. (1994) Electrostatic potential of the acetylcholine binding sites in the nicotinic receptor probed by reactions of binding-site cysteines with charged methanethiosulfonates. *Biochemistry* **33**(22), 6840-6849

202. Kimura-Someya, T., Iwaki, S., and Yamaguchi, A. (1998) Site-directed chemical modification of cysteine-scanning mutants as to transmembrane segment II and its flanking regions of the Tn10-encoded metal-tetracycline/H^+ antiporter reveals a transmembrane water-filled channel. *J. Biol. Chem.* **273**(49), 32806-32811

203. Loo, T. W., and Clarke, D. M. (1999) Identification of residues in the drug-binding domain of human P-glycoprotein. Analysis of transmembrane segment 11 by cysteine-scanning mutagenesis and inhibition by dibromobimane. *J. Biol. Chem.* **274**(50), 35388-35392

204. Wang, J.J., Hodges, R. S., and Sykes, B. D. (1995) Generating multiple conformations of flexible peptides in solution based on NMR nuclear Overhauser effect data: Application to desmopressin. *J. Am. Chem. Soc.* **117**, 8627-8634

205. Spadaccini, R., and Temussi, P. A. (2001) Natural peptide analgesics: the role of solution conformation. *Cell. Mol. Life Sci.* **58**(11), 1572-1582

206. Girvin, M. E., Rastogi, V. K., Abildgaard, F., Markley, J. L., and Fillingame, R. H. (1998) Solution structure of the transmembrane H^+-transporting subunit c of the F_1F_0 ATP synthase. *Biochemistry* **37**(25), 8817-8824

207. Katragadda, M., Alderfer, J. L., and Yeagle, P. L. (2001) Assembly of a polytopic membrane protein structure from the solution structures of overlapping peptide fragments of bacteriorhodopsin. *Biophys. J.* **81**(2), 1029-1036

208. Henry, G. D., and Sykes, B. D. (1994) Methods to study membrane protein structure in solution. *Methods Enzymol.* **239**, 515-535

209. Fimmel, A. L., Jans, D. A., Langman, L., James, L. B., Ash, G. R., Downie, J. A., Senior, A. E., Gibson, F., and Cox, G. B. (1983) The F_1F_0-ATPase of *Escherichia coli*. Substitution of proline by leucine at position 64 in the c-subunit causes loss of oxidative phosphorylation. *Biochem. J.* **213**(2), 451-458

210. Dmitriev, O. Y., and Fillingame, R. H. (2001) Structure of Ala(20) --> Pro/Pro(64) --> Ala substituted subunit c of *Escherichia coli* ATP synthase in which the essential proline is switched between transmembrane helices. *J. Biol. Chem.* **276**(29), 27449-27454

211. Rimon, A., Gerchman, Y., Kariv, Z., and Padan, E. (1998) A point mutation (G338S) and its suppressor mutations affect both the pH response of the NhaA-Na^+/H^+ antiporter as well as the growth phenotype of *Escherichia coli*. *J. Biol. Chem.* **273**(41), 26470-26476

212. Kaback, H. R. (1997) A molecular mechanism for energy coupling in a membrane transport protein, the lactose permease of *Escherichia coli*. *Proc. Natl. Acad. Sci. U.S.A.* **94**(11), 5539-5543

213. Qiu, Z., Nicoll, D. A., and Philipson, K. D. (2001) Helix packing of functionally important regions of the cardiac Na^+-Ca^{2+} exchanger. *J. Biol. Chem.* **276**(1), 194-199

214. Loo, T. W., and Clarke, D. M. (2000) The packing of the transmembrane segments of human multidrug resistance P-glycoprotein is revealed by disulfide cross-linking analysis. *J. Biol. Chem.* **275**(8), 5253-5256

215. Wu, J., Hardy, D., and Kaback, H. R. (1999) Site-directed chemical cross-linking demonstrates that helix IV is close to helices VII and XI in the lactose permease. *Biochemistry* **38**(6), 1715-1720

216. Wu, J., and Kaback, H. R. (1996) A general method for determining helix packing in membrane proteins in situ: helices I and II are close to helix VII in the lactose permease of *Escherichia coli*. *Proc. Natl. Acad. Sci. U.S.A.* **93**(25), 14498-14502

217. Rice, W. J., Green, N. M., and MacLennan, D. H. (1997) Site-directed disulfide mapping of helices M4 and M6 in the Ca^{2+} binding domain of SERCA1a, the Ca^{2+} ATPase of fast twitch skeletal muscle sarcoplasmic reticulum. *J. Biol. Chem.* **272**(50), 31412-31419

218. Loo, T. W., and Clarke, D. M. (1996) Inhibition of oxidative cross-linking between engineered cysteine residues at positions 332 in predicted transmembrane segments (TM) 6 and 975 in predicted TM12 of human P-glycoprotein by drug substrates. *J. Biol. Chem.* **271**(44), 27482-27487